USGS
science for a changing world

Forecasting Igneous Activity in Germany—A Multi-Criteria Approach

Chapter C of
Distributed Volcanism—Characteristics, Processes, and Hazards

Professional Paper 1890

U.S. Department of the Interior
U.S. Geological Survey

Cover. Photograph showing the Ulmener Maar, the youngest volcano in Germany. It is located within the Vulkaneifel United Nations Educational, Scientific and Cultural Organization (UNESCO) Global Geopark, Germany. Photograph by Franz May, Federal Institute for Geosciences and Natural Resources.

Forecasting Igneous Activity in Germany—A Multi-Criteria Approach

By Alexander Bartels, Lisa Rummel, and Franz May

Chapter C of
Distributed Volcanism—Characteristics, Processes, and Hazards

Edited by Michael P. Poland, Michael H. Ort, Wendy K. Stovall, R. Greg Vaughan, Charles B. Connor, and M. Elise Rumpf

Professional Paper 1890

U.S. Department of the Interior
U.S. Geological Survey

U.S. Geological Survey, Reston, Virginia: 2026

Suggested citation:
Bartels, A., Rummel, L., and May, F., 2026, Forecasting igneous activity in Germany—A multi-criteria approach, chap. C *of* Poland, M.P., Ort, M.H., Stovall, W.K., Vaughan, R.G., Connor, C.B., and Rumpf, M.E., eds., Distributed volcanism—Characteristics, processes, and hazards: U.S. Geological Survey Professional Paper 1890, 42 p., https://doi.org/10.3133/pp1890C.

ISSN 2330-7102 (online)

Acknowledgments

We highly appreciate the detailed comments by Brittain Hill, Chuck Connor, and an anonymous reviewer, which helped to improve the paper significantly. Funding was provided by the Federal Institute for Geosciences and Natural Resources, Germany.

Contents

Figures

Table

Conversion Factors

International System of Units to U.S. customary units

Multiply	By	To obtain
	Length	
meter (m)	3.281	foot (ft)
kilometer (km)	0.6214	mile (mi)

Datums

Vertical coordinate information is referenced to the European Terrestrial Reference System 1989 (ETRS 1989).

Horizontal coordinate information is referenced to the European Terrestrial Reference System 1989 (ETRS 1989).

Altitude, as used in this report, refers to distance above the vertical datum.

Abbreviations

BGE	Bundesgesellschaft für Endlagerung [Federal Company for Radioactive Waste Disposal]
BGR	Bundesanstalt für Geowissenschaften und Rohstoffe [Federal Institute for Geosciences and Natural Resources]
DLF	deep low frequency
GÜK250	Geological Map of the Federal Republic of Germany 1:250,000
HLW	high-level radioactive waste
IAEA	International Atomic Energy Agency
ka	kilo-annum; thousand years before present
LAB	lithosphere-asthenosphere boundary
Ma	mega-annum; million years before present
Moho	Mohorovičić discontinuity
m.y.	million years
StandAG	Repository Site Selection Act of 2017 (Standortauswahlgesetz)
USGS	U.S. Geological Survey

Distributed Volcanism—Characteristics, Processes, and Hazards
Edited by Poland, Ort, Stovall, Vaughan, Connor, and Rumpf
Professional Paper 1890

Chapter C

Forecasting Igneous Activity in Germany—A Multi-Criteria Approach

By Alexander Bartels,[1] Lisa Rummel,[1] and Franz May[1]

Abstract

Igneous activity, including shallow intrusions and volcanism, has the potential to disrupt underground critical infrastructure. Notably, future underground infrastructure projects like high-level radioactive waste repositories must be sited in areas of extremely low disruption probability by igneous activity. In Germany, according to the Repository Site Selection Act of 2017 (Standortauswahlgesetz, or StandAG), areas in which Quaternary volcanism is either present or future volcanic activity is expected within the next 1 million years (m.y.) must be excluded from the site selection process. Although the locations of regions with Quaternary volcanism are reasonably well known in Germany, forecasting potential igneous activity at intraplate volcanic fields is challenging, as many processes and their interactions control the spatial distribution of volcanic centers. Here, a semi-quantitative, multi-criteria approach is proposed for a regional evaluation of the relative potential of future igneous activity in Germany. A variety of geoscientific indicators are used, including seismic anomalies in Earth's mantle, gravity data, tectonic activity, sutures, ground motion, earthquakes, mantle degassing centers, and geochronological data of volcanic rocks. The indicators describe the sequence of processes from potential melt generation in Earth's mantle, through ascent and accumulation of melt within the lithosphere, to eruption at Earth's surface. In total, 15 out of 30 proposed geoscientific indicators are selected and quantified using 20 total assigned parameters. Defined threshold values are used to spatially delimit relevant parameter properties to focus on areas with higher potential of future magmatic activity. To consider uncertainties of parameters and their underlying processes, which are usually more spatially extensive below ground, buffer zones are defined in which values of relevance decrease with increasing distance from the initial lateral shape of a parameter. Normalized parameters are combined into an index, whose spatial value distribution is used to differentiate the relative potential of future igneous activity (within the next 1 m.y.). The sensitivity of the results is shown by varying the weighting factors for the relevant parameters in country-wide index maps. Thereby, profiles illustrate the distribution of the resulting index values and respective index fractions of various parameters. Different index maps for the relative potential of future igneous activity are presented and can be used for hazard assessments.

Introduction

Igneous activity must be evaluated critically when looking for a repository location for high-level radioactive waste (HLW) in deep geological formations. HLW, such as waste from nuclear power plants, must be isolated to protect people and the environment from harmful radiation. Many nations have elected to pursue isolation of HLW in underground repositories. Such repositories are expected to operate for hundreds of years, after which they will be permanently closed and the HLW will be inaccessible as the radioactive material decays to safe background levels over hundreds of thousands of years. To ensure the long-term stability of an underground repository site for HLW, areas that might be affected by future igneous activity must be excluded from consideration (International Atomic Energy Agency [IAEA], 2016; Bundesgesellschaft für Endlagerung [BGE], 2020, 2022b). Considering the local geology, storage concepts, and technical feasibility of construction, repository mines are recommended to be built at depths between 300 meters (m) and 1,500 m below surface (BGE, 2020). Additionally, HLW must be retrievable for the duration of repository operation and up to 500 years after closure. In Germany, according to the Repository Site Selection Act of 2017 (Standortauswahlgesetz, referred to herein as "StandAG, 2017")[2], areas in which either Quaternary volcanism is present or future volcanic activity is expected in the next 1 million years (m.y) must be excluded from the site selection process. No specific criteria for the term "expected" are given in the description of the repository site criteria within the StandAG; however, the long-term protection for society and the environment against ionizing radiation and other harmful effects of radioactive waste must be guaranteed for the next 1 m.y. (StandAG, 2017). Although Quaternary volcanic activity has been identified by previous geological mapping and geochronological data (for example, the Geological Map of the Federal Republic of Germany [GÜK250; BGR, 2019]; Wilson and Downes, 2006; and

[1]Federal Institute for Geosciences and Natural Resources, Germany.

[2]https://www.gesetze-im-internet.de/standag_2017/index.html#BJNR107410017BJNE001200000.

references therein), forecasting potential igneous activity is more challenging, especially if past eruptions occurred long before the Quaternary and volcanic fields became active again after several million years of quiescence. To consider the potential resurgence of volcanism in different regions of Germany, this report includes the complete spatiotemporal sequence of Cenozoic volcanism for hazard assessment of potential future igneous activity.

Worldwide, quantitative probability analyses of volcanic hazards are available for individual Quaternary volcanic fields (Weller and others, 2006; Connor and others, 2009; IAEA, 2016; Marrero and others, 2019; Ang and others, 2020). Also, forecasting the activity and general behavior of large, already existing polygenetic volcanoes such as stratovolcanoes or shield volcanoes is possible; these volcanoes may be active over tens to hundreds of thousands of years and their history can therefore be studied extensively (for instance, Ubide and Kamber, 2018). Monitoring volcanic unrest with geophysical methods can only provide information on imminent volcanic eruptions usually on the timescale of days to months (Deligne and others, 2018; Carlino, 2019; Barsotti and others, 2023; Eckel and others, 2023)—much less than the time needed to retrieve HLW from a threatened repository. Different precursory phenomena, such as changes in seismic activity, ground deformation, gravity and temperature, magnetic and electric fields, or gas flows and concentrations are observed over the span of several years, but usually only experience drastic changes minutes to months before an eruption. The ascent of primitive magmas from Earth's mantle to the surface can occur within hours to days (O'Reilly and Griffin, 2010). The time between eruptions of a single volcano can be days (Passarelli and Brodsky, 2012) or even thousands of years (Connor and others, 2006). In distributed volcanic fields, recurrence rates are low (10^{-4} to 10^{-5} vents per year) compared to the longevity of the fields (10^5 to 10^6 years) (Molloy and others, 2009). Investigations by Rout and Wörner (2020) on igneous rocks of the Laacher See volcano in Germany reveal that during the entire lifespan of the underlying magma reservoir, a timespan tens of thousands of years, there was periodic recharge with no eruptions until recently, in the late Pleistocene. Consequently, the absence of historical (or even Holocene) activity or unrest is not an accurate measure of potential for future igneous activity during the next 1 m.y.

Forecasting the timing and location of eruptions in monogenetic volcanic fields, like those in Germany, are challenging because of their short-lived activity and the numerous geodynamic processes and structural influences of overlying continental crust on melt migration. In addition, most intraplate volcanic systems are distributed over large areas, and new eruptions almost always occur at localities that have not previously experienced volcanic activity (Connor and others, 2019). Recent studies on forecasting new vent formation in young monogenetic volcanic fields focus on regions in which the spatiotemporal distribution of former eruptions is well known (Connor and others, 2009; El Difrawy and others, 2013; Germa and others, 2013; Bartolini and others, 2015; Galindo Jiménez and others, 2016; Mazzarini and others, 2016; van den Hove and others, 2017). Kernel density estimation is a statistical method widely used to calculate probable locations of eruptive vents (Connor and others, 2019); however, this method requires sufficient knowledge of the spatial and temporal distribution of vent localities within a certain volcanic field. This knowledge is not given for most of the volcanic fields in Germany, especially for older fields where volcanic rocks have been subjected to strong erosion and for which the recurrence rate of eruptions is uncertain. Given that many complex processes control the occurrence of volcanic vents in intraplate settings, additional geoscientific indicators, such as seismic anomalies, tectonic activity, ground motion, earthquakes, and mantle degassing centers must be considered for forecasting igneous activity. These indicators may provide information about recent or possible future processes connected to magmatic activity and its potential to culminate in an eruption.

Jentzsch (2001, 2013) proposed spatially differentiating areas within the Quaternary East and West Eifel volcanic fields in western Germany and Saxony and its surroundings in eastern Germany (fig. 1) by their respective likelihoods of future volcanic activity on the basis of different geoscientific indicators. A similar approach was taken by Schreiber and Jentzsch (2021) for Germany as a whole. Based on the distribution of Cenozoic igneous rocks and occurrence of different indicators (for example, swarm earthquakes, seismic low velocity anomalies in the mantle, helium isotopes in fluids with mantle signature, the occurrence of mofettes [CO_2-rich gas emanation] and bicarbonate water), Schreiber and Jentzsch (2021) defined areas with different relative probabilities of possible future volcanism by unequal evaluation of individual indicators and regions. In contrast, the multi-criteria approach proposed here considers more geoscientific indicators, which are processed for Germany as a whole to ensure a fair and unbiased procedure for all federal states. The spatiotemporal history of igneous activity within individual volcanic fields therefore only contributes proportionally to the multi-criteria approach (with 2 geoscientific indicators out of 14, table 1) and thus to the overall hazard assessment.

Geological Background

The Cenozoic volcanic fields in Germany are part of the much larger European Cenozoic Volcanic Province, which extends over approximately 1,200 kilometers (km) from France (Massif Central) through central Germany to the Czech Republic and Poland. According to the geological map GÜK250 and the charted igneous rocks therein (BGR, 2019), the Cenozoic volcanic fields in Germany form several groups within the European Cenozoic Volcanic Province (fig. 1). The northern volcanic fields present an extensive volcanic belt that runs in an easterly direction, parallel to the deformation front of the Alps, from the Eifel, Siebengebirge and Westerwald over the Vogelsberg, the Hessian Depression, the Rhön and Heldburger Gangschar to the complex volcanic fields of the Eger Rift and southwestern Poland (Schreiber and Jentzsch, 2021). To the south, individual occurrences of igneous rocks follow along the Upper Rhine Graben and within the adjacent areas of exposed Paleozoic basement rocks. The smaller Hegau, Urach, and Kaiserstuhl volcanic fields form a second belt close to the Alps (fig. 1).

In Germany, the volcanic activity of the European Cenozoic Volcanic Province started during the Late Cretaceous to early Paleocene, with isolated volcanic activity along the Upper Rhine Graben and southwest of the Vogelsberg (Horn and others, 1972; Schmitt and others, 2007; Martha and others, 2014; Nesbor, 2018). In the middle Eocene, volcanism started in the Hocheifel volcanic field, where it lasted until the late Oligocene and was characterized by two activity maxima during 44–39 mega-annum (million years before present, Ma) and 37–35 Ma (Fekiacova and others, 2007). The second period coincides with the first phase of volcanic

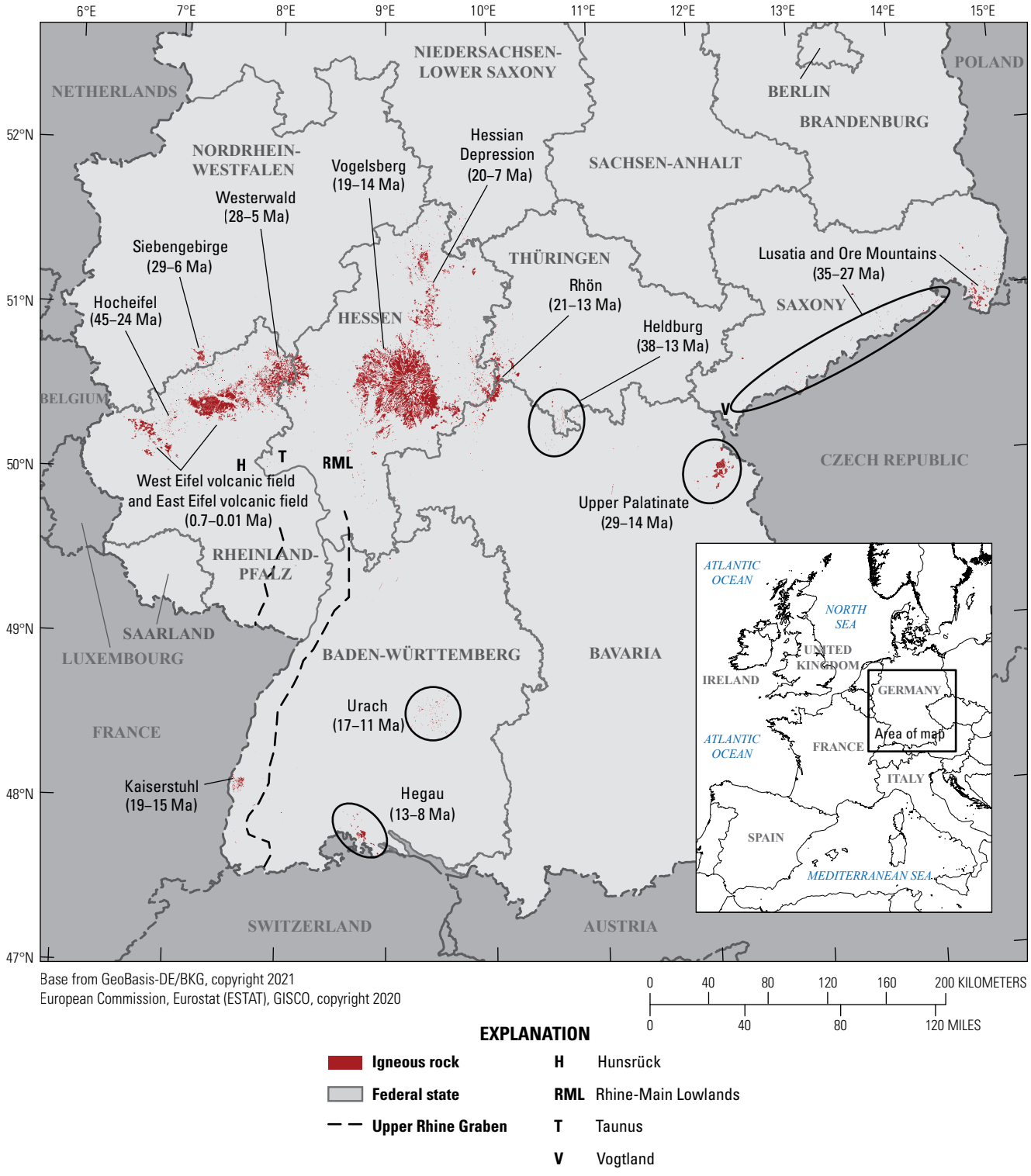

Figure 1. Map showing the location of Cenozoic igneous rocks in Germany and their ages (in millions of years) within volcanic fields. Ages are based on geochronological data (see compilation in Rummel and others, 2021b). Distribution of igneous rocks according to the geological map GÜK250 (BGR, 2019).

activity (38–25 Ma) in the Heldburger Gangschar volcanic field (Pfänder and others, 2018), as well as volcanism within the Lusatia volcanic field and the Ore Mountains (35–27 Ma; Abratis and others, 2015; Büchner and others, 2015), the latter associated with the main phase of volcanic activity in the Eger Rift. In the period between 29 and 14 Ma, a peak of volcanic activity in Central Europe, volcanism developed in the Upper Palatinate region (Todt and Lippolt, 1975; Ackerman and others, 2013) and the main parts of Siebengebirge and Westerwald volcanic fields (Lippolt, 1976; Lippolt and Todt, 1978; Turk and others, 1984; Przybyla and others, 2017), followed by the Rhön volcanic field (21–13 Ma; Lippolt, 1983), the Vogelsberg volcanic field (19–14 Ma; van den Bogaard and others, 2001; Turk and others, 1984) and volcanism in the Hessian Depression (20–7 Ma; Wedepohl and others, 1994). Concurrently and following, the second phase of activity in the Heldburger Gangschar volcanic field began (16–13 Ma; Abratis and others, 2007). Around the same time, activity commenced at the Kaiserstuhl volcanic field (19–15 Ma), in the Hegau volcanic field (13–8 Ma), and around Bad Urach (17–11 Ma) in southern Germany (Lippolt and others, 1963; Weiskirchner, 1972; Baranyi and others, 1976; Kröchert and others, 2009; Rahn and Handt, 2013; Schmid and others, 2014; Binder and others, 2022).

From the late Miocene to early Pliocene, a second phase of volcanic activity developed in the Westerwald volcanic field and within the area between Westerwald and Siebengebirge (Lippolt, 1976; Turk and others, 1984). In addition, two Quaternary events in the Westerwald volcanic field are assigned in the literature to the Quaternary volcanism of the Eifel volcanic fields (Lippolt and Todt, 1978). During the Quaternary, volcanism revived and formed the separate East and West Eifel volcanic fields, with the most recent activity in the East Eifel volcanic field at around 12.9 thousand years before present (ka; Laacher See) and the most recent activity in the West Eifel volcanic field at around 11 ka (Ulmener Maar) (Brauer and others, 2000). Additionally, some Quaternary eruption centers also formed in the Tertiary Hocheifel volcanic field, between the focal points for the eruptions of the East and West Eifel volcanic fields, as well as in the region of Upper Palatinate close to the border between Germany and the Czech Republic.

Presently, no scientific consensus exists on the underlying mechanisms and causes of igneous activity in Germany during the Cenozoic. The temporal and spatial distribution of volcanic fields, however, show that volcanism repeatedly shifted during the Cenozoic and in some cases reactivated within individual volcanic fields after long periods of quiescence (for example, the Eifel and Westerwald volcanic fields). This observed activity indicates a dynamic, long-lasting, and potentially reactivable magmatic system. The nature of this magmatic system necessitates the inclusion of the complete spatiotemporal sequence of Cenozoic volcanism in the hazard assessment of future igneous activity for the next 1 m.y., though this inclusion does not imply future activity exclusively occurring within known volcanic fields; new volcanic fields may form elsewhere or activity may resume in existing Quaternary fields during the next 1 m.y. Using the proposed multi-criteria approach, where all assigned parameters of the indicators are combined into an overall hazard index (see "Methods" section), the distribution of past eruptions represents a small fraction of the calculated index (see also "Parameter Components of the Index Values" section). Therefore, past, especially Tertiary, igneous activity might only become relevant if additional parameters used within this report point to potential future igneous activity.

Methods

Quantification of Indicators Using Assigned Parameters

To spatially differentiate the relative potential of future igneous activity in Germany, a variety of geoscientific indicators were used in a multi-criteria approach. Geoscientific indicators, referred to hereinafter as indicators, were identified considering the results of a proposal about the forecast of volcanic activity in Germany by using and evaluating existing data for volcanism related processes (May, 2019) and two expert surveys (Bartels and others, 2020; Rummel and others, 2021a). The purpose of these surveys was to gain an understanding of the scientific consensus and existing knowledge gaps concerning magmatism and volcanism in Germany, and decisions about the exclusion of regions in the site selection process for a HLW repository. Further, the experts were asked to rate the relevance of possible indicators regarding forecasts of volcanic activity in Germany. In these surveys, a total of 30 indicators were suggested that provided information about past and possibly recent magmatic processes and geological conditions that might indicate the potential for future eruptions.

Although all identified indicators are assumed to provide valid insight into forecasting eruptions in the next 1 m.y., suitable data are still needed to quantify the indicators across Germany. Considering both validity and availability of data, 15 suitable indicators were identified for use in the multi-criteria approach, and each indicator was quantified using at least one parameter (20 parameters in total for all indicators, tables 1 and 1.1). It should be noted, however, that the two indicators "distribution of Cenozoic volcanic fields and volcanic rocks" and "isolated Cenozoic volcanoes" within the 30 indicators proposed by Rummel and others (2021a) were combined into a single indicator, "distribution of Cenozoic volcanic fields and rocks" (table 1). The indicators reflect a complete magmatic lifespan (later also referred to as a process chain) from (1) potential melt generation in Earth's mantle, (2) ascent of melt through the lithosphere, and (3) eruption at Earth's surface. To enable a comprehensive assessment of potential future igneous activity, the parameters were processed and applied to all federal states of Germany. Parameter values were assigned to a 1 km by 1 km spatial grid that covers the entire country. Some parameters, such as seismic anomalies (ΔV_S, ΔV_P), vary continuously, whereas others vary categorically, such as distribution of bicarbonate springs. Continuous variables may have an assigned value of 0 where data are unavailable. For categorical variables, a value of 0 indicates the respective feature is absent.

Table 1. Quantifiable parameters for indicators of volcanic activity across Germany.

[ΔV_P and ΔV_S, seismic velocities of primary and secondary waves relative to horizontal mean; DLF, deep low frequency; LAB, lithosphere-asthenosphere boundary; σ_3, minimum principal stress; Moho, Mohorovičić discontinuity; He, helium; $^3He/^4He$ ratio (R) in relation to the atmospheric $^3He/^4He$ ratio (R_A)]

Indicator	Quantifiable parameter
Geochemical and isotopic analysis of mantle fluids	He isotopes (R/R_A values)
Teleseismic anomalies	ΔV_S ΔV_P
Ground motions	Uplift Dilatational component of strain rate Second invariant of strain rate
Temperature field and heat flux density	Depth of LAB
Gravity anomalies	Gravity anomalies in Earth's mantle
DLF-earthquakes	Occurrence of DLF-earthquakes (epicenters)
Swarm earthquakes	Occurrence of swarm earthquakes (epicenters)
Mofettes and bicarbonate water	Occurrence of mofettes and bicarbonate water
Neotectonic activity	Seismic hazard areas Structures of the European Cenozoic Rift System
Old faults and sutures	Occurrence of sutures and terrane boundaries Occurrence of deep and large-scale faults
Stress field	Magnitude of σ_3 Critical fluid pressure for fracturing
Deep seismic structures	Depth of Moho
Geochronological data	Geochronological data of volcanic rocks
Distribution of Cenozoic volcanic fields and rocks	Occurrence of igneous rocks (according to geological maps)

The multi-criteria approach is based on an independent consideration of all indicators and related parameters; therefore, the forecast is thought to be unbiased with regards to the distribution of past volcanic eruptions, as future igneous activity may occur elsewhere in and around distributed volcanic fields. The multi-criteria approach is thus based on a variety of overlapping parameters and can be applied as long as the parameters from all critical steps of the process chain are considered.

Data Processing

The parameters described in table 1 require assessment in terms of quality, uncertainties owing to data collection procedures and preprocessing methods, and uncertainties in relation to long-term and large-scale geodynamic and magmatic processes. Based on these assessments, processing strategies were developed for individual parameters to combine them into a semi-quantitative index value of the relative potential of future igneous activity in Germany, without being able to determine absolute numbers for the eruption probability for a certain location.

Data Uncertainty

Apart from natural heterogeneities and variations, all parameters have uncertainty owing to data collection procedures, interpretation, and preprocessing strategies. Uncertainties exist for both the spatial distribution of data points and their underlying properties. Different kinds of uncertainties are identified, caused by (1) interpolation of properties between adjacent data points, (2) preparation and evaluation of data (for example, treatment of outliers or filtering and correction), (3) defined constraints (for example, for numerical simulations or other calculations), (4) attributed coordinates, (5) measurement errors, (6) data quality, and (7) generalizations and interpretations.

Parameters determined by geophysical methods are strongly dependent on the available monitoring network (especially the density of observation points) and the applied methods for data acquisition and processing, both of which might influence the resolution of the parameter results. For non-interpolated data, uncertainties regarding data collection, position coordinates, measurement errors (for instance, for hypocenters of earthquakes or for the assigned position coordinates of geochronological data of volcanic rocks), or generalizations of parameters and their interpretations (for example, for faults and sutures [former plate or terrane boundaries]) are taken into account by assigning uncertainty zones of different shapes adequate to the specific parameter (see "Processing Strategies" section). Underlying large-scale geodynamic and magmatic processes, which might affect a much larger area than the available dataset represents, are accounted for by additional buffer zones around the lateral extension of different parameters and their possible uncertainty zones. Within these buffer zones, the values of relevance for a specific parameter linearly decrease with increasing distance from the initial lateral shape or uncertainty zone of a parameter (see "Processing Strategies" section for more details). For example, the occurrence of igneous rocks at Earth's surface can be assumed to only represent a small amount of the total melt ascending from Earth's mantle, as most of the melt stalls during its ascent through

the lithosphere (Sparks and others, 2019). Similarly, geodynamic processes associated with the formation of the European Cenozoic Rift System or suture zones must be much wider in subsurface regions than expected from observed near-surface structures. Although we mostly rely on surface observations in quantifying the spatial extent of a parameter, we assume that most of the deeper processes (such as dike or crack propagation) affecting the depth level of a repository mine for HLW (for example, between 300 m and 1,500 m below the surface) are covered by the applied buffer zones.

The described general application of uncertainty and buffer zones (see "Processing Strategies" section) for a specific parameter is only a first approximation for the region most likely affected by a parameter, given the possible underlying large-scale processes and uncertainties in a country-wide application of the multi-criteria approach. Accordingly, the uncertainty and buffer zones could be adjusted in the future in more regional applications depending on the local geological conditions, especially if more precise data or additional information are available for certain parameters, or if data densities facilitate the application of geostatistical methods or machine learning.

Processing Strategies

The parameters and their data are heterogeneous with respect to their quality and spatial coverage. Data collected with geophysical or geodetic methods (for instance, seismic anomalies in Earth's mantle, depth of the Mohorovičić discontinuity [Moho] and the lithosphere-asthenosphere boundary [LAB], gravity anomalies, ground motion) as well as results from numerical simulations (for example, of the stress field) are mostly available for the whole of Germany (appendix 2). However, other datasets are limited to the surface expression of igneous rocks (for instance, geochronological data or distribution of igneous rocks) or form selective clusters or point data (for example, degassing centers and earthquakes). Evaluation of parameters is limited by the availability of data and information from different institutions and research groups. For areas in which no data are available for a certain parameter, a value of 0 is assumed with reference to the current data availability and knowledge base for the parameter. For some clustered information, like the occurrence of bicarbonate springs that have been used since at least ancient Roman times, the data can be assumed to be close to complete, and the lack of data reflects the absence of occurrences.

Depending on the parameter, threshold values are defined on the basis of (1) the statistical distribution of data within a reference region of different size (for example, for seismic anomalies, depth of Moho and LAB, gravity anomalies, stress field, ground motion, and seismic hazard areas), (2) specific levels of significance given in the literature (such as for helium isotopes), or (3) the sole existence of a parameter itself (for example, for the occurrence of igneous rocks, earthquakes, faults, and sutures). Depending on the parameter, the reference region in (1) is defined by (1a) an area in northern Germany unaffected by Cenozoic volcanism or the thickening of the lithosphere as a result of deformation related to the Alpine orogeny (for example, for depth of Moho and LAB), (1b) Germany as a whole (for instance, for seismic hazard), or (1c) Germany and adjacent areas (for example, for seismic anomalies, gravity anomalies, and stress fields). A detailed description of the threshold and the demarcation criteria for each parameter is given in appendix 1, table 1.1.

To compare and combine different parameters into hazard potential maps, their relevant values (delimited by the threshold value) are normalized to a uniform standard scale with values between 0 and 10, where 0 represents the lowest potential hazard and 10 the highest potential hazard of a certain parameter. However, the occurrence of a single parameter does not constitute an overall hazard for volcanism, as only elevated values of the index calculated from the combination of all parameters indicate a higher relative potential for future igneous activity. When values outside Germany are considered in the normalization procedure of specific parameters, the maximum value of this uniform standard scale of relevance may not be located inside Germany. Where interpolated data are available, the values are directly converted to the uniform standard scale of relevance (see strategy 1). Parameters for which only a spatially limited interpolation is available within individual clusters of point data (for example, for helium isotope data; see strategy 2) are also directly converted to the uniform standard scale of relevance. For parameters whose existence itself acts as quantifiable property, the highest relevance is allocated to the initial lateral shape or uncertainty zone of the parameter (with surrounding buffer zones of decreasing values; refer to strategy 3).

References for the data used are given in the supplementary material (appendix 2). A detailed description of the datasets and the processing for each parameter is provided in the technical reports of Bartels and others (2022) and Rummel and others (2023). Data processing for individual parameters can be grouped into three strategies, which are briefly described here with examples illustrated in figures 2–4.

Strategy 1 is used for continuous parameters for which interpolated, country-wide data records are available (ΔV_S and ΔV_P [seismic velocities of secondary and primary waves relative to horizontal mean], depth of LAB and Moho, magnitude of σ_3 [minimum principal stress], critical fluid pressure for fracturing, seismic hazard areas, uplift, second invariant of strain rate, dilatation, and gravity anomalies); an example showing seismic velocities of secondary waves is given in figure 2. To begin, the datasets (fig. 2*A*) are further interpolated to a 1 km by 1 km spatial grid (applied for all indicators) using a cubic or nearest neighbor interpolation method depending on the parameter (fig. 2*B*). Thresholds are defined (appendix 1, table 1.1) on the basis of the frequency distribution of all (or only positive or negative) values depending on the parameter using the average or the standard deviation of the respective data to determine critical values to be considered in hazard assessment (fig. 2*C*). Finally, the data between the proposed threshold value and the minimum or maximum value (in the example of seismic velocity for secondary waves, this minimum or maximum value is the most negative value of the anomaly; fig. 2*C*) are normalized to the chosen uniform standard scale of relevance with values between 0 and 10 (fig. 2*D*). If different datasets are available for a certain parameter, an average is computed before the normalization procedure (for example, for Moho and LAB depth). Other datasets were combined after normalization (for instance, three depth layers

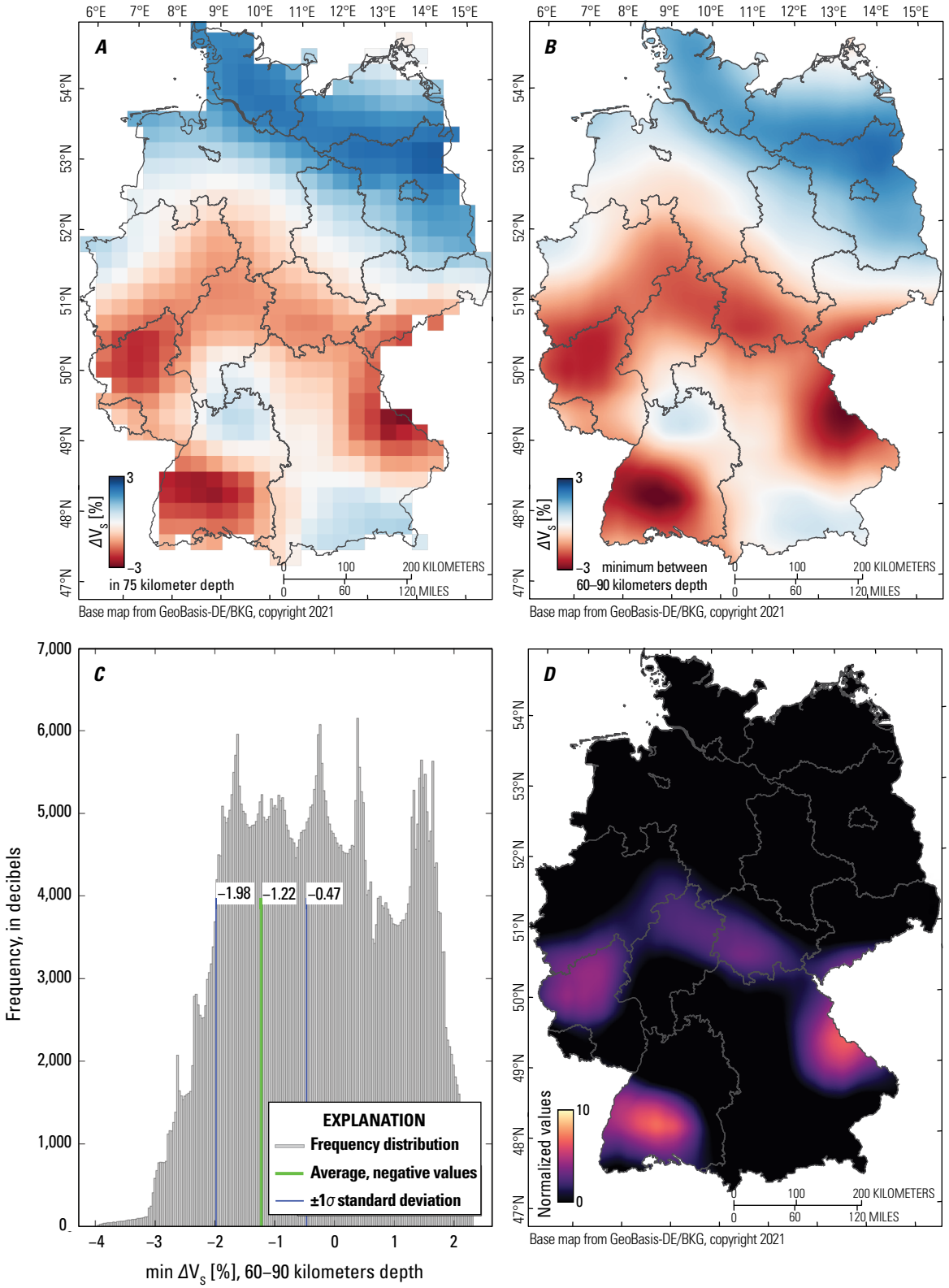

Figure 2. Maps and a frequency distribution of data processing strategy 1 showing seismic velocities of secondary waves (V_S). Strategy 1 is generally used for interpolated, country-wide data records, whose value range can be directly converted to the uniform standard scale of relevance. *A*, Map of initial interpolated, country-wide data and their resolution (from Collaborative Seismic Earth Model described in Fichtner and others, 2018) at 75 kilometers (km) depth after determining the deviation of absolute isotropic velocities from horizontal mean (V_S to ΔV_S), or isotropic anomaly. *B*, Map of the determined minimum values of ΔV_S [min ΔV_S] within 60–90 km depth (assumed here as the melting depth for each location), and interpolation of "min ΔV_S" to a 1 km by 1 km spatial grid using a cubic interpolation method. *C*, Graph of threshold values from the negative "min ΔV_S" distribution. *D*, Map that shows the scaling of "min ΔV_S" between the proposed relevant threshold value and the most negative value of the anomaly to values between 0 and 10. %, percent.

of the stress field, two sets of ΔV_S) as only their normalized value distribution could be compared owing to different parameter scales. For example, stress generally increases with increasing depth. To consider only the lateral variation of the least compressive stress (σ_3) in each depth level and not the total amount of stress, the data of the individual depth levels were processed separately and normalized to the uniform standard scale of relevance. The resulting normalized values were combined into a single layer for σ_3.

Strategy 2 is applied for point datasets, which are further processed by either calculating a spatially limited interpolation (for example, for helium isotopes) or determining the spatial density of point data. An example of the latter is shown in figure 3 for the occurrence of mofettes and bicarbonate water using a planar kernel density method with an automatically determined bandwidth, modeled after Silverman (1986). In both cases, the resulting values are converted directly into the uniform standard scale of relevance (fig. 3*B*).

Strategy 3 is used for point, line, and polygon datasets that can be related to underlying large-scale processes that might affect a much larger area than the available datasets represent. For point or line data (for example, earthquakes, faults, and sutures), a surrounding area (for instance, a circular area for points and a belt for lines) with a specific spatial range is assigned to consider the uncertainties associated with the measurement, collection, and interpretation of data (for example, fig. 4*B*; see also "Data Uncertainty" section). The spatial range of these areas varies depending on the assumed uncertainty (for instance, 1 km radius around epicenters of DLF [deep low frequency] earthquakes, 10 km width for suture zones, 5 km width for generalized fault zones). For these uncertainty zones, a value of 10 (the highest value of the uniform standard scale), equivalent to the highest relevance of a parameter, is used. For parameters with polygon datasets (for example, structures of the European Cenozoic Rift System or distribution of igneous rocks), the area with highest relevance is already defined by the polygons. Uncertainties regarding the underlying large-scale processes are considered for all datasets by assigning additional buffer zones that surround the defined area with the highest relevance. Depending on the parameter, the spatial range of the buffer zone varies (for instance, 1 km for fault zones and 10 km for occurrences of igneous rocks). Within these buffer zones, the values of relevance linearly decrease with increasing distance to the center, from 10 (high relevance) to 0 (no relevance).

Besides these general applications of the third strategy, the parameter "geochronological data of volcanic rocks" is processed differently. For example, the available geochronological data are grouped into different age categories. The first category comprises the period of the Quaternary between 2.6 Ma and today, in accordance with the exclusion criterion "volcanic activity" stated in the StandAG. The second category is based on the specifications of the International Atomic Energy Agency (IAEA) for the safety of nuclear installations (IAEA, 2016) and covers the age range between 10.0 and 2.6 Ma. The other categories are divided into

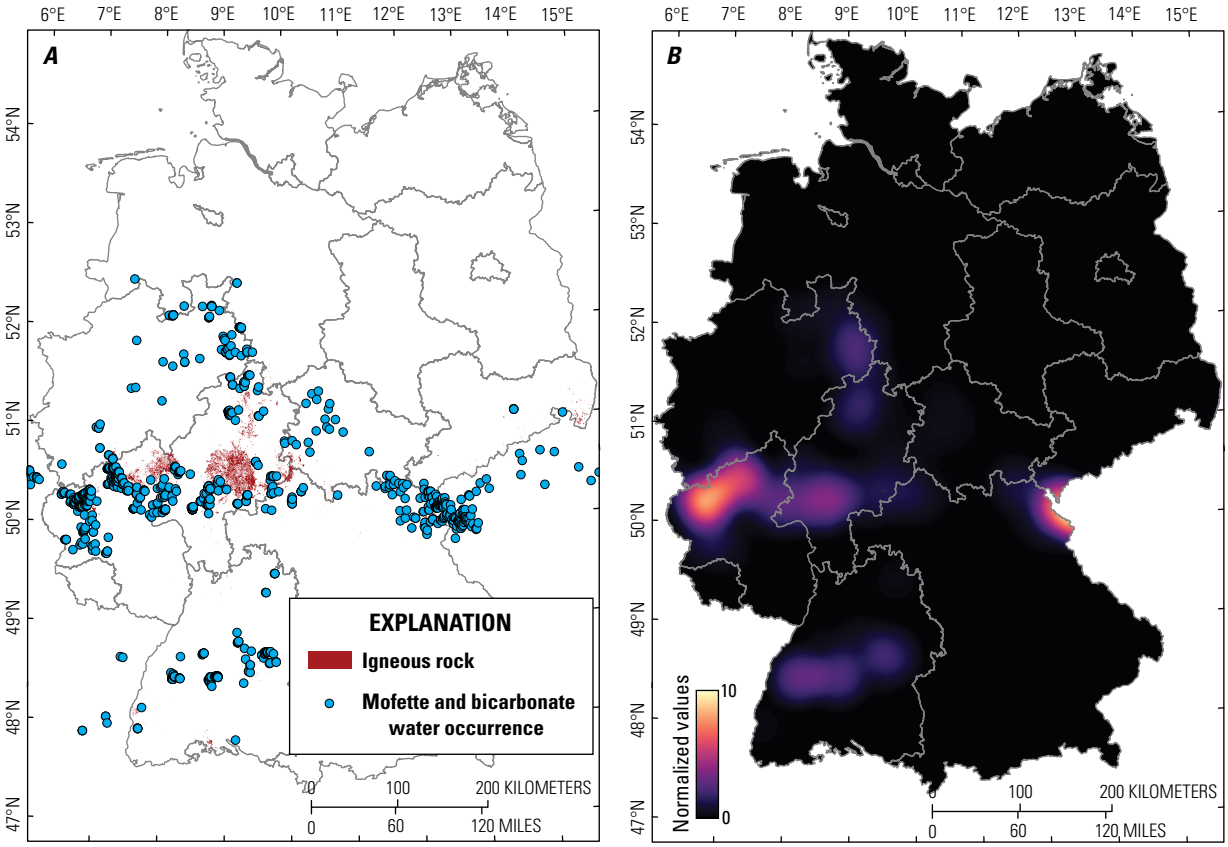

Figure 3. Maps showing an example of data processing strategy 2. Strategy 2 is generally used for point datasets with limited spatial interpolation. The resulting values can be converted directly into the uniform standard scale of relevance. *A*, Map of occurrences of mofettes and bicarbonate water in Germany and adjacent areas after Bartels and others (2022). References for the data are given in the supplementary material (appendix 2). *B*, Map showing normalized spatial density of the point data given in *A*.

steps of 10 Ma up to an age of 60 Ma. To account for earlier volcanism possibly related to the European Cenozoic Volcanic Province, the last category includes all ages greater than 60 Ma up to 145 Ma. Because of the importance of young volcanism for the hazard assessment of future volcanic eruptions, values of relevance are assigned to the selected categories following an exponential function. A country-wide assignment of values determined in this way to igneous units rather than to individual rocks cannot be made because of heterogeneous datasets related to different regional stratigraphic scales and definitions used by various authors. Alternatively, the values are applied to allocated circular areas with a uniform radius of 2.5 km around the position coordinate of the analyzed rock sample (assigned to a specific age datum). The size of the circle is defined by an assumed average size of volcanic structures (vents, craters, lava flows, and so on) in the volcanic fields of Germany. The chosen radius also covers most of the sizes of possible subvolcanic dikes, which might affect an underground repository. Uncertainties regarding the lateral distribution of the volcanic structures and magma conduits from lithospheric or asthenospheric magma reservoirs, which in some cases are larger than the assigned circular area with a 2.5 km radius, are taken into account by assigning 10 km wide buffer zones, with a gradual decrease of values from the respective prescribed value of relevance (fig. 4*B*). For the combined consideration of all age data, the individual age categories, together with their respective buffer zones (fig. 4*C*), are added and scaled between 0 and 10 (fig. 4*D*).

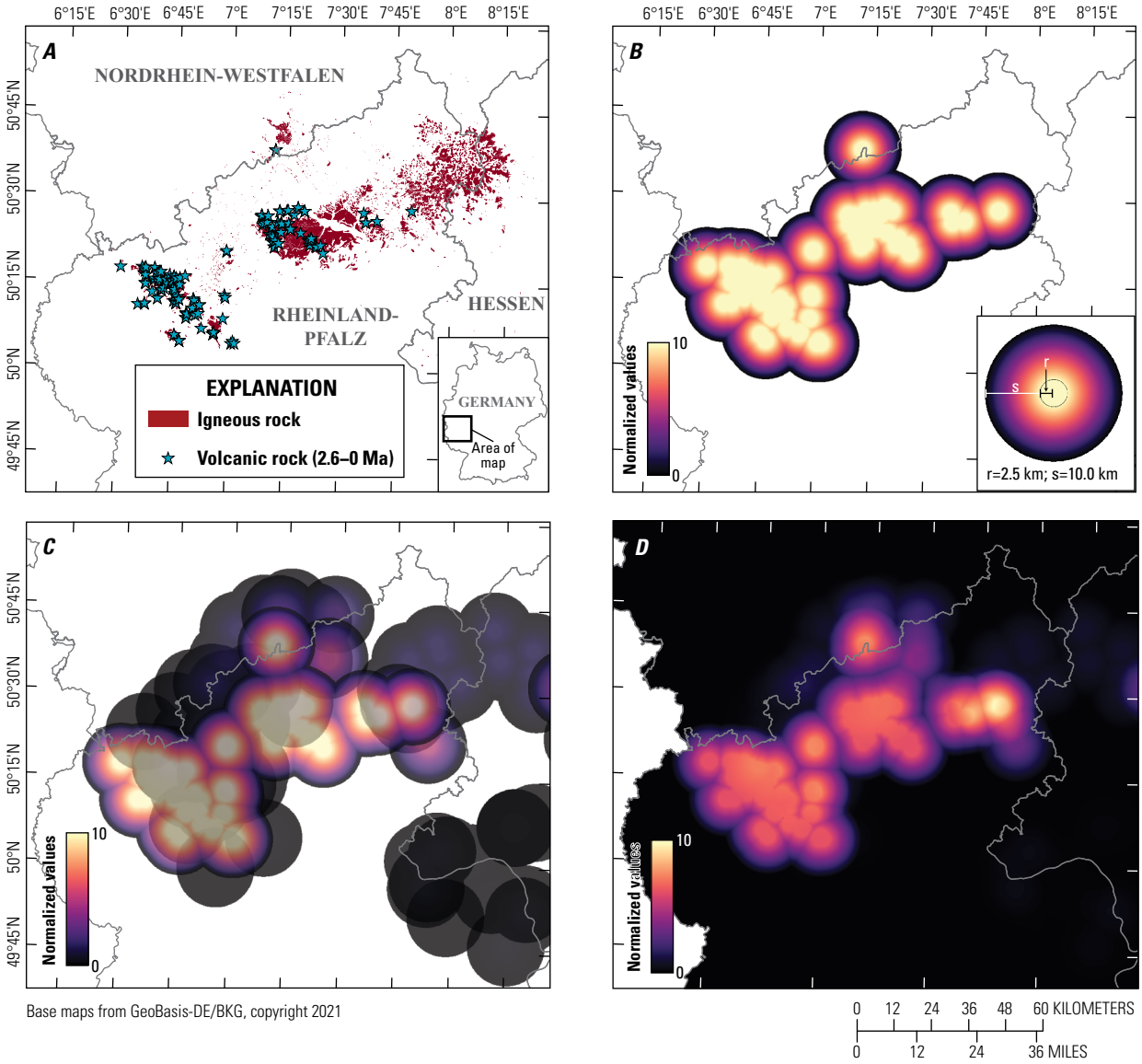

Figure 4. Maps of the results from extended data processing strategy 3 showing geochronological data of volcanic rocks. Strategy 3 is generally used for point, line, and polygon datasets that can be related to underlying large-scale processes that might affect a much larger area than the available datasets represent. All maps represent the same area shown on inset regional map. *A*, Map of available geochronological data of volcanic rocks in the Eifel volcanic fields and adjacent areas for a defined age category (2.6–0 million years ago). References for the data are given in the supplementary material (appendix 2). *B*, Map of assigned circular areas (radius of 2.5 kilometers [km]) and additional buffer zones of 10 km width around a sample position coordinate with normalized values of defined relevance. *C*, Map showing the superposition of all age categories investigated (visualized with 30 percent transparency). *D*, Map showing the result for the parameter "geochronological data of volcanic rocks" after adding the calculated values of given age categories from *C* and normalization to the uniform standard scale of relevance between 0 and 10. r, radius; s, width of buffer zone.

The advantage of this approach is the general consideration of recurring volcanic activity within different periods of time without having to distinguish between episodic volcanism or long-lasting and persistent activity.

Combination of Parameters to a Single Index Value

The aim of the combined consideration of all 20 parameters is to develop a semi-quantitative index value for potential future igneous activity in Germany during the next 1 m.y. To compare different parameters (refer to the "Processing Strategies" section), their relevant values are normalized to a uniform standard scale. These normalized parameters are used to develop an index value for each geographical location of the 1 km by 1 km grid by multiplying the parameter values with defined weighting factors and adding them together. The higher the index value, the higher the assumed potential for future igneous activity in the respective region. Four different approaches are computed to account for different relevance of indicators and assigned parameters by using different individual weighting factors.

The expert surveys regarding forecasting volcanism in Germany (Bartels and others, 2020; Rummel and others, 2021a) conducted according to the Delphi method (Häder, 2009) yielded differences in expected relevance for individual indicators. In these surveys, indicators were ranked according to five possible categories. Assigned values varied between one (very low relevance) and five (very high relevance; Bartels and others, 2020; Rummel and others, 2021a). However, since the average ranking from all experts is used for each indicator, the resulting weighting factors after normalization are similar (table 1.2, approach 1). In approach 1, the respective parameters are weighted using the relevance for the indicators obtained from the expert surveys.

For approach 2, the parameters are assigned to different categories of processes that lead to a volcanic eruption. Parameters that provide information on possible melt formation in Earth's mantle are separated into one process category, separate from processes that provide information on possible pathways for melts within the lithosphere. A third process category comprises volcanic surface features (indicative of a past eruption), including the distribution of igneous rocks based on geological maps and their ages (table 1.2). To equally account for all three process categories, the sum of the weighting factors within each category must be equal to one third (table 1.2, approach 2). This procedure guarantees that processes for which many quantifiable parameters are available do not become disproportionately high in relevance when all parameters are summed.

Approach 3 is a combination of approach 1 and approach 2 and includes both the results of the expert surveys as well as the different process categories.

To test for the sensitivity of the multi-criteria approach, a statistical approach 4 is used, where the weighting factors within the process categories of approach 2 were computed using a random number generator with a uniform distribution. Weighting factors between 0 and 1 with a resolution of 0.01 were calculated and normalized to one third within each process category. Based on the resulting weighting factors, 1,000 possible realizations for the index were calculated and are used to determine the mean index value for each geographical location.

The results of the different approaches are described in the "Results" section and are illustrated in respective index maps (fig. 5).The approach 3, which considers both the results of the expert surveys as well as different process categories, is further used to calculate hazard index maps to determine the relative potential of future igneous activity in Germany for the next 1 m.y. (see "Index Maps of Relative Hazard Potential" section).

Results

For approach 1, high index values are observed for the Eifel region, with maximum values in the East Eifel volcanic field. Additionally, north of the Eifel volcanic fields around the Siebengebirge and southeast of the Eifel volcanic fields in the Hunsrück and Rhine-Main lowlands, higher values of the calculated index are present compared to the surrounding areas. Other regions that show an elevated potential for future igneous activity during the next 1 m.y., based on the results of approach 1, are the Hessian Depression, Upper Palatinate and the southern Vogtland, as well as parts of the southern Upper Rhine Graben. Slightly lower, but still elevated, index values are present in southern Germany around Bad Urach and the Hegau volcanic field. Lineaments of faults and sutures are observed within the resulting index maps throughout Germany, with slightly elevated values compared to the surrounding areas (fig. 5*A*).

The results of calculated index values using approach 2 show clear differences to approach 1 (fig. 5*A*, fig. 5*B*). By considering process categories (as done in approach 2), the regions with substantially increased index values can be correlated with surface expressions of Cenozoic igneous rocks. Similar to approach 1, the maximum values appear in the area of the Eifel volcanic fields, but the lateral extensions of the maximum values for approach 2 are more pronounced (fig. 5*B*). In the areas of northeastern Hunsrück, Taunus, Rhine-Main lowlands, Hessian Depression, Upper Palatinate, southern Vogtland, and southern Upper Rhine Graben, values of the calculated index are slightly higher relative to the results of approach 1. Other regions that show an elevated potential for future igneous activity are around Vogelsberg, Rhön, Heldburger Gangschar, and the southern volcanic fields around Bad Urach and in the Hegau.

The results of the combined approach 3 (fig. 5*C*) are almost identical to those of approach 2 (fig. 5*B*), with the highest index values in regions where volcanism has occurred in the Cenozoic. The same can be observed for the statistical approach 4, with the difference being that the maximum values of the calculated averaged index are generally more pronounced when compared to approach 2 and approach 3 (fig. 5*B*, *C*, *D*).

To quantify differences between approaches and evaluate the multi-criteria approach's sensitivity in terms of different weighting factors, the absolute differences of index values between two different approaches were computed (fig. 6). The results show distinct differences between approach 1 and approach 2, with an average difference between index values of 0.16 and a maximum difference of 1.75. This difference illustrates the substantial effect of normalizing weighting factors within respective process categories instead of considering all parameters after sole expert valuation in the computed index values. When random weighting

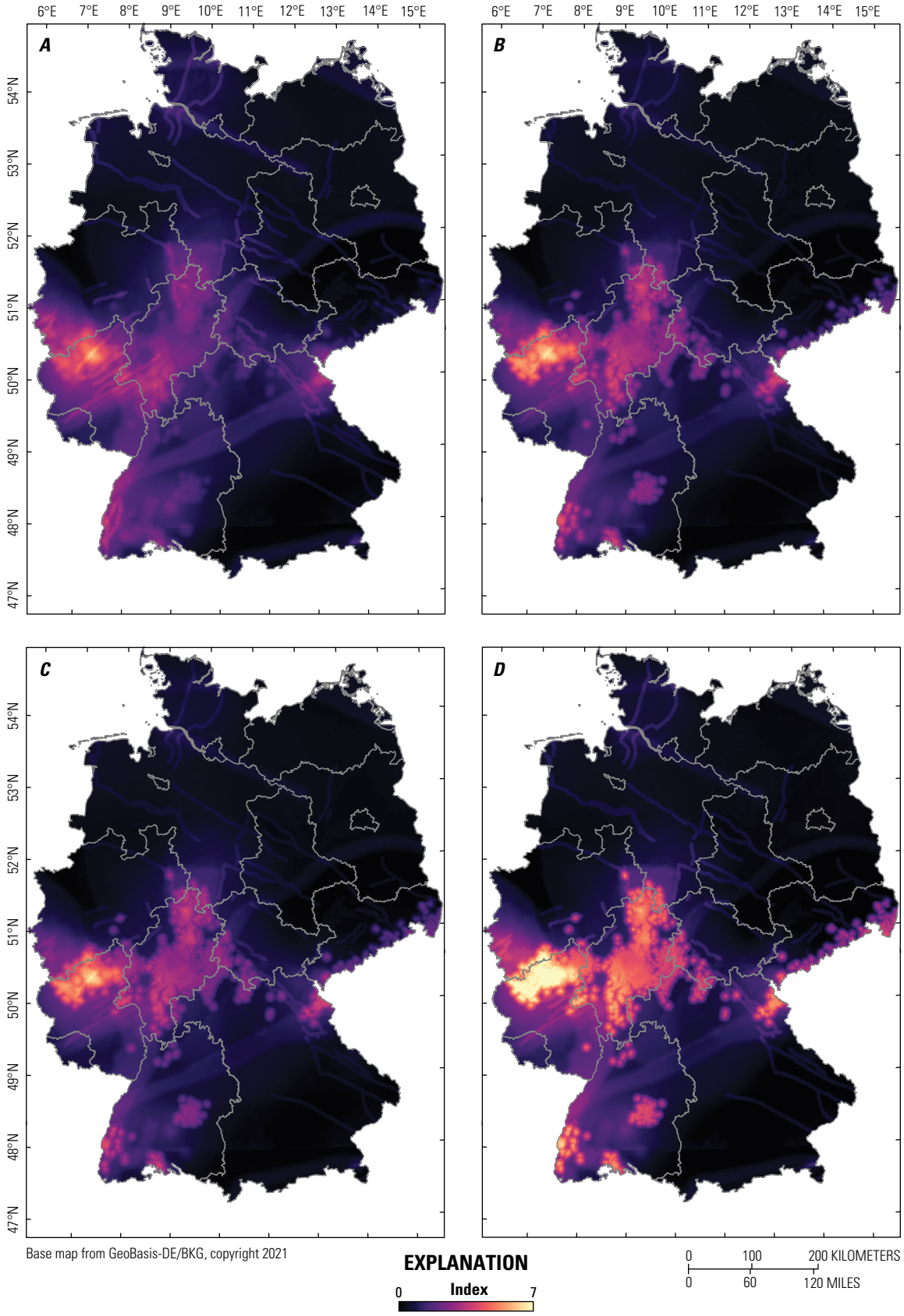

Figure 5. Maps of the spatial distribution of computed index values for four different approaches. *A*, Approach 1: considering results from expert surveys in the weighting factors. *B*, Approach 2: considering process categories for the weighting factors. *C*, Approach 3: a combination of approach 1 and approach 2. *D*, Approach 4: statistically determined weighting factors. An index value of 7 corresponds to the highest relative potential for the occurrence of future igneous activity in Germany.

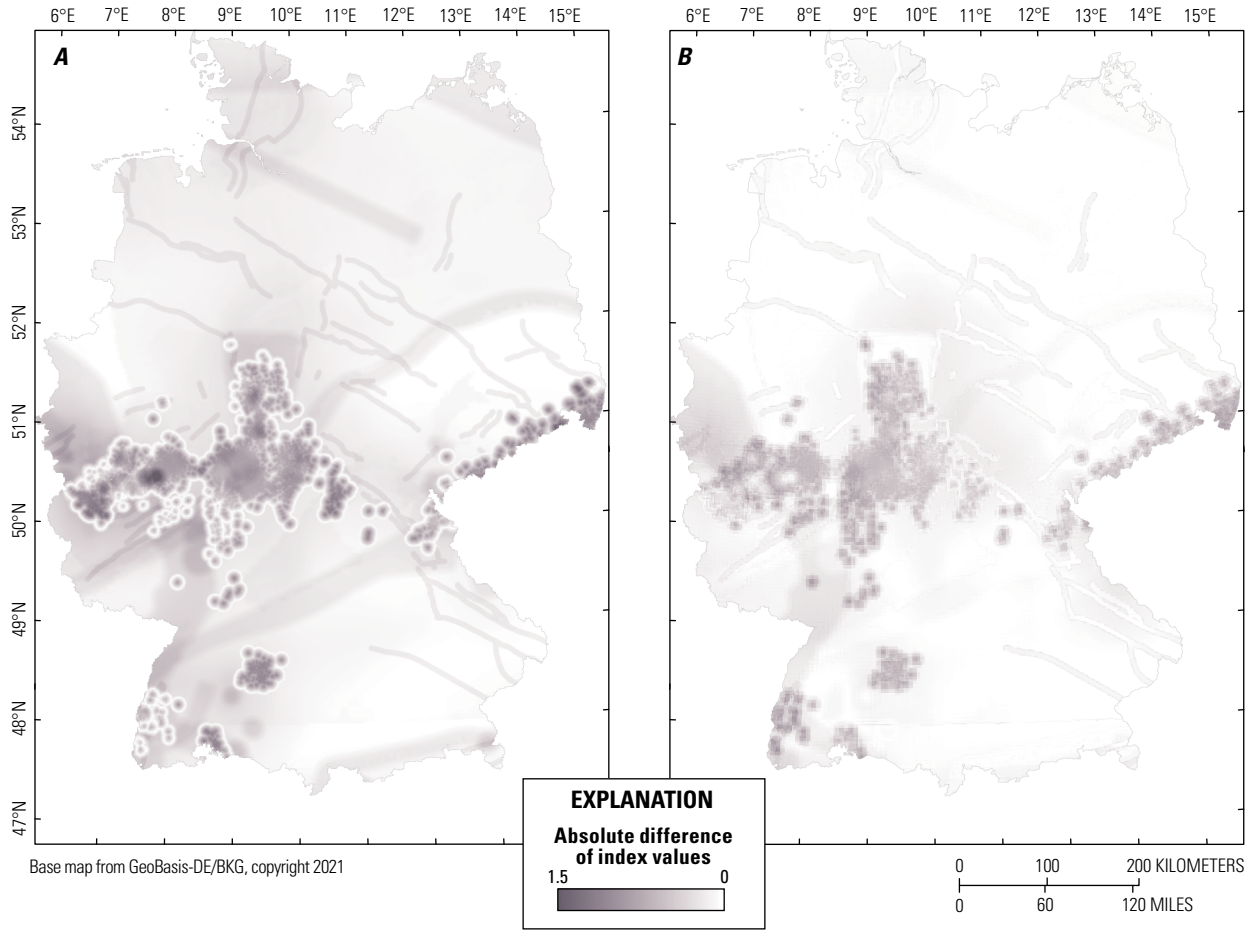

Figure 6. Maps showing the quantitative comparison of the different approaches shown by the absolute differences of their index values. *A*, Map that shows the comparison between approach 1 (considering results from expert surveys in the weighting factors) and approach 2 (considering process categories for the weighting factors). *B*, Map that shows the comparison between approach 3 (as combination of approach 1 and approach 2) and approach 4 (statistically determined weighting factors).

factors are used (approach 4) instead of factors obtained from expert surveys (approach 3) in the process categories, the average difference is smaller (0.08) but still clearly visible in the comparison map (fig. 6*B*). Nevertheless, the resulting images of the spatial distribution of index values are still similar (fig. 5), although the magnitude of the index regarding the potential of future igneous activity may vary regionally depending on approach. Accordingly, the proposed multi-criteria approach appears mostly insensitive to the effects of different weighting schemes because of the large number of parameters considered in determining areas that have a relatively higher potential for future igneous activity in the next 1 m.y.

Discussion

In the following sections, the effects of individual parameters on the resulting index are shown, and it is discussed how the distribution of index values can contribute to a hazard assessment of future igneous activity. Furthermore, limitations of the multi-criteria approach are identified, and the possible transferability of the multi-criteria approach to other intra-plate settings related to volcanism is presented.

Parameter Components of the Index Values

To quantitatively evaluate and visualize the results, the index values of the combined approach 3 are presented along defined profiles (fig. 7). The north-south oriented profile, profile *A*–*A*′ (fig. 7*A*), shows a minor relative potential for future igneous activity in northern Germany and an increased potential in central and southern Germany (for instance, around the Tertiary volcanic field around Bad Urach). The west-east oriented profile, profile *B*–*B*′ (fig.7*B*), passes through the Quaternary East and West Eifel volcanic fields. The index values are generally higher than along the north-south profile and form a plateau in the west, with values between 5 and 6 (with a maximum value of 6.1 in the East Eifel volcanic field). These values decrease eastward, where another plateau with index values of about 3 occurs in the areas of Vogelsberg and Rhön volcanic field.

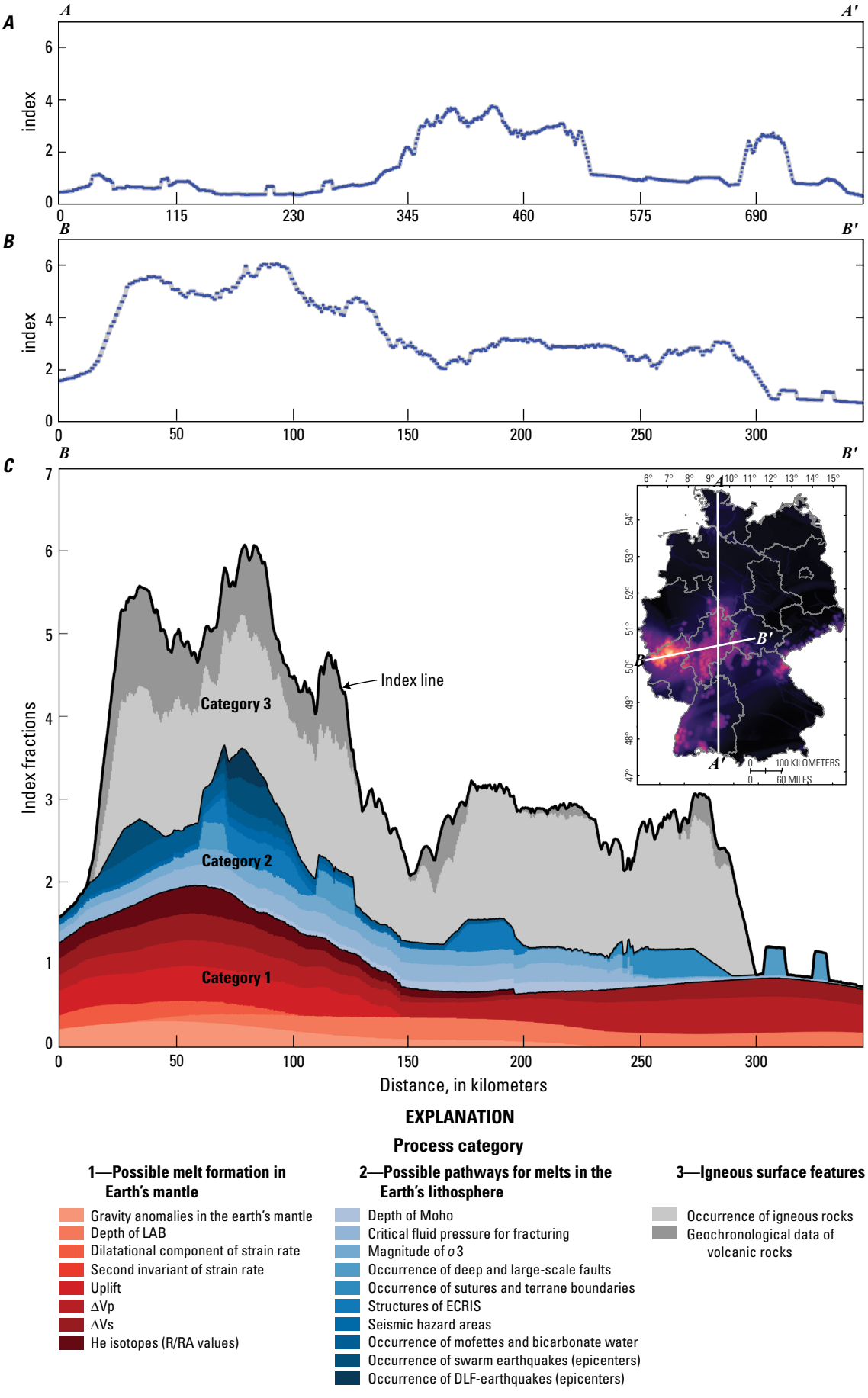

Figure 7. Graphs of index value distribution and its underlying index fractions from parameters of the combined approach 3 (considering results from expert surveys and process categories for the weighting factors). *A*, Index value distribution along north-south profile *A*–*A*′. *B*, Index value distribution along west-east profile *B*–*B*′. Note the x-axis scales on the profiles in *A* and *B* are different. *C*, Index fractions of individual parameters for profile *B*–*B*′ divided into the three process categories: possible melt formation in Earth's mantle, possible pathways for melts within the lithosphere, and igneous surface features. The index fractions represent normalized parameter values multiplied by respective weighting factors (approach 3, table 1.2), summed up to form an index. LAB, lithosphere-asthenosphere boundary; ΔV_P and ΔV_S, seismic velocities of primary and secondary waves relative to horizontal mean; He, helium; $^3He/^4He$ ratio (R) in relation to the atmospheric $^3He/^4He$ ratio (R_A); Moho, Mohorovičić discontinuity; σ_3, minimum principal stress; ECRIS, European Cenozoic Rift System; DLF, deep low frequency.

An indirect indication of the factors that cause an increase or decrease of the index values is provided by the value distributions of individual parameters that in sum represent the index values. The relative distribution of index values along the profiles is controlled by the characteristics of all parameters and their respective weighting factors. Parameters with normalized values larger than the calculated index led to a general increase of the absolute index values, whereas normalized values smaller than the calculated index led to a decrease of the absolute index values. Figure 7*C* shows the relative fractions of normalized and weighted parameters of the index for profile *B*–*B*′. In areas where multiple parameters are present, the index values are generally elevated. Highly elevated index values around the Eifel region are due to the relative fractions of the following parameters: occurrence of igneous rocks, uplift, critical fluid pressure for fracturing, ΔV_S, ΔV_P, gravity anomalies in Earth's mantle, occurrence of mofettes and bicarbonate water, and helium isotopes—expected characteristics of a volcanic field that was most recently active about 11 ka (West Eifel volcanic field) and that would likely have a higher potential for eruptions in the next 1 m.y. Small variations along profile *B*–*B*′ are further induced by DLF and swarm earthquakes, geochronological data of volcanic rocks, structures of the European Cenozoic Rift System, and the distribution of faults, sutures, and terrane boundaries (fig. 7). However, the large number of considered parameters and their superposition make it difficult to link local variations of index values to the effect of specific parameters.

Index Maps of Relative Hazard Potential

Based on the spatial distribution of the index values, a country-wide hazard index map with continuous trends of the relative potential for future igneous activity is proposed, as illustrated in the map section shown in figure 8.

The continuous distribution of index values results in a more differentiated image of the relative hazard potential compared to the results of Schreiber and Jentzsch (2021), who outlined areas

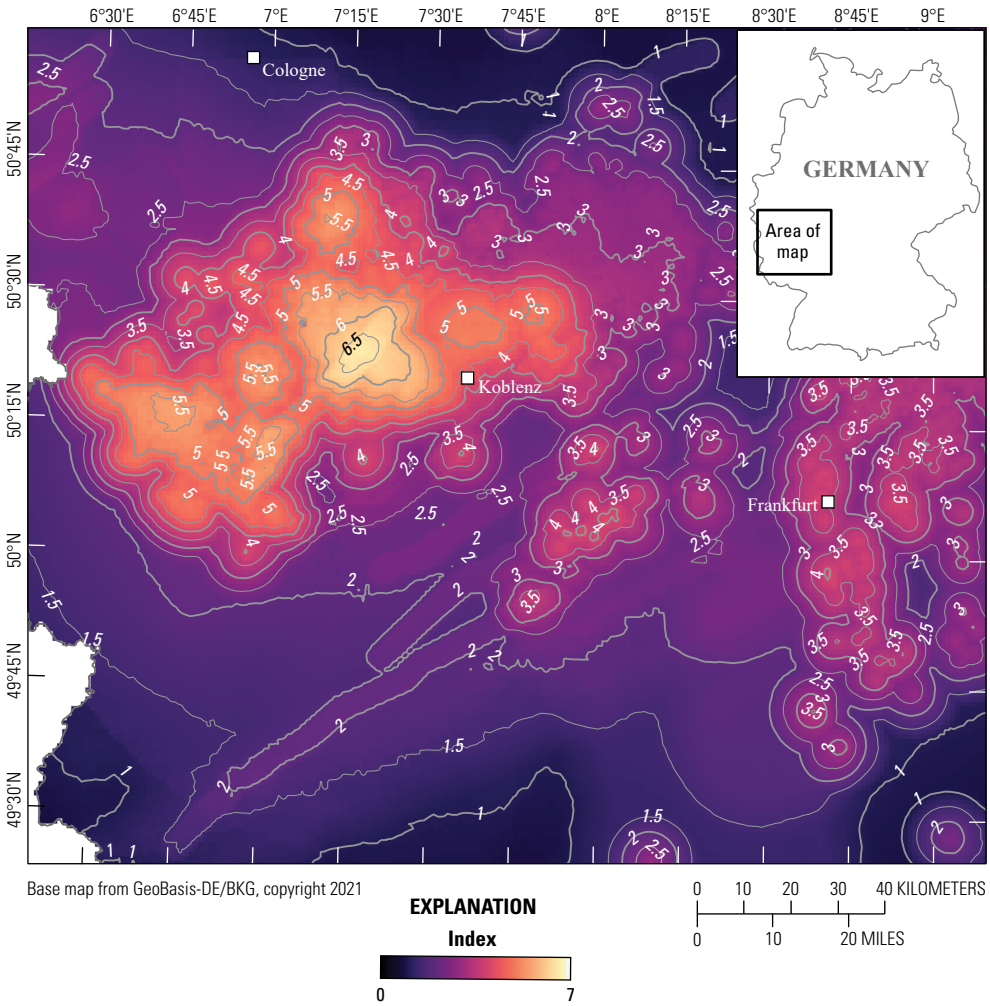

Figure 8. Map of area in western Germany showing relative potential for future igneous activity using continuously changing index values calculated using approach 3 (considering results from expert surveys and process categories for the weighting factors). Contour lines are shown at index intervals of 0.5. An index value of 7 corresponds to the highest potential for the occurrence of future igneous activity relative to other areas in Germany.

in Germany with or without "expected" future volcanic activity based on the occurrence of individual parameters. Furthermore, with the procedure recommended here, possible threshold values, which can be used for the assessment of the hazards from potential future igneous activity, can be displayed within the map using contour lines (isolines of the calculated index). Whether an area falls into a certain hazard class of potential future igneous activity depends on the individual assessment of the calculated index of the chosen approach (approach 1–approach 4) and the defining class boundaries for different hazard potentials. Figure 8 illustrates the calculated index values and their isolines for the combined approach 3 from the Eifel region to the Rhine-Main lowlands. The area west of Koblenz, called East Eifel, is characterized by the highest values of the hazard index, with values > 6.5.

An alternative approach to create hazard maps is to define hazard classes based on the frequency distribution of index values using different data classification methods—for example, by using quantiles, equal-sized subranges, or natural breaks. Depending on the classification method used, the limits of individual classes vary considerably. The assignment of local index values to a specific hazard class of potential future igneous activity is therefore strongly dependent on the classification method and the definition of critical thresholds. Furthermore, areas could be differentiated according to the number of existing parameters. The local value of an existing parameter (if greater than 0) can be ignored or incorporated by multiplying those numbers by defined factors representing the value distribution or the potential relevance of a parameter for the hazard assessment. Using a specific number of existing parameters as a required condition may better highlight the most likely regions of future volcanism by decreasing the values of relevance in areas that are not supported by enough parameters. Index maps with a different number of underlying parameters can be added to a more amplified hazard map. In figure 9, the results of classifying the index values using natural breaks (Jenks and Caspall, 1971; De Smith and others, 2007) with five possible classes are shown. In this classification method, similar values are grouped together, and the limits of classes are defined where large changes of data values occur.

However, the use of generalized classes with assigned potential future activity values (fig. 9) should be avoided when spatially differentiating the relative potential for future igneous activity, and only be used for simplicity. Classes defined in this way and the values standardized therein reduce the information content and

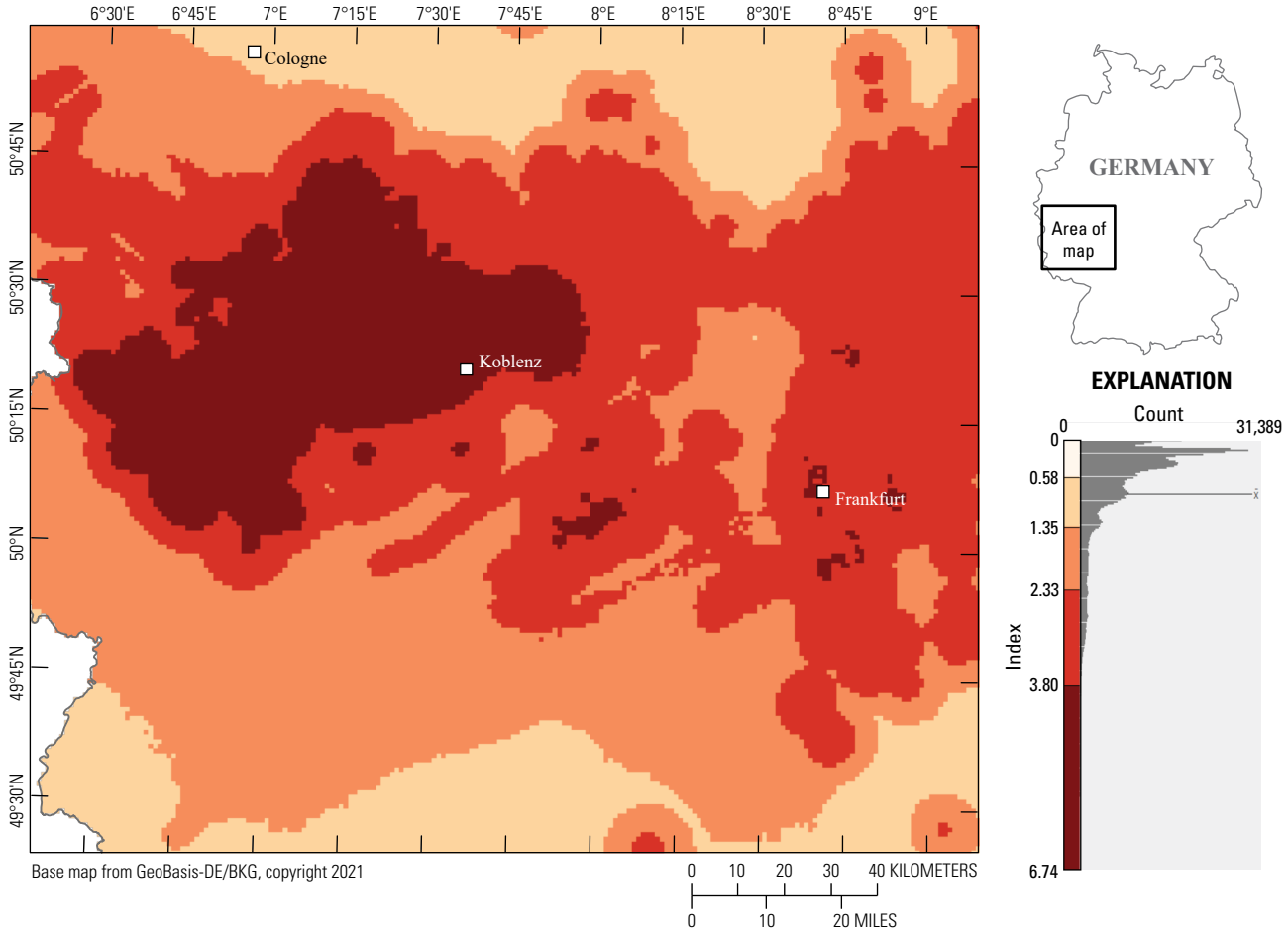

Figure 9. Map of area in western Germany showing defined possible hazard classes of the relative potential for future igneous activity for approach 3 (considering both the results from expert surveys and process categories for the definition of weighting factors) using the classification method of natural breaks modeled after Jenks and Caspall (1971) and De Smith and others (2007). The histogram of index values shows the respective classes which are transferred to the map.

the possibilities for differentiation within a class and maximize the apparent difference between the classes, potentially leading to misinterpretations. Furthermore, fixed hazard classes do not reflect the current state of scientific knowledge about processes subject to volcanism nor the uncertainties in the underlying data when used for forecasting the potential of igneous activity in Germany.

Defining areas to be excluded for an underground repository for HLW because of potential future igneous activity should be linked to some threshold based on the calculated index. Volcanic hazards and related near-surface igneous processes are, however, only one among many criteria used in the site selection process for underground HLW repositories. In particular, the proposed 1 m.y. performance period for a repository significantly exceeds the timeframe typically considered in traditional societal risk decisions (usually less than 100 years). In the end, pros and cons of candidate repository sites for HLW must be balanced—a process that can consider the local differences in the hazard index. As areas in Germany with index values of 0 are few, not discarding the information of index values below arbitrary thresholds is important, as those data could be used to compare different candidate sites during the final rounds of the selection process.

In addition to the geoscientific indicators considered in the multi-criteria approach presented here, other indicators exist that do not provide information about the potential of future igneous activity. Rather, these indicators provide information regarding the type of volcanic eruption that may occur in the future and its effects on repository performance, as well as near-surface environment and infrastructure (Jentzsch, 2001; Lorenz, 2007; IAEA, 2012, 2016; Jentzsch, 2013; Bartels and others, 2022). The influence of volatiles, fragmentation of magma, and distribution of volcanic products, as well as regional hydrogeological conditions and local topography might be of importance for understanding the consequences of any future eruptions. For example, Schmincke (2014) has shown that the distribution of the Laacher See tephra (deposited by the youngest volcanic event in the East Eifel volcanic field, just under 13 ka) is widespread in Central Europe. Additional calculations from Leder and others (2017) indicate that the effects of another eruption similar to that of Laacher See would not only affect nearby cities such as Koblenz, but also more distant cities like Frankfurt, owing to the prevailing westerly winds. Large deposits of tephra could therefore lead to significant damage. Additional volcanic processes, such as the formation of lahars or the damming of rivers like the Rhine because of lava flows and tephra deposits and possible subsequent dam failures, could occur in the future—events that could lead to considerable damage in the surrounding regions (Park and Schmincke, 1997; Jentzsch, 2001; Schreiber and Jentzsch, 2021). Other processes and phenomena that can have a direct result on the safety of nuclear installations, and therefore also on the safety of repositories for HLW during the operational and possible recovery phases (about 500 years; StandAG, 2017), are described in reports of the IAEA (IAEA, 2012, 2016).

These site-specific parameters could be considered separately after a country-wide or regional application of the proposed multi-criteria approach and may be important for the assessment of safety zones for critical infrastructure, such as for HLW repositories.

Limitations of the Multi-Criteria Approach

In addition to uncertainties associated with individual parameters and those produced by data processing, described in the "Data Uncertainty" section and in more detail by Bartels and others (2022), further uncertainties in the assessment of potential future igneous activity result from the combination of parameters to form an index value. Depending on the approach used, the spatial dependencies of the calculated index values and the derived distribution of the hazard index in Germany are different. Accordingly, the choice of a specific approach is critical for the evaluation of the results in regard to the relative potential for igneous activity in the next 1 m.y., and the definition of hazard classes. The comparison of the various approaches (see "Results" section), however, also shows that the derived hazard maps are similar despite their differences in the absolute index values. The insensitivity of the proposed multi-criteria approach to the effects of different weighting schemes is further supported by the results of approach 4, which considers a statistical variation of weighting factors for individual parameters inside each process category. The importance of considering process categories, included in approaches 2–4, is apparent as all available quantifiable parameters that can provide information about the relative potential of future igneous activity are considered in the multi-criteria approach. Accordingly, a different number of parameters is used to describe a specific phenomenon that can be related to magmatic processes. To prevent processes with many available indicators and assigned parameters from being given disproportionally high weighting in a multi-criteria approach, the same sum of weighting factors is used for each of the defined process categories to which different numbers of parameters are assigned.

The results are affected by data availability, completeness, resolution, and parameter quality to provide information about potential future igneous activity. Depending on the applied methods for data collection and processing and methods constraints, the spatial characteristics of different parameters may vary (Bartels and others, 2022). The data were analyzed considering the current state of knowledge and existing supra-regional datasets. Areas in which no suitable data are currently available are described by a parameter value of 0. A 0 value may influence the value distribution of the index (as a sum of all normalized parameter values) but is necessary because of insufficient data records and missing process understanding for some parameters (for example, for helium isotopes). Using random parameter values, instead of a value of 0 as proposed, without reference to process understanding or existing measured or computed values should be avoided, because the results would not be based on reliable data and could suggest a higher volcanic hazard than is the actual case in certain regions. The results from the multi-criteria approach are thus a conservative estimation of hazard potential.

The multi-criteria approach allows the incorporation of new datasets into the hazard assessment, if such data should become available. Additional knowledge of individual parameters may be used to further refine the hazard index. During a progressively focused search for repository sites for HLW, datasets that are only locally available and therefore could not be used in the

Germany-wide hazard assessments can now be used in a regional application of the multi-criteria approach to further improve the assessment results. Moreover, the use of regional scale geophysical datasets or geological maps with higher resolution and (or) a higher degree of precision is recommended when focusing the search for a repository site for HLW on smaller regions.

The indicators used and their assigned parameters can only provide information about areas with a higher relative potential for future extrusive or near-surface intrusive magmatic activity over the timescale of long-term geodynamic and magmatic processes in Earth's mantle and crust (thousands to millions of years). The long-term processes include plate tectonic movements within Europe, which will lead to uplift, tectonic faults, crustal extension, subsidence, earthquakes, and magmatic activity. Similarly, mantle convection and smaller mantle upwellings (plumes, diapirs, and compensatory upwellings at plate boundaries) occur slowly compared to the million-year timeframe required for a safe repository for HLW. Decompression in Earth's mantle has led, and will probably continue to lead, to the formation of partial melts, from which magmas can develop and rise to Earth's surface. Examining the age data of the volcanic fields in Germany reveals that, during the Cenozoic era, volcanic activity was sometimes very long-lasting, but there was also renewed activity after periods of dormancy lasting several million years (Rummel and others, 2021b). Therefore, a resurgence of volcanism cannot be ruled out in the future. Thus, although the multi-criteria approach cannot be used to quantify the absolute probability or timing of a future volcanic eruption, the results can indicate the relative potential for future igneous activity over the long term.

Transferability of the Multi-Criteria Approach to Other Regions

The multi-criteria approach presented here is, in principle, applicable for the hazard assessment of long-term (over the next 1 m.y.) near-surface igneous activity related to distributed volcanic fields in general. A crucial requirement is the availability of data with high quality and resolution that describe individual parameters relevant to potential future magmatic activity. Depending on the available data, some parameters might be treated differently with respect to data processing in the assessments of other areas; for example, other indicators might be extended by additional parameters, or existing parameters could be quantified more precisely. Additionally, applying the multi-criteria approach to other regions requires enough parameters (meaning that the inclusion or omission of a single parameter should not have a significant effect on the results) to be considered in the index value determination and that each of the different process categories (table 1.2) is represented by multiple parameters. Although such an index approach can be adapted to other magmatic provinces, the underlying data will always be different. As index maps are produced for specific regions and normalized to a uniform standard scale, however, the results for the relative potential of future igneous activity can provide important insights into potential future volcanic hazards. Using the index approach presented here allows for the rough differentiation of regions in terms of their relative potential of future igneous activity, and easily adapted threshold values can be used for the spatial demarcation of hazard potential. However, the multi-criteria approach should primarily be regarded as a semi-quantitative opportunity to indicate a relative potential of possible future igneous activity on a long-term scale (for instance, over the next 1 m.y.). The multi-criteria approach is not a substitute for existing quantitative probability analyses of volcanic hazard in Quaternary volcanic fields (Weller and others, 2006; Connor and others, 2009; IAEA, 2016; Marrero and others, 2019; Ang and others, 2020), rather a supplementary means of extending such assessments or providing insights in the absence of such assessments.

Application of the multi-criteria approach in recently active intraplate volcanic settings could help constrain indicators and parameters that might be critical for forecasting volcanic or igneous activity, assuming equal threshold values and normalized scales for individual parameters. Comparisons of different fields might reveal indicators of particular importance for forecasts. This knowledge would facilitate decisions about the applicability and further development of the multi-criteria approach described here.

Summary and Conclusion

A semi-quantitative, multi-criteria approach is presented that can be used for a spatial differentiation of the relative potential for future igneous activity in Germany during the next 1 million years (m.y.). Various geoscientific indicators thought to provide information about recent or possible future processes connected to magmatic activity are evaluated using 20 quantifiable parameters. Different strategies to define values of relevance are described for the parameters applied. Thresholds are established for each parameter using statistical distribution of data, specific levels of significance given in the literature, or the sole existence of a parameter itself (appendix 1, table 1.1). Data collected with geophysical or geodetic methods, as well as results from numerical simulations, are mostly available for the whole of Germany and can therefore be converted directly into a uniform standard scale of relevance, but other datasets are more spatially limited, forming selective clusters or point data. For spatially limited datasets, underlying large-scale processes that might affect a much larger area than the available data and their assigned uncertainty zones represent, are considered by applying additional buffer zones around areas of different shapes, across which the values of relevance linearly decrease. The combination of all parameters results in a multi-criteria index that presents the relative potential for future igneous activity in Germany over the next 1 m.y.

Four different approaches are presented for evaluating all criteria, with the difference between approaches being due to the weighting factors for individual parameters. In approach 1, the respective parameters are weighted using the relevance for the indicators obtained from expert surveys. A disproportional weighting of specific processes for which many quantifiable parameters are available is avoided in approaches 2 and 3 by utilizing standardized weighting factors within process

categories. The results of approach 3, used for the final hazard assessment, show that the highest relative potential for future igneous activity in Germany exists in the Eifel region, followed by the Siebengebirge, the area of the northeastern Hunsrück and western Taunus, the Rhine-Main lowlands, the Hessian Depression, the Vogelsberg, the Upper Palatinate, the southern Upper Rhine Graben, and the Hegau. Further areas with relatively lower index values are in the southern Vogtland, in the Rhön, in the region of the Heldburger Gangschar, and around Bad Urach. The results of this analysis can help to identify potential locations of a high-level radioactive waste (HLW) repository, as opposed to a more arbitrary assessment; for example, where only regions with Quaternary volcanism (like the Eifel region) are excluded. The results of all approaches indicate that igneous activity during the next 1 m.y. may have the potential to occur in regions that have not been locations of Cenozoic volcanism. Low index values, indicating a low but not zero chance of igneous activity in the next 1 m.y., are present throughout Germany, reflecting the uncertainties in understanding the magmatic and geodynamic processes leading to intraplate volcanism. Accordingly, an absolute exclusion of volcanic activity within the next 1 m.y. is probably not possible anywhere in Germany.

The sensitivity of the model results with regard to different weighting factors is tested using statistical approach 4 in which the individual parameter values are weighted randomly with 100 possible realizations within each process category when calculating the index. The tests reveal only minor differences in the resulting index distribution when compared to those of approach 2 and approach 3.

To estimate the relative hazard potential for future igneous activity, a spatial distribution of continuous index values is recommended (fig. 8). The results of the semi-quantitative, multi-criteria approach form an objective basis for a comprehensive (equal and transparent) assessment of areas with elevated potential for future igneous activity in Germany. This multi-criteria approach can thus be used in the geoscientific long-term evaluation of possible repository sites for HLW.

References Cited

Abratis, M., Mädler, J., Hautmann, S., Leyk, H.-J., Meyer, R., Lippolt, H., and Viereck-Götte, L., 2007, Two distinct Miocene age ranges of basaltic rocks from the Rhön and Heldburg areas (Germany) based on $^{40}Ar/^{39}Ar$ step heating data: Chemie der Erde, v. 67, no. 2, p. 133–150, https://doi.org/10.1016/j.chemer.2006.03.003.

Abratis, M., Viereck, L., Pfänder, J., and Hentschel, R., 2015, Geochemical composition, petrography and $^{40}Ar/^{39}Ar$ age of the Heldburg phonolite—Implications on magma mixing and mingling: International Journal of Earth Sciences, v. 104, no. 8, p. 2033–2055, https://doi.org/10.1007/s00531-015-1207-x.

Ackerman, L., Špaček, P., Magna, T., Ulrych, J., Svojtka, M., Hegner, E., and Balogh, K., 2013, Alkaline and carbonate-rich melt metasomatism and melting of subcontinental lithospheric mantle—Evidence from mantle xenoliths, NE Bavaria, Bohemian massif: Journal of Petrology, v. 54, no. 12, p. 2597–2633, https://doi.org/10.1093/petrology/egt059.

Ang, P.S., Bebbington, M.S., Lindsay, J.M., and Jenkins, S.F., 2020, From eruption scenarios to probabilistic volcanic hazard analysis—An example of the Auckland volcanic field, New Zealand: Journal of Volcanology and Geothermal Research, v. 397, no. 106871, p. 106871, at https://doi.org/10.1016/j.jvolgeores.2020.106871.

Baranyi, I., Lippolt, H.J., and Todt, W., 1976, K-Ar Altersbestimmungen an tertiären Vulkaniten des Oberrheingraben-Gebietes—II. Die Alterstraverse vom Hegau nach Lothringen [Potassium-Argon age determinations on Tertiary volcanites of the Upper Rhine Graben region: II. The age traverse from Hegau to Lorraine]: Oberrheinische Geologische Abhandlungen, v. 25, p. 41–62.

Barsotti, S., Parks, M.M., Pfeffer, M.A., Óladóttir, B.A., Barnie, T., Titos, M.M., Jónsdóttir, K., Pedersen, G.B., Hjartardóttir, Á.R., Stefansdóttir, G., Johannsson, T., Arason, Þ., Gudmundsson, M.T., Oddsson, B., Þrastarson, R.H., Ófeigsson, B.G., Vogfjörd, K., Geirsson, H., Hjörvar, T., von Löwis, S., Petersen, G.N., and Sigurðsson, E.M., 2023, The eruption in Fagradalsfjall (2021, Iceland)—How the operational monitoring and the volcanic hazard assessment contributed to its safe access: Natural Hazards, v. 116, no. 3, p. 3063–3092, https://doi.org/10.1007/s11069-022-05798-7.

Bartels, A., Rummel, L., and May, F., 2020, Dokumentation und Auswertung einer Expertenbefragung zur langfristigen Vorhersage vulkanischer Aktivität in Deutschland [Documentation and evaluation of an expert survey on the long-term forecast of volcanic activity in Germany]: Hannover, Germany, Bundesanstalt für Geowissenschaften und Rohstoffe (BGR), 104 p.

Bartels, A., Rummel, L., and May, F., 2022, Quantifizierung von Indikatoren für die Prognose einer vulkanischen Aktivität in Deutschland [Quantification of indicators to forecast volcanic activity in Germany]: Hannover, Germany, Bundesanstalt für Geowissenschaften und Rohstoffe (BGR), 167 p.

Bartolini, S., Bolós, X., Martí, J., Pedra, E.R., and Planagumà, L., 2015, Hazard assessment at the quaternary La Garrotxa volcanic field (NE Iberia): Natural Hazards, v. 78, no. 2, p. 1349–1367, https://doi.org/10.1007/s11069-015-1774-y.

Bundesgesellschaft für Endlagerung [BGE], 2020, Zwischenbericht Teilgebiete gemäß § 13 StandAG [Sub-areas Interim Report pursuant to Section 13 StandAG]: Peine, Germany, Bundesgesellschaft für Endlagerung mbH, 444 p., accessed December 12, 2025, at https://www.bge.de/fileadmin/user_upload/Standortsuche/Wesentliche_Unterlagen/Zwischenbericht_Teilgebiete/Zwischenbericht_Teilgebiete_barrierefrei.pdf.

Bundesgesellschaft für Endlagerung [BGE], 2022a, Konzept zur Durchführung der repräsentativen vorläufigen Sicherheitsuntersuchungen gemäß Endlagersicherheitsuntersuchungsverordnung [Concept for conducting the representative preliminary safety assessments in accordance with the final repository safety investigation ordinance]: Peine, Germany, Bundesgesellschaft für Endlagerung mbH, 62 p., accessed December 12, 2025, at https://www.bge.de/fileadmin/user_upload/Standortsuche/Wesentliche_Unterlagen/Methodik/Phase_I_Schritt_2/rvSU-Methodik/20220328_Konzept_zur_Durchfuehrung_der_rvSU_barrierefrei.pdf.

Bundesgesellschaft für Endlagerung [BGE], 2022b, Methodenbeschreibung zur Durchführung der repräsentativen vorläufigen Sicherheitsuntersuchungen gemäß Endlagersicherheitsuntersuchungsverordnung [Method description for conducting the representative preliminary safety assessments in accordance with the final repository safety investigation ordinance]: Peine, Germany, Bundesgesellschaft für Endlagerung mbH, 744 p., accessed December 12, 2025, at https://www.base.bund.de/shareddocs/ip6/base/de/20220328_Methodenpapier_rvSU.html.

Bundesanstalt für Geowissenschaften und Rohstoffe [BGR], 2019, Geologische Übersichtskarte der Bundesrepublik Deutschland (GÜK250) [Geological overview of the Federal Republic of Germany]: BGR interactive map, accessed December 12, 2025, at https://geoportal.bgr.de/mapapps/resources/apps/geoportal/index.html?lang=en#/datasets/portal/f1780a06-69b6-44b0-855e-dc0f8da9a1d4.

Binder, T., Marks, M.A., Gerdes, A., Walter, B.F., Grimmer, J., Beranoaguirre, A., Wenzel, T., and Markl, G., 2022, Two distinct age groups of melilitites, foidites, and basanites from the southern Central European volcanic province reflect lithospheric heterogeneity: International Journal of Earth Sciences, v. 112, no. 3, p. 881–905, https://doi.org/10.1007/s00531-022-02278-y.

van den Bogaard, P., Wörner, G., and Henjes-Kunst, F., 2001, Chemical stratigraphy and origin of volcanic rocks from the drill-core "Forschungsbohrung Vogelsberg 1996": Geologische Abhandlungen Hessen, v. 107, p. 69–99.

Brauer, A., Endres, C., Zolitschka, B., and Negendank, J.F.W., 2000, AMS radiocarbon and varve chronology from the annually laminated sediment record of Lake Meerfelder maar, Germany: Radiocarbon, v. 42, no. 3, p. 355–368, https://doi.org/10.1017/S0033822200030307.

Büchner, J., Tietz, O., Viereck, L., Suhr, P., Abratis, M., and van den Bogaard, P., 2015, Volcanology, geochemistry and age of the Lausitz volcanic field: International Journal of Earth Sciences, v. 104, no. 8, p. 2057–2083, at https://doi.org/10.1007/s00531-015-1165-3.

Carlino, S., 2019, Correction to: Neapolitan Volcanoes—A Trip Around Vesuvius, Campi Flegrei and Ischia: Cham, Germany, Springer International Publishing, 312 p. https://doi.org/10.1007/978-3-319-92877-7.

Connor, C.B., Chapman, N.A., and Connor, L.J. [eds.], 2009, Volcanic and tectonic hazard assessment for nuclear facilities: Cambridge, United Kingdom, Cambridge University Press, 655 p., https://doi.org/10.1017/CBO9780511635380.

Connor, C.B., Connor, L.J., Germa, A., Richardson, J.A., Bebbington, M.S., Gallant, E., and Saballos, A., 2019, How to use kernel density estimation as a diagnostic and forecasting tool for distributed volcanic vents: Statistics in Volcanology, v. 4, no. 1, p. 1–25, https://doi.org/10.5038/2163-338X.4.3.

Connor, C.B., McBirney, A.R., and Furlan, C., 2006, What is the probability of explosive eruption at a long-dormant volcano? *in* Coles, C.B., Connor, C.B., Connor, L.J., and Mader, H.M., eds., Statistics in Volcanology: London, United Kingdom, Geological Society of London, p. 39–46, https://doi.org/10.1144/IAVCEI001.4.

De Smith, M.J., Goodchild, M.F., and Longley, P., 2007, Geospatial analysis—A comprehensive guide to principles, techniques and software tools—Market Harborough: United Kingdom, Troubador Publishing, 394 p.

Deligne, N.I., Jolly, G.E., Taig, T., and Webb, T.H., 2018, Evaluating life-safety risk for fieldwork on active volcanoes—The volcano life risk estimator (VoLREst), a volcano observatory's decision-support tool: Journal of Applied Volcanology, v. 7, no. 1, 19 p., https://doi.org/10.1186/s13617-018-0076-y.

Eckel, F., Langer, H., and Sciotto, M., 2023, Monitoring sources of volcanic activity at Mount Etna using pattern recognition techniques on infrasound signals: Geophysical Journal International, v. 232, no. 1, p. 1–16, https://doi.org/10.1093/gji/ggac278.

El Difrawy, M., Runge, M., Moufti, M., Cronin, S., and Bebbington, M., 2013, A first hazard analysis of the Quaternary Harrat Al-Madinah volcanic field, Saudi Arabia: Journal of Volcanology and Geothermal Research, v. 267, p. 39–46, https://doi.org/10.1016/j.jvolgeores.2013.09.006.

Fekiacova, Z., Mertz, D.F., and Renne, P.R., 2007, Geodynamic Setting of the Tertiary Hocheifel Volcanism (Germany), Part I—$^{40}Ar/^{39}Ar$ geochronology, *in* Ritter, J.R.R., and Christensen, U.R., eds., Mantle Plumes—A Multidisciplinary Approach: Berlin, Heidelberg, Springer Berlin Heidelberg, p. 185–206, https://doi.org/10.1007/978-3-540-68046-8_6.

Fichtner, A., van Herwaarden, D.P., Afanasiev, M., Simutė, S., Krischer, L., Çubuk-Sabuncu, Y., Taymaz, T., Colli, L., Saygin, E., Villaseñor, A., Trampert, J., Cupillard, P., Bunge, H.-P., and Igel, H., 2018, The collaborative seismic earth model—Generation 1: Geophysical Research Letters, v. 45, no. 9, p. 4007–4016, https://doi.org/10.1029/2018GL077338.

Galindo Jiménez, I., Romero Ruíz, M.C., Sánchez Jiménez, M.N., and Morales de Francisco, J.M., 2016, Quantitative volcanic susceptibility analysis of Lanzarote and Chinijo Islands based on kernel density estimation via a linear diffusion process: Scientific Reports, v. 6, no. 27381, 10 p.

Germa, A., Connor, L.J., Cañon-Tapia, E., and Le Corvec, N., 2013, Tectonic and magmatic controls on the location of post-subduction monogenetic volcanoes in Baja California, Mexico, revealed through spatial analysis of eruptive vents: Bulletin of Volcanology, v. 75, no. 782, p. 1–14, https://doi.org/10.1007/s00445-013-0782-6.

Häder, M., 2009, Delphi-Befragungen—Ein Arbeitsbuch [Delphi surveys—A workbook]: Wiesbaden, Springer VS Wiesbaden, 221 p., https://doi.org/10.1007/978-3-531-91926-3.

Horn, P., Lippolt, H.J., and Todt, W., 1972, Kalium-Argon-Altersbestimmungen an tertiären Vulkaniten des Oberrheingrabens—I. Gesamtgesteinsalter [Potassium-argon age determinations on Tertiary volcanites of the Upper Rhine Graben: I. Total rock age]: Eclogae Geologicae Helvetiae, v. 65, no. 1, p. 131–156.

van den Hove, J., Grose, L., Betts, P.G., Ailleres, L., Van Otterloo, J., and Cas, R.A., 2017, Spatial analysis of an intra-plate basaltic volcanic field in a compressional tectonic setting—South-eastern Australia: Journal of Volcanology and Geothermal Research, v. 335, p. 35–53, https://doi.org/10.1016/j.jvolgeores.2017.02.001.

International Atomic Energy Agency [IAEA], 2012, Volcanic Hazards in Site Evaluation for Nuclear Installations: Vienna, International Atomic Energy Agency, 106 p., accessed December 2025, at https://www.iaea.org/publications/8774/volcanic-hazards-in-site-evaluation-for-nuclear-installations.

International Atomic Energy Agency [IAEA], 2016, Volcanic Hazard Assessments for Nuclear Installations—Methods and Examples in Site Evaluation: Vienna, International Atomic Energy Agency, 261 p., accessed December 2025, at https://www-pub.iaea.org/MTCD/Publications/PDF/TE1795web.pdf.

Jenks, G.F., and Caspall, F.C., 1971, Error on choroplethic maps—Definition, measurement, reduction: Annals of the Association of American Geographers, v. 61, no. 2, p. 217–244, https://doi.org/10.1111/j.1467-8306.1971.tb00779.x.

Jentzsch, G., 2001, Vulkanische Gefährdung in Deutschland—Entwicklung eines Kriteriums zum Ausschluss von Gebieten für die weitere Untersuchung hinsichtlich der Eignung als Standort eines Endlagers für radioaktive Abfälle [Volcanic hazards in Germany—Development of criteria for excluding areas from further investigation regarding their suitability as sites for a final repository for radioactive waste]: Prepared on behalf of the working group 'Kriterienentwicklung' (AG-Krit) of the working committee 'Auswahlverfahren Endlagerstandorte' (AKEnd) of the Federal Ministry for Environment, Nature Conservation, and Nuclear Safety (Germany), 48 p.

Jentzsch, G., 2013, Ausarbeitung Vulkanische Gefährdung in Sachsen [Preparation Volcanic hazard in Saxony]: Unpublished expert opinion for the Saxon State Office for Environment, Agriculture, and Geology, 35 p.

Kröchert, J., Schmieder, M., Theye, T., and Buchner, E., 2009, Das Alter und die Dauer der vulkanischen Aktivität im Urach-Kirchheimer Vulkangebiet (SW-Deutschland) [The age and duration of volcanic activity in the Urach-Kirchheim volcanic area (SW-Germany)]: Zeitschrift der Deutschen Gesellschaft für Geowissenschaften, v. 160, no. 4, p. 325–331.

Leder, J., Wenzel, F., Daniell, J.E., and Gottschämmer, E., 2017, Loss of residential buildings in the event of a re-awakening of the Laacher See Volcano (Germany): Journal of Volcanology and Geothermal Research, v. 337, p. 111–123, https://doi.org/10.1016/j.jvolgeores.2017.02.019.

Lippolt, H.J., 1976, Das pliozäne Alter der Bertenauer Basalte/Westerwald [The Pliocene age of the Bertenau basalts/Westerwald]: Der Aufschluss, v. 27, p. 205–208.

Lippolt, H.J., 1983, Distribution of volcanic activity in space and time, *in* Fuchs, K., von Gehlen, K., Mälzer, H., Murawski, H., and Semmel, A., eds., Plateau Uplift, p. 112–120.

Lippolt, H.J., Gentner, W., and Wimmenauer, W., 1963, Altersbestimmungen nach der Kalium-Argon-Methode an tertiären Eruptivgesteinen Südwestdeutschlands [Age determinations using the potassium-argon method on Tertiary igneous rocks of southwest Germany]: Jahresheft der geologischen Landesanstalt Baden-Württemberg, v. 6, p. 507–538.

Lippolt, H.J., and Todt, W., 1978, Isotopische Altersbestimmungen an Vulkaniten des Westerwaldes [Isotopic dating of volcanic rocks from the Westerwald]: Neues Jahrbuch für Geologie und Paläontologie, v. 1978, no. 6, p. 332–352.

Lorenz, V., 2007, Syn-and posteruptive hazards of maar–diatreme volcanoes: Journal of Volcanology and Geothermal Research, v. 159, nos. 1-3, p. 285–312, https://doi.org/10.1016/j.jvolgeores.2006.02.015.

Marrero, J.M., García, A., Berrocoso, M., Llinares, Á., Rodríguez-Losada, A., and Ortiz, R., 2019, Strategies for the development of volcanic hazard maps in monogenetic volcanic fields—The example of La Palma (Canary Islands): Journal of Applied Volcanology, v. 8, no. 6, p. 1–21, https://doi.org/10.1186/s13617-019-0085-5.

Martha, S.O., Zulauf, G., Dörr, W., Nesbor, H.-D., Petschick, R., Prinz-Grimm, P., and Gerdes, A., 2014, The Saxothuringian-Rhenohercynian boundary underneath the Vogelsberg volcanic field—Evidence from basement xenoliths and U-Pb zircon data of trachyte: Zeitschrift der Deutschen Gesellschaft für Geowissenschaften, v. 165, no. 3, p. 373–394, https://doi.org/10.1127/1860-1804/2014/0079.

May, F., 2019, Möglichkeiten der Prognose zukünftiger vulkanischer Aktivität in Deutschland [Possibility of prediction of volcanic activity in Germany]: Hannover, Germany, Bundesanstalt für Geowissenschaften und Rohstoffe (BGR), 87 p.

Mazzarini, F., Le Corvec, N., Isola, I., and Favalli, M., 2016, Volcanic field elongation, vent distribution, and tectonic evolution of a continental rift—The Main Ethiopian Rift example: Geosphere, v. 12, no. 3, p. 706–720, https://doi.org/10.1130/GES01193.1.

Molloy, C., Shane, P., and Augustinus, P., 2009, Eruption recurrence rates in a basaltic volcanic field based on tephra layers in maar sediments—Implications for hazards in the Auckland volcanic field: Geological Society of America Bulletin, v. 121, nos. 11–12, p. 1666–1677, https://doi.org/10.1130/B26447.1.

Nesbor, H.-D., 2018, Das Vulkangebiet Vogelsberg [The Vogelsberg volcanic region]: Geologisches Jahrbuch Hessen, v. 139, p. 5–41.

O'Reilly, S.Y., and Griffin, W., 2010, Rates of magma ascent—Constraints from mantle-derived xenoliths, chap. 6 of Dosseto, A., Turner, S., and Van Orman, J., eds., Timescales of magmatic processes, from core to atmosphere: Blackwell Publishing, 255 p. https://doi.org/10.1002/9781444328509.ch6

Park, C., and Schmincke, H.-U., 1997, Lake formation and catastrophic dam burst during the Late Pleistocene Laacher See eruption (Germany): Die Naturwissenschaften, v. 84, no. 12, p. 521–525, https://doi.org/10.1007/s001140050438.

Passarelli, L., and Brodsky, E.E., 2012, The correlation between run-up and repose times of volcanic eruptions: Geophysical Journal International, v. 188, no. 3, p. 1025–1045, https://doi.org/10.1111/j.1365-246X.2011.05298.x.

Pfänder, J.A., Jung, S., Klügel, A., Münker, C., Romer, R.L., Sperner, B., and Rohrmüller, J., 2018, Recurrent local melting of metasomatised lithospheric mantle in response to continental rifting—Constraints from basanites and nephelinites/melilitites from SE Germany: Journal of Petrology, v. 59, no. 4, p. 667–694, https://doi.org/10.1093/petrology/egy041.

Przybyla, T., Pfänder, J., Münker, C., Kolb, M., Becker, M., and Hamacher, U., 2017, High-resolution $^{40}Ar/^{39}Ar$ geochronology of volcanic rocks from the Siebengebirge (Central Germany)—Implications for eruption timescales and petrogenetic evolution of intraplate volcanic fields: International Journal of Earth Sciences, v. 107, no. 4, p. 1465–1484, https://doi.org/10.1007/s00531-017-1553-y.

Rahn, M., and Handt, A., 2013, Tracing the time-resolved magmatic evolution of the Hegau volcanic field (Southern Germany) through apatites [abs.], *in* Goldschmidt Conference, 23rd, Florence, Italy, August 25–30, 2013, p. 2020.

Rout, S.S., and Wörner, G., 2020, Constraints on the pre-eruptive magmatic history of the Quaternary Laacher See volcano (Germany): Contributions to Mineralogy and Petrology, v. 175, no. 73, 22 p., https://doi.org/10.1007/s00410-020-01710-3.

Rummel, L., Bartels, A., and May, F., 2021a, Dokumentation und Auswertung einer zweiten Expertenbefragung zur langfristigen Vorhersage vulkanischer Aktivität in Deutschland [Documentation and evaluation of a second expert survey on the long-term forecast of volcanic activity in Germany]: Hannover, Germany, Bundesanstalt für Geowissenschaften und Rohstoffe, 73 p.

Rummel, L., Bartels, A., and May, F., 2021b, Känozoischer Vulkanismus in Deutschland - Stand der Forschung zur Geodynamik und Magmengenese [Cenozoic volcanism in Germany – state of research for geodynamics and magma genesis]: Hannover, Germany, Bundesanstalt für Geowissenschaften und Rohstoffe, 361 p.

Rummel, L., Bartels, A., and May, F., 2023, Deutschlandweite Anwendung eines multikriteriellen Ansatzes zur räumlichen Differenzierung von Wahrscheinlichkeiten eines zukünftig möglichen Vulkanismus [Germany-wide application of a multi-criteria approach for spatial differentiation of the likelihood of possible future volcanism]: Hannover, Germany, Bundesanstalt für Geowissenschaften und Rohstoffe, 113 p.

Schmid, R., Franz, L., Rahn, M., Gautheron, C., and Capitani, C., 2014, Petrography and geochronology of phonolites of the Hegau volcanic field, SW Germany, *in* 12th Swiss Geoscience Meeting 2014, Fribourg, p. 114–115.

Schmincke, H.-U., 2014, Vulkane der Eifel: Heidelberg, Springer Berlin, 161 p., https://doi.org/10.1007/978-3-8274-2985-8

Schmitt, A.K., Marks, M.A., Nesbor, H.D., and Markl, G., 2007, The onset and origin of differentiated Rhine Graben volcanism based on U-Pb ages and oxygen isotopic composition of zircon: European Journal of Mineralogy, v. 19, no. 6, p. 849–857, https://doi.org/10.1127/0935-1221/2007/0019-1776.

Schreiber, U., and Jentzsch, G., 2021, Vulkanische Gefährdung in Deutschland—Bewertung möglicher vulkanischer Aktivitäten der nächsten 1 Million Jahre in Deutschland inklusive Festlegung der Gebiete mit einer Eintrittswahrscheinlichkeit in diesem Zeitraum [Volcanic hazard in Germany—Assessment of possible volcanic activities in Germany over the next 1 million years, including the definition of areas with a probability of occurance during this period]: Bonn, Germany, Bundesgesellschaft für Endlagerung, 132 p.

Silverman, B.W., 1986, Density estimation for statistics and data analysis: Bath, United Kingdom, CRC press, 22 p.

Sparks, R., Annen, C., Blundy, J., Cashman, K., Rust, A., and Jackson, M., 2019, Formation and dynamics of magma reservoirs: Philosophical Transactions of the Royal Society A, v. 377, no. 2139, 42 p.

Todt, W., and Lippolt, H.J., 1975, K-Ar-Altersbestimmungen an Vulkaniten bekannter paläomagnetischer Feldrichtung—I. Oberpfalz und Oberfranken [K-Ar dating of volcanic rocks with known paleomagnetic field directions: I. Upper Palatinate and Upper Franconia]: Journal of Geophysics, v. 41, p. 43–61.

Turk, P.G., Lohse, H.H., Schürmann, K., Fuhrmann, U., and Lippolt, H.J., 1984, Petrographische und Kalium-Argon-Untersuchungen an basischen tertiären Vulkaniten zwischen Westerwald und Vogelsberg [Petrographic and potassium-argon investigations on basic Tertiary volcanites between Westerwald and Vogelsberg]: Geologische Rundschau, v. 73, no. 2, p. 599–617, https://doi.org/10.1007/BF01824974.

Ubide, T., and Kamber, B.S., 2018, Volcanic crystals as time capsules of eruption history: Nature Communications, v. 9, no. 326, p. 326, https://doi.org/10.1038/s41467-017-02274-w.

Wedepohl, K.H., Gohn, E., and Hartmann, G., 1994, Cenozoic alkali basaltic magmas of western Germany and their products of differentiation: Contributions to Mineralogy and Petrology, v. 115, no. 3, p. 253–278, https://doi.org/10.1007/BF00310766.

Weiskirchner, W., 1972, Einführung zur Exkursion in den Hegau [Introduction to the excursion to the Hegau]: Fortschritte der Mineralogie, v. 50, p. 70–84.

Weller, J.N., Martin, A.J., Connor, C.B., Connor, L.J., and Karakhanian, A., 2006, Modelling the spatial distribution of volcanoes—An example from Armenia: Statistics in Volcanology, v. 1, p. 77–87, https://doi.org/10.1144/IAVCEI001.7.

Wilson, M., and Downes, H., 2006, Tertiary-Quaternary intra-plate magmatism in Europe and its relationship to mantle dynamics: Geological Society of London, Memoirs, v. 32, no. 1, p. 147–166, at https://doi.org/10.1144/GSL.MEM.2006.032.01.09.

Appendixes 1–2

Appendix 1

The threshold values used to normalize parameters to values of significance as well as the demarcation criteria for each parameter are described in table 1.1. Additionally, the relation that each parameter might have to different kinds of magmatic processes is provided. Although most parameters are not uniquely related to magmatic activity during the next 1 m.y., the presence of values exceeding the thresholds of any single parameter enhances the potential of future igneous activity within the range of this datum.

A semi-quantitative index value for the relative potential of igneous activity in Germany is computed by summing weighted normalized parameter values. The sum of the weighting factors is one. Four different approaches are used to show the sensitivity of the multi-criteria approach. Approach 1 includes results from the expert valuations for the relevance of individual indicators to forecast volcanism (Bartels and others, 2020; Rummel and others, 2021a), approach 2 classifies the parameters into three groups representing different kinds of magmatic or geodynamic processes, and approach 3 represents a combination of approach 1 and approach 2. Approach 4 averages 1,000 statistically determined index maps with randomly weighted parameters and is therefore not listed here. Table 1.2 shows the weighting factors of the individual parameters used for approaches 1, 2, and 3.

Table 1.1. Threshold values, demarcation criteria, and relation to magmatic processes for each of the used parameters.

[He, helium; R/R_A, $^3He/^4He$ ratio (R) in relation to the atmospheric $^3He/^4He$ ratio (R_A); ΔV_S, seismic velocities of secondary waves relative to horizontal mean; %, percent; km, kilometer; ΔV_P, seismic velocities of primary waves relative to horizontal mean; yr^{-1}, per year; mm/yr, millimeter per year; LAB, lithosphere-asthenosphere boundary; mGal, milligal; DLF, deep low frequency; m/s^2, meter per second squared; MPa, megapascal; Moho, Mohorovičić discontinuity; σ_3, minimum principal stress]

Parameter	Threshold [units]	Demarcation criteria	Possible relation of parameter to igneous activity
He isotopes (R/R_A values)	0.1 R/R_A	R/R_A values greater than 0.1 are indicative for a mantle component in the gas phase	Measured R/R_A greater than 0.1 may indicate large-scale magmatic processes in Earth's mantle and pathways for melt ascent to Earth's surface
ΔV_S	−1.2 [%]; −1.9 [%]	Average of negative values of minimum of ΔV_S between 60–90 km depth for two different models, and determined relative to horizontal mean	Negative ΔV_S values are related to higher temperatures or existing fluids/melts that all can promote melt formation
ΔV_P	−0.9 [%]	Average of negative values of minimum of ΔV_P between 60–90 km depth, and determined relative to horizontal mean	Negative ΔV_P values are related to higher temperatures or existing fluids/melts that all can promote melt formation
Uplift	0.23 [mm/yr]	Average of uplift	Hints for uprising mantle material, potential decompression melting
Second invariant of strain rate	$1.84 * 10^{-9}$ [yr^{-1}]	+1σ standard deviation of the second invariant	Hints for uprising mantle material and lithospheric deformation
Dilatational component of strain rate	$0.89 * 10^{-9}$ [yr^{-1}]	Average of positive values (extension) of the dilatational component	Hints for uprising mantle material and lithospheric deformation, potential for opening conduits in the upper crust
Depth of LAB	96 [km]	−1σ standard deviation of the LAB from a region in northern Germany	A shallower LAB indicates elevated mantle temperatures that could promote melt formation
Gravity anomalies in Earth's mantle	−40 [mGal]	Average of negative values from the gravity anomalies	Negative anomalies in Earth's mantle are produced by low density material and thus higher temperatures or existing fluids/melts
Occurrence of DLF-earthquakes (epicenters)	None	Occurrence itself 1 km radius of uncertainty zone for each epicenter 10 km width of surrounding buffer zone	Connected to the ascent of magma or magmatic fluids in the lithosphere

Table 1.1. Threshold values, demarcation criteria, and relation to magmatic processes for each of the used parameters.—Continued

[He, helium; R/R_A, $^3He/^4He$ ratio (R) in relation to the atmospheric $^3He/^4He$ ratio (R_A); ΔV_S, seismic velocities of secondary waves relative to horizontal mean; %, percent; km, kilometer; ΔV_P, seismic velocities of primary waves relative to horizontal mean; yr^{-1}, per year; mm/yr, millimeter per year; LAB, lithosphere-asthenosphere boundary; mGal, milligal; DLF, deep low frequency; m/s^2, meter per second squared; MPa, megapascal; Moho, Mohorovičić discontinuity; σ_3, minimum principal stress]

Parameter	Threshold [units]	Demarcation criteria	Possible relation of parameter to igneous activity
Occurrence of swarm earthquakes (epicenters)	None	Occurrence itself Radius of uncertainty zone surrounding epicenters of individual swarms is proportional to their areal extent 10 km width of surrounding buffer zone	Connected to fluids related to magmatic processes Hints for possible melt pathways in the upper crust
Occurrence of mofettes and bicarbonate water	None	Occurrence itself Processed by kernel density method	Hints for magmatic processes at depth releasing CO_2 and indicating melt pathways to Earth's surface
Seismic hazard areas	1 [m/s^2]	Average of mean spectral response acceleration with a mean return period of 2,475 years	Connected to zones of crustal deformation, where faults could facilitate the ascent of melts
Structures of the European Cenozoic Rift System	None	Occurrence itself 10 km width of surrounding buffer zone	Related to a shallowing of the crust and mantle lithosphere promoting melt formation and ascent Mechanically weakened zone of the crust
Occurrence of sutures and terrane boundaries	None	Occurrence itself 10 km minimum width of uncertainty zone 10 km width of surrounding buffer zone	Possible reactivation of pathways for ascending melts through the lithosphere
Occurrence of deep and large-scale faults	None	Occurrence itself 5 km width of uncertainty zone 1 km width of surrounding buffer zone	Possible pathways for ascending melts through the crust
Magnitude of σ_3	118 [MPa]; 223 [MPa]; 345 [MPa]	Average of σ_3 in 7, 12, and 19 km depth, respectively	The smaller the minor principal stress, the easier it is to open fractures for ascending melts
Critical fluid pressure for fracturing	102 [MPa]; 187 [MPa]; 285 [MPa]	Average of critical fluid pressure in 7, 12, and 19 km depth, respectively	The smaller the needed fluid pressure to generate new fractures, the easier it is to break the rocks
Depth of Moho	31 [km]	Average of the Moho from a region in northern Germany	The shallower the Moho depth, the easier the ascent of melts
Geochronological data of volcanic rocks	None	Available literature data 2.5 km width of uncertainty zone 10 km width of surrounding buffer zone	The presence of Cenozoic volcanism enhances the possibility of future volcanic activity according to the principle of actualism Indicating melt pathways to Earth's surface
Occurrence of igneous rocks	None	Occurrence itself 10 km width of surrounding buffer zone	The presence of Cenozoic volcanic rocks enhances the possibility of future volcanic activity according to the principle of actualism Indicating melt pathways to Earth's surface

Table 1.2. Weighting factors for the different approaches (approach 1–approach 3) to calculate the index values used to forecast igneous activity in Germany.

[He, helium; R/R_A, $^3He/^4He$ ratio (R) in relation to the atmospheric $^3He/^4He$ ratio (R_A); ΔV_S, seismic velocities of secondary waves relative to horizontal mean; ΔV_P, seismic velocities of primary waves relative to horizontal mean; LAB, lithosphere-asthenosphere boundary; DLF, deep low frequency; Moho, Mohorovičić discontinuity; σ_3, minimum principal stress]

Parameter	Approach 1	Approach 2	Approach 3
Possible melt formation in Earth's mantle			
He isotopes (R/R_A values)	0.0565	0.0417	0.0471
ΔV_S	0.0532	0.0417	0.0444
ΔV_P	0.0532	0.0417	0.0444
Uplift	0.0516	0.0417	0.0431
Second invariant of strain rate	0.0516	0.0417	0.0431
Dilatational component of strain rate	0.0516	0.0417	0.0431
Depth of LAB	0.0428	0.0417	0.0357
Gravity anomalies in Earth's mantle	0.0387	0.0417	0.0323
Possible pathways for melts within the lithosphere			
Occurrence of DLF-earthquakes (epicenters)	0.0581	0.0333	0.0395
Occurrence of swarm earthquakes (epicenters)	0.0546	0.0333	0.0371
Occurrence of mofettes and bicarbonate water	0.0519	0.0333	0.0352
Seismic hazard areas	0.0490	0.0333	0.0333
Structures of the European Cenozoic Rift System	0.0490	0.0333	0.0333
Occurrence of sutures and terrane boundaries	0.0475	0.0333	0.0323
Occurrence of deep and large-scale faults	0.0475	0.0333	0.0323
Magnitude of σ_3	0.0451	0.0333	0.0307
Critical fluid pressure for fracturing	0.0451	0.0333	0.0307
Depth of Moho	0.0424	0.0333	0.0288
Igneous surface features			
Geochronological data of volcanic rocks	0.0569	0.1667	0.1711
Occurrence of igneous rocks	0.0538	0.1667	0.1619

Appendix 2

Table 2.1. References of data used to quantify the parameters listed in alphabetical order.

[R/R_A, ^{3}Helium/^{4}Helium ratio (R) in relation to the atmospheric ^{3}Helium/^{4}Helium ratio (R_A); ΔV_S, seismic velocities of secondary waves relative to horizontal mean; ΔV_P, seismic velocities of primary waves relative to horizontal mean; LAB, lithosphere-asthenosphere boundary; DLF, deep low frequency; σ_3, minimum principal stress; Moho, Mohorovičić discontinuity]

Parameter	Data source
Helium isotopes (R/R_A values)	Aeschbach-Hertig and others (1996); Bräuer and others (2008); Bräuer and others (2003); Bräuer and others (2004); Bräuer and others (2007); Bräuer and others (2011); Bräuer and others (2013, 2018); Bräuer and others (2014); Griesshaber and others (1992); Kämpf and others (2007); Kämpf and others (2013); O'Nions and others (1989); Schäffer and others (2021); Ufrecht (2006); Weinlich (1998); Weinlich and others (1999); Weinlich and others (2003)
ΔV_S	Fichtner and others (2018); Zhu and others (2015)
ΔV_P	Zhu and others (2015)
Uplift	Kreemer and others (2020)
Second invariant of strain rate	Kreemer and others (2020)
Dilatational component of strain rate	Kreemer and others (2020)
Depth of LAB	Anikiev and others (2019); Artemieva (2019)
Gravity anomalies in Earth's mantle	Kaban and others (2010)
Occurrence of DLF-earthquakes (epicenters)	Hensch and others (2019); Landeserdbebendienst Rheinland-Pfalz (2022)
Occurrence of swarm earthquakes (epicenters)	Audin and others (2002); Buchholz and others (2013); Buchholz and others (2016); Buchholz and others (2019); Camelbeeck (1993); Dahlheim and others (1997); Dahm and others (2008); Dahm and others (2019); Erdbebendienst Bayern (2021); Fischer and Horálek (2003); Fischer and Michálek (2008); Fischer and others (2014); GeoSphere Austria (2022); Grünthal and others (1990); Hannemann and others (2021); Heinicke and others (2018); Hemmann (2002); Hensch and others (2019); Homuth (2020); Homuth and Rümpker (2017); Horálek and others (1996); Institute of Geophysics of the Czech Academy of Science (2021); Kämpf and others (2019); Korn and others (2008); Kraft and others (2006); LfULG (2021); Neunhöfer and Hemmann (2005); Schwezerischer Erdbebendienst (2022); Skapski (2022); Weber (2012); Weinlich and others (2006); Wirth and others (2000)
Occurrence of mofettes and bicarbonate water	Bräuer and others (2003); Bräuer and others (2007); Bräuer and others (2008); Bräuer and others (2011); Bräuer and others (2018); Carlé (1975); Fassbender (1990); Franzensbad (2020); Giggenbach and others (1991); Griesshaber and others (1992); Kämpf and others (2007); Kämpf and others (2013); Information Centre of the City of Karlovy Vary (2021); Konstantinsbad (2021); Köppen (1987); Langguth and Plum (1984); Mariánské Lázně Tourist Portal (2021); May (2002a); May (2002b); Rogge and Nowag (2018); Schäffer and others (2021); Schloz and Stober (2006); Schöttker (2022); Staatsbad (2022); Weinlich (1998); Weinlich and others (1999); Weinlich and others (2003); Weise and others (2001)
Seismic hazard areas	GFZ Helmholtz-Zentrum Potsdam (2022); Grünthal and others (2018)
Structures of the European Cenozoic Rift System	Bundesanstalt für Geowissenschaften und Rohstoffe (2023); Cajz and others (2004); Dèzes and others (2004); Egli and others (2017); Geluk and others (1994); Grimmer and others (2017); Lang (2007); Meschede (2015); Meyer (2013); Meyer and Stets (2002); Prinz and McCann (2021); Rajchl and others (2009); Reicherter and others (2008); Ring and Bolhar (2020); Rupf and Nitsch (2008); Schneider and Bankwitz (2003); Schreiber and Rotsch (1998); Schulz and others (2013); Sissingh (2003); Sissingh (2006); Stanek and others (2016); Thews (1996); Ziegler and Dèzes (2006)
Occurrence of sutures and terrane boundaries	Babuška and others (2010); Babuška and Plomerová (2013); Berthelsen (1992); Blundell and others (1992); Brandes and others (2019); Franke (2014); Franke and Hoffmann (1999); Hann and others (2003); Hetényi and others (2018); Huth and Zedler (2019); Lyngsie and Thybo (2007); Maystrenko and others (2008); Maystrenko and Scheck-Wenderoth (2013); Meschede (2015); Müller and others (2019); Pharaoh (1999); Reinhold (2005); Scheck and others (2002); Schmid and others (2004); Shaw and Johnston (2016); Sintubin and others (2009); Smit and others (2016); The PACE TMR Network Team and Winchester (2002)
Occurrence of deep and large-scale faults	Agemar and others (2014a); Agemar and others (2014b); Agemar and others (2016); Decker and others (1994); Dehner and others (2015); DEKORP-Research-Group and others (1991); Egger (1997); Freudenberger and Schwerd (1996); Frisch and Kockel (2004); Kley and others (2008); Kockel (1998); LfULG (2022); Meyer and Stets (2000); Oncken and others (2000); Reinhold (2005); Ribbert (2010); Ribbert (2012); Scheck and others (2002); Schulz and others (2013); Thews (1996); Wrede (2017)

Table 2.1. References of data used to quantify the parameters.—Continued

[R/R_A, ^{3}Helium/^{4}Helium ratio (R) in relation to the atmospheric ^{3}Helium/^{4}Helium ratio (R_A); ΔV_S, seismic velocities of secondary waves relative to horizontal mean; ΔV_P, seismic velocities of primary waves relative to horizontal mean; LAB, lithosphere-asthenosphere boundary; DLF, deep low frequency; σ_3, minimum principal stress; Moho, Mohorovičić discontinuity]

Parameter	Data source
Magnitude of σ_3	Ahlers and others (2022)
Critical fluid pressure for fracturing	Ahlers and others (2022)
Depth of Moho	Anikiev and others (2019); Grad and others (2009); Molinari and Morelli (2011); Tesauro and others (2008);
Geochronological data of volcanic rocks	Abratis and others (2007); Abratis and others (2015); Ackerman and others (2007); Ackerman and others (2013); Alibert and others (1987); Bednarz and Schmincke (1990); Binder and others (2022); Birkenmajer and Pécskay (2002); Birkenmajer and others (2002a, 2002b, 2004, 2007, 2011); Blanchard (unpub. data, 2002); Bogaard (2000); van den Bogaard and others (1989); van den Bogaard and others (1987); van den Bogaard and others (2001); Brauer and others (2000); Büchel and Lorenz (1982); Büchner and others (2015); Cajz and others (2012); Cantarel and Lippolt (1977); Dersch-Hansmann and others (1999); Fekiacova and others (2007); Förster and Sirocko (2016); Frechen and Lippolt (1965); Frechen and Vieten (1970); Frechen and others (1999); Friedrich and others (1999); Fuhrmann (1983); Fuhrmann and Lippolt (1985); Fuhrmann and Lippolt (1986, 1987a); Fuhrmann and Lippolt (1987b); Gögen and Wagner (2000); Hajdas and others (1995); Hofbauer (2007); Horn and others (1972); Kaiser and Pilot (1986); Keller (2001); Keller and others (2002); Kraml and others (1995); Kraml and others (1999); Kreuzer (1973); Kröchert and others (2009); Lenz and others (2015); Leyk and Lippolt (1999); Linthout and others (2009); Lippolt (1961, 1974, 1976, 1983); Lippolt and Fuhrmann (1980); Lippolt and Todt (1978); Lorenz (1978); Lorenz and Büchel (1980); Lustrino and Wilson (2007); Mertes and Schmincke (1983); Mertz and others (2000); Mertz and others (2015); Mertz and Renne (2005); Meyer (2013); Mrlina and others (2007); Müller-Sohnius and Huckenholz (1989); Negendank and others (1990); Nesbor (2018); Paulick and others (2008); Pécskay and others (2009); Pfänder and others (2018); Preusser and others (2011); Przybyla and others (2017); Reinig and others (2021); Rohrmüller and others (2017); Schaber and Sirocko (2005); Schleicher (1986); Schmid and others (2014); Schmidt and others (2017); Schmincke and Mertes (1979); Schmitt and others (2007); Schnepp (1996); Schnepp and Hradetzky (1994); Schubert and others (2015); Schweigert (1990); Shrbený and Vokurka (unpub. data, 1985); Sibrava and Havlicek (1980); Singer and others (2008); Stanek and others (2003); Todt and Lippolt (1975a, 1975b, 1980); Turk and others (1984); Ulrych and others (2002); Ulrych and others (2003); Ulrych and others (2006); Ulrych and others (2008); Ulrych and others (2013); Viereck (1983); Wagner (1976); Wagner and others (2002); Wedepohl (1982); Wilson and others (1994); Wimmenauer (2003); Woda and others (2001); Zirkler and others (2021); Zolitschka (1998); Zolitschka and others (1995); Zöller (1991); Zöller and Blanchard (2009)
Occurrence of igneous rocks	Bundesanstalt für Geowissenschaften und Rohstoffe (2023)

References Cited

Abratis, M., Mädler, J., Hautmann, S., Leyk, H.-J., Meyer, R., Lippolt, H., and Viereck- Götte, L., 2007, Two distinct Miocene age ranges of basaltic rocks from the Rhön and Heldburg areas (Germany) based on $^{40}Ar/^{39}Ar$ step heating data: Chemie der Erde—Geochemistry, v. 67, no. 2, p. 133–150, https://doi.org/10.1016/j.chemer.2006.03.003.

Abratis, M., Viereck, L., Pfänder, J., and Hentschel, R., 2015, Geochemical composition, petrography and $^{40}Ar/^{39}Ar$ age of the Heldburg phonolite—Implications on magma mixing and mingling: International Journal of Earth Sciences, v. 104, no. 8, p. 2033–2055, https://doi.org/10.1007/s00531-015-1207-x.

Ackerman, L., Mahlen, N., Jelínek, E., Medaris, G., Ulrych, J., Strnad, L., and Mihaljevič, M., 2007, Geochemistry and evolution of subcontinental lithospheric mantle in Central Europe—Evidence from peridotite xenoliths of the Kozákov volcano, Czech Republic: Journal of Petrology, v. 48, no. 12, p. 2235–2260, https://doi.org/10.1093/petrology/egm058.

Ackerman, L., Špaček, P., Magna, T., Ulrych, J., Svojtka, M., Hegner, E., and Balogh, K., 2013, Alkaline and carbonate-rich melt metasomatism and melting of subcontinental lithospheric mantle—Evidence from mantle xenoliths, NE Bavaria, Bohemian Massif: Journal of Petrology, v. 54, no. 12, p. 2597–2633, https://doi.org/10.1093/petrology/egt059.

Aeschbach-Hertig, W., Kipfer, R., Hofer, M., Imboden, D.M., Wieler, R., and Signer, P., 1996, Quantification of gas fluxes from the subcontinental mantle—The example of Laacher See, a maar lake in Germany: Geochimica et Cosmochimica Acta, v. 60, no. 1, p. 31–41, https://doi.org/10.1016/0016-7037(95)00370-3.

Agemar, T., Alten, J.-A., Ganz, B., Kuder, J., Kühne, K., Schumacher, S., and Schulz, R., 2014a, The geothermal information system for Germany–GeotIS: Zeitschrift der Deutschen Gesellschaft für Geowissenschaften, v. 165, no. 2, p. 129–144, https://doi.org/10.1127/1860-1804/2014/0060.

Agemar, T., Alten, J.A., Gorling, L., Gramenz, J., Kuder, J., Suchi, E., Moeck, I., Weber, J., von Hartmann, H., Stober, I., Hese, F., and Thomsen, C., 2016, Die Rolle von tiefreichenden Störungszonen bei der geothermischen Energienutzung—Verbundvorhaben "StörTief", Teilprojekt A [The role of deep fault zones in geothermal energy utilization—Joint project "StörTief, subproject A]: Hannover, Germany, Leibniz-Institut für Angewandte Geophysik, final report, 91 p.

Agemar, T., Weber, J., and Schulz, R., 2014b, Deep geothermal energy production in Germany: Energies, v. 7, no. 7, p. 4397–4416, https://doi.org/10.3390/en7074397.

Ahlers, S., Röckel, L., Hergert, T., Reiter, K., Heidbach, O., Henk, A., Müller, B., Morawietz, S., Scheck-Wenderoth, M., and Anikiev, D., 2022, The crustal stress field of Germany—A refined prediction: Geothermal Energy, v. 10, no. 1, p. 1–32, https://doi.org/10.1186/s40517-022-00222-6.

Alibert, C., Leterrier, J., Panasiuk, M., and Zimmermann, J., 1987, Trace and isotope geochemistry of the alkaline Tertiary volcanism in southwestern Poland: Lithos, v. 20, no. 4, p. 311–321, https://doi.org/10.1016/S0024-4937(87)80004-X.

Anikiev, D., Lechel, A., Gomez Dacal, M.L., Cacace, M., and Scheck-Wenderoth, M., 2019, 3-D-Deutschland (3-DD)—A three-dimensional lithospheric-scale thermal model of Germany: GFZ Data Services, https://doi.org/10.5880/GFZ.4.5.2019.005.

Artemieva, I.M., 2019, Lithosphere structure in Europe from thermal isostasy: Earth-Science Reviews, v. 188, p. 454–468, https://doi.org/10.1016/j.earscirev.2018.11.004.

Audin, L., Avouac, J.P., Flouzat, M., and Plantet, J.L., 2002, Fluid-driven seismicity in a stable tectonic context—The Remiremont fault zone, Vosges, France: Geophysical Research Letters, v. 29, no. 6, p. 13-1–13-4, at https://doi.org/10.1029/2001GL012988.

Babuška, V., Fiala, J., and Plomerová, J., 2010, Bottom to top lithosphere structure and evolution of western Eger Rift (Central Europe): International Journal of Earth Sciences, v. 99, no. 4, p. 891–907, https://doi.org/10.1007/s00531-009-0434-4.

Babuška, V., and Plomerová, J., 2013, Boundaries of mantle–lithosphere domains in the Bohemian Massif as extinct exhumation channels for high-pressure rocks: Gondwana Research, v. 23, no. 3, p. 973–987, https://doi.org/10.1016/j.gr.2012.07.005.

Bartels, A., Rummel, L., and May, F., 2020, Dokumentation und Auswertung einer Expertenbefragung zur langfristigen Vorhersage vulkanischer Aktivität in Deutschland [Documentation and evaluation of an expert survey on the long-term forecast of volcanic activity in Germany]: Hannover, Germany, Bundesanstalt für Geowissenschaften und Rohstoffe (BGR), 104 p.

Bednarz, U., and Schmincke, H.-U., 1990, Evolution of the Quaternary melitite-nephelinite Herchenberg volcano (East Eifel): Bulletin of Volcanology, v. 52, no. 6, p. 426–444, https://doi.org/10.1007/BF00268924.

Berthelsen, A., 1992, From Precambrian to Variscan Europe, chap. 6.2 *of* Blundell, D.J., Freeman, R., Mueller, S., and Button, S., eds., A continent revealed—The European Geotraverse: Cambridge, United Kingdom, Cambridge University Press, 231 p.

Bundesanstalt für Geowissenschaften und Rohstoffe, 2023, Geoportal der Bundesanstalt für Geowissenschaften und Rohstoffe [Geoportal of the Federal Institute for Geosciences and Natural Resources]: Hannover, Germany, Bundesanstalt für Geowissenschaften und Rohstoffe (BGR), accessed January 1, 2023, at https://geoportal.bgr.de/mapapps/resources/apps/geoportal/index.html?lang=de#/.

Binder, T., Marks, M.A., Gerdes, A., Walter, B.F., Grimmer, J., Beranoaguirre, A., Wenzel, T., and Markl, G., 2022, Two distinct age groups of melilitites, foidites, and basanites from the southern Central European Volcanic Province reflect lithospheric heterogeneity: International Journal of Earth Sciences, v. 112, no. 3, p. 881–905, https://doi.org/10.1007/s00531-022-02278-y.

Birkenmajer, K., and Pécskay, Z., 2002, Radiometric dating of the Tertiary volcanics in Lower Silesia, Poland. I. Alkali basaltic rocks of the Opole region: Bulletin of the Polish Academy of Sciences. Earth Sciences, v. 50, no. 1, p. 31–50.

Birkenmajer, K., Pécskay, Z., Grabowski, J., Lorenc, M.W., and Zagożdżon, P.P., 2002a, Radiometric dating of the Tertiary volcanics in Lower Silesia, Poland. II. K-Ar and palaeomagnetic data from Neogene basanites near Lądek Zdrój, Sudetes Mts: Annales Societatis Geologorum Poloniae, v. 72, p. 119–129.

Birkenmajer, K., Pécskay, Z., Grabowski, J., Lorenc, M.W., and Zagożdżon, P.P., 2002b, Radiometric dating of the Tertiary volcanics in Lower Silesia, Poland. III. K-Ar and palaeomagnetic data from Early Miocene basaltic volcanics near Jawor, Fore-Sudetic Block: Annales Societatis Geologorum Poloniae, v. 72, p. 241–253.

Birkenmajer, K., Pécskay, Z., Grabowski, J., Lorenc, M.W., and Zagożdżon, P.P., 2004, Radiometric dating of the Tertiary volcanics in Lower Silesia, Poland. IV. Further K-Ar and palaeomagnetic data from Late Oligocene to Early Miocene basaltic rocks of the Fore-Sudetic Block: Annales Societatis Geologorum Poloniae, v. 74, p. 1–19.

Birkenmajer, K., Pécskay, Z., Grabowski, J., Lorenc, M.W., and Zagożdżon, P.P., 2007, Radiometric dating of the Tertiary volcanics in Lower Silesia, Poland. V. K-Ar and palaeomagnetic data from Late Oligocene to Early Miocene basaltic volcanics of the North-Sudetic Depression: Annales Societatis Geologorum Poloniae, v. 77, p. 1–16.

Birkenmajer, K., Pécskay, Z., Grabowski, J., Lorenc, M.W., and Zagożdżon, P.P., 2011, Radiometric dating of the Tertiary volcanics in Lower Silesia, Poland. VI. K-Ar palaeomagnetic data from basaltic rocks of the West Sudety Mountains and their northern foreland: Annales Societatis Geologorum Poloniae, v. 81, p. 115–131.

Blundell, D.J., Freeman, R., Mueller, S., and Button, S., eds., 1992, A continent revealed—The European Geotraverse, structure and dynamic evolution: Cambridge, United Kingdom, Cambridge University Press, 232 p., https://doi.org/10.1017/CBO9780511608261.

van den Bogaard, P., 2000, Temporal evolution of the Vogelsberg volcano, central Germany—Mantle sources, melting processes and magma differentiation—Reconstructed from the 'Forschungsbohrung Vogelsberg 1996': Göttingen, Germany, Georg August Universität Göttingen, Ph.D. dissertation.

van den Bogaard, P., Hall, C.M., Schmincke, H.-U., and York, D., 1987, 40Ar/39Ar laser dating of single grains—Ages of Quaternary tephra from the East Eifel Volcanic Field, FRG: Geophysical Research Letters, v. 14, no. 12, p. 1211–1214, https://doi.org/10.1029/GL014i012p01211.

van den Bogaard, P., Hall, C.M., Schmincke, H.-U., and York, D., 1989, Precise single-grain 40Ar/39Ar dating of a cold to warm climate transition in Central Europe: Nature, v. 342, no. 6249, p. 523–525, https://doi.org/10.1038/342523a0.

van den Bogaard, P., Wörner, G., and Henjes-Kunst, F., 2001, Chemical stratigraphy and origin of volcanic rocks from the drill-core "Forschungsbohrung Vogelsberg 1996": Geologische Abhandlungen Hessen, v. 107, p. 69–99.

Brandes, C., Plenefisch, T., Tanner, D.C., Gestermann, N., and Steffen, H., 2019, Evaluation of deep crustal earthquakes in northern Germany—Possible tectonic causes: Terra Nova, v. 31, no. 2, p. 83–93, https://doi.org/10.1111/ter.12372.

Brauer, A., Endres, C., Zolitschka, B., and Negendank, J.F.W., 2000, AMS radiocarbon and varve chronology from the annually laminated sediment record of Lake Meerfelder maar, Germany: Radiocarbon, v. 42, no. 3, p. 355–368, https://doi.org/10.1017/S0033822200030307.

Bräuer, K., Kämpf, H., Strauch, G., and Weise, S.M., 2003, Isotopic evidence ($^{3}He/^{4}He$, $^{13}C_{CO_2}$) of fluid-triggered intraplate seismicity: Journal of Geophysical Research, v. 108, B2, p. 1–11, at https://doi.org/10.1029/2002JB002077.

Bräuer, K., Kämpf, H., Niedermann, S., Strauch, G., and Weise, S.M., 2004, Evidence for a nitrogen flux directly derived from the European subcontinental mantle in the Western Eger Rift, central Europe: Geochimica et Cosmochimica Acta, v. 68, no. 23, p. 4935–4947, https://doi.org/10.1016/j.gca.2004.05.032.

Bräuer, K., Kämpf, H., Koch, U., Niedermann, S., and Strauch, G., 2007, Seismically induced changes of the fluid signature detected by a multi-isotope approach (He, CO_2, CH_4, N_2) at the Wettinquelle, Bad Brambach (central Europe): Journal of Geophysical Research, v. 112, B4, p. 2006JB004404, at https://doi.org/10.1029/2006JB004404.

Bräuer, K., Kämpf, H., Niedermann, S., Strauch, G., and Tesař, J., 2008, Natural laboratory NW Bohemia—Comprehensive fluid studies between 1992 and 2005 used to trace geodynamic processes: Geochemistry, Geophysics, Geosystems, v. 9, no. 4, p. 2007GC001921, at https://doi.org/10.1029/2007GC001921.

Bräuer, K., Kämpf, H., Koch, U., and Strauch, G., 2011, Monthly monitoring of gas and isotope compositions in the free gas phase at degassing locations close to the Nový Kostel focal zone in the western Eger Rift Czech Republic: Chemical Geology, v. 290, nos. 3–4, p. 163–176, https://doi.org/10.1016/j.chemgeo.2011.09.012.

Bräuer, K., Kämpf, H., Niedermann, S., and Strauch, G., 2013, Indications for the existence of different magmatic reservoirs beneath the Eifel area (Germany)—A multi-isotope (C, N, He, Ne, Ar) approach: Chemical Geology, v. 356, p. 193–208, https://doi.org/10.1016/j.chemgeo.2013.08.013.

Bräuer, K., Kämpf, H., and Strauch, G., 2014, Seismically triggered anomalies in the isotope signatures of mantle-derived gases detected at degassing sites along two neighboring faults in NW Bohemia, central Europe: Journal of Geophysical Research. Solid Earth, v. 119, no. 7, p. 5613–5632, https://doi.org/10.1002/2014JB011044.

Bräuer, K., Kämpf, H., Niedermann, S., and Strauch, G., 2018, Monitoring of helium and carbon isotopes in the western Eger Rift area (Czech Republic)—Relationships with the 2014 seismic activity and indications for recent (2000–2016) magmatic unrest: Chemical Geology, v. 482, p. 131–145, https://doi.org/10.1016/j.chemgeo.2018.02.017.

Büchel, G., and Lorenz, V., 1982, Zum Alter des Maarvulkanismus der Westeifel [The age of maar volcanism in the West Eifel]: Neues Jahrbuch für Geologie und Paläontologie, v. 163, p. 1–22.

Buchholz, P., Estrella, H.F., Funke, S., Korn, M., Lerbs, N., Sonnabend, L., Wendt, S., Hänel, F., Hellwig, O., Burghardt, T., van Laaten, M., Schönwald, D., Wegler, U., Domigall, D., Krentz, O., Witthauer, B., Martin, J., Pustal, I., and Rappsilber, I., 2019, Erdbebenbeobachtung in Mitteldeutschland—Dreijahresbericht 2016–2018 [Earthquake monitoring in central Germany—Three-year report 2016–2018]: Dresden, Germany, Sächsisches Landesamt für Umwelt, Landwirtschaft und Geologie, 66 p.

Buchholz, P., Funke, S., Korn, M., Wendt, S., Hänel, F., Mittag, R., Novak, E., Rappsilber, I., Burghardt, T., Schönwald, D., Pustal, I., Koch, U., Krentz, O., Witthauer, B., and Neunhöfer, H., 2013, Erdbebenbeobachtung im Freistaat Sachsen—Dreijahresbericht 2010–2012 [Earthquake monitoring in Saxony—Three-year report 2010–2012]: Dresden, Germany, Sächsisches Landesamt für Umwelt, Landwirtschaft und Geologie, 42 p.

Buchholz, P., Funke, S., Wendt, S., Hänel, F., Mittag, R., Novak, E., Burghardt, T., Schönwald, D., Busch, P., Eberlein, L., Horwath, M., Schröder, L., Rappsilber, I., Pustal, I., Krentz, O., and Witthauer, B., 2016, Erdbebenbeobachtung in Mitteldeutschland—Dreijahresbericht 2013–2015 [Earthquake monitoring in central Germany—Three-year report 2013–2015]: Dresden, Germany, Sächsisches Landesamt für Umwelt, Landwirtschaft und Geologie, 54 p.

Büchner, J., Tietz, O., Viereck, L., Suhr, P., and Abratis, M., 2015, Erratum to Volcanology, geochemistry and age of the Lausitz Volcanic Field: International Journal of Earth Sciences, v. 104, no. 8, p. 2057–2083, at https://doi.org/10.1007/s00531-015-1165-3.

Cajz, V., Adamovič, J., Rapprich, V., and Valigurský, L., 2004, Newly identified faults inside the volcanic complex of the České středohoří Mts., Ohře/Eger Graben, North Bohemia: Acta Geodynamica et Geomaterialia, v. 1, no. 2, p. 213–222.

Cajz, V., Schnabl, P., Pécskay, Z., Skácelová, Z., Venhodová, D., Slechta, S., and Čížková, K., 2012, Chronological implications of the paleomagnetic record of the Late Cenozoic volcanic activity along the Moravia-Silesia border (NE Bohemian Massif): Geologica Carpathica, v. 63, no. 5, p. 423–435, https://doi.org/10.2478/v10096-012-0033-3.

Camelbeeck, T., 1993, Mécanisme au foyer des tremblements de terre et contraintes tectoniques—Le cas de la zone intraplaque belge [Earthquake focal mechanism and tectonic stresses—The case of the Belgian intraplate zone]: Louvin-la-Neuve, Belgium, Université Catholique de Louvain, Ph.D. dissertation, 295 p.

Cantarel, P., and Lippolt, H.J., 1977, Alter und Abfolge des Vulkanismus in der Hocheifel [Age and sequence of volcanism in the Hocheifel]: Neues Jahrbuch für Geologie und Paläontologie, v. 10, p. 600–612.

Carlé, W., 1975, Die Mineral- und Thermalwässer von Mitteleuropa—Geologie, Chemismus, Genese [The mineral and thermal waters of Central Europe: geology, chemistry, genesis]: Stuttgart, Germany, Wissenschaftliche Verlagsgesellschaft Stuttgart, 643 p.

Czech Academy of Science, 2021, Recent swarm activity in the western Bohemia/Vogtland region: Institute of Geophysics, accessed January 1, 2021, at https://www.ig.cas.cz/en/recent-swarm-activity-in-the-western-bohemia-vogtland-region/.

Dahlheim, H.A., Gebrande, H., Schmedes, E., and Soffel, H., 1997, Seismicity and stress field in the vicinity of the KTB location: Journal of Geophysical Research, v. 102, no. B8, no. B8, p. 18493–18506, https://doi.org/10.1029/96JB02812.

Dahm, T., Fischer, T., and Hainzl, S., 2008, Mechanical intrusion models and their implications for the possibility of magma-driven swarms in NW Bohemia region: Studia Geophysica et Geodaetica, v. 52, no. 4, p. 529–548, https://doi.org/10.1007/s11200-008-0036-9.

Dahm, T., Wörner, G., Ritter, J., and Walter, T., 2019, Vulkanismus in der Eifel—Wissenschaftliche Einschätzung, Bewertung aktueller Prozesse und Forschungsbedarf [Volcanism in the Eifel—Scientific assessment, evaluation of current processes and research needs]: Mitteilungen—Deutsche Geophysikalische Gesellschaft, v. 2 p. 5–15.

Decker, K., Peresson, H., and Faupl, P., 1994, Die miozäne Tektonik der östlichen Kalkalpen—Kinematik, Paläospannungen und Deformationsaufteilung während der "lateralen Extrusion" der Zentralalpen [Miocene tectonics of the Eastern Limestone Alps—kinematics, paleostresses, and deformation partitioning during the "lateral extrusion" of the Central Alps]: Jahrbuch der Geologischen Bundesanstalt, v. 137, no. 1, p. 5–18.

Dehner, U., Grad, J., Hohberger, K.-H., Weidenfeller, M., Wiesner, T., Baumeister, C., Demuth, N., Kampf, J., Meuser, A., Plaul, W., Steinrücken, U., and Schreiber, U., 2015, Hydrogeologische Kartierung Westerwaldkreis [Hydrogeological mapping of the Westerwald district]: Mainz, Germany, Landesamt für Geologie und Bergbau Rheinland-Pfalz and Landesamt für Umwelt Wasserwirtschaft und Gewerbeaufsicht Rheinland-Pfalz, 136 p.

DEKORP-Research-Group, Anderle, H.-J., Bittner, R., Bortfeld, R., Bouckaert, J., Büchel, G., Dohr, G., Dürbaum, H.-J., Durst, H., Fielitz, W., Flüh, E., Gundlach, T., Hance, L., Henk, A., Jordan, F., Kläschen, D., Klöckner, M., Meissner, R., Meyer, W., Oncken, O., Reichert, C., Ribbert, K.-H., Sadowiak, P., Schmincke, H.-U., Schmoll, J., Walter, R., Weber, K., Weihrauch, U., and Wever, T., 1991, Results of the DEKORP 1 (BELCORP-DEKORP) deep seismic reflection studies in the western part of the Rhenish Massif: Geophysical Journal International, v. 106, no. 1, p. 203–227, https://doi.org/10.1111/j.1365-246X.1991.tb04612.x.

Dersch-Hansmann, M., Ehrenberg, K., Heggemann, H., Hottenrott, M., Kaufmann, E., Keller, T., Königshof, P., Kött, A., Nesbor, H., and Theuerjahr, A., 1999, Geotope in Hessen—Exkursionen zu Geotopen in Hessen und Rheinland-Pfalz sowie zu naturwissenschaftlichen Beobachtungspunkten Johann Wolfgang Goethes in Böhmen [Geotopes in Hesse—Excursions to geotopes in Hesse and Rhineland-Palatinate, as well as to Johann Wolfgang Goethe's natural science observation points in Bohemia]: Schriftenreihe der Deutschen Geologischen Gesellschaft, v. 8, p. 69–126.

Dèzes, P., Schmid, S., and Ziegler, P., 2004, Evolution of the European Cenozoic Rift system—Interaction of the Alpine and Pyrenean orogens with their foreland lithosphere: Tectonophysics, v. 389, nos. 1–2, p. 1–33, https://doi.org/10.1016/j.tecto.2004.06.011.

Egger, H., 1997, Das sinistrale Innsbruck-Salzburg-Amstetten-Blattverschiebungssystem—Ein weiterer Beleg für die miozäne laterale Extrusion der Ostalpen [The sinistral Innsbruck-Salzburg-Amstetten strike-slip fault system—Further evidence for the Miocene lateral extrusion of the Eastern Alps]: Jahrbuch der Geologischen Bundesanstalt, v. 140, no. 1, p. 47–50.

Egli, D., Mosar, J., Ibele, T., and Madritsch, H., 2017, The role of precursory structures on Tertiary deformation in the Black Forest—Hegau region: International Journal of Earth Sciences, v. 106, no. 7, p. 2297–2318, https://doi.org/10.1007/s00531-016-1427-8.

Fassbender, M., 1990, Untersuchungen von kohlensäurehaltigen Quellen südöstlich Hillesheim/Eifel [Investigations of carbonic acid springs southeast of Hillesheim/Eifel].: Aachen, Germany, Technische Hochschule Aachen, 103 p.

Fekiacova, Z., Mertz, D.F., and Renne, P.R., 2007, Geodynamic Setting of the Tertiary Hocheifel Volcanism (Germany), Part I—$^{40}Ar/^{39}Ar$ geochronology, *in* Ritter, J.R.R., and Christensen, U.R., eds., Mantle plumes—A multidisciplinary approach: Berlin, Heidelberg, Springer Berlin Heidelberg, p. 185–206, https://doi.org/10.1007/978-3-540-68046-8_6.

Fichtner, A., van Herwaarden, D.P., Afanasiev, M., Simutė, S., Krischer, L., Çubuk-Sabuncu, Y., Taymaz, T., Colli, L., Saygin, E., Villaseñor, A., Trampert, J., Cupillard, P., Bunge, H.-P., and Igel, H., 2018, The collaborative seismic earth model—Generation 1: Geophysical Research Letters, v. 45, no. 9, p. 4007–4016, https://doi.org/10.1029/2018GL077338.

Fischer, T., and Horálek, J., 2003, Space-time distribution of earthquake swarms in the principal focal zone of the NW Bohemia/Vogtland seismoactive region—Period 1985–2001: Journal of Geodynamics, v. 35, nos. 1–2, p. 125–144, https://doi.org/10.1016/S0264-3707(02)00058-3.

Fischer, T., Horálek, J., Hrubcová, P., Vavryčuk, V., Bräuer, K., and Kämpf, H., 2014, Intra-continental earthquake swarms in west-Bohemia and Vogtland—A review: Tectonophysics, v. 611, p. 1–27, https://doi.org/10.1016/j.tecto.2013.11.001.

Fischer, T., and Michálek, J., 2008, Post 2000-swarm microearthquake activity in the principal focal zone of West Bohemia/Vogtland—Space-time distribution and waveform similarity analysis: Studia Geophysica et Geodaetica, v. 52, no. 4, p. 493–512, https://doi.org/10.1007/s11200-008-0034-y.

Förster, M.W., and Sirocko, F., 2016, The ELSA tephra stack—Volcanic activity in the Eifel during the last 500,000 years: Global and Planetary Change, v. 142, p. 100–107, https://doi.org/10.1016/j.gloplacha.2015.07.012.

Franke, D., and Hoffmann, N., 1999, Das Elbe-Lineament—bedeutende Geofraktur oder Phantomgebilde?—Teil 1—Die Referenzgebiete [The Elbe Lineament—Significant geofracture or phantom formation?—Part 1—The reference areas]: Zeitschrift für Geologische Wissenschaften, v. 27, p. 279–318.

Franke, W., 2014, Topography of the Variscan orogen in Europe—Failed–not collapsed: International Journal of Earth Sciences, v. 103, no. 5, p. 1471–1499, https://doi.org/10.1007/s00531-014-1014-9.

Franzensbad, 2020, Franzensbader Quellen [Franzensbad springs]: Frantoškovy Láznê, accessed January 1, 2021, at https://www.frantiskovy-lazne.info/de/kur-und-wellness/kolonnaden-und-quellen.

Frechen, J., and Vieten, K., 1970, Petrographie der Vulkanite des Siebengebirges—Die peralkalische Gesteinsreihe Alkalitrachyt—Sanidinbasanit [Petrography of the volcanic rocks of the Siebengebirge—The peralkaline rock series alkali trachyte—sanidine basanite]: Decheniana, v. 122, p. 357–377.

Frechen, J.V., and Lippolt, H., 1965, Kalium-Argon-Daten zum Alter des Laacher Vulkanismus, der Rheinterrassen und der Eiszeiten [Potassium-argon data for the age of the Laacher volcanism, the Rhine terraces and the ice ages]: E&G Quaternary Science Journal, v. 16, no. 1, p. 5–30., https://doi.org/10.3285/eg.16.1.01.

Frechen, M., Boenigk, W., Hambach, U., and Reinders, J., 1999, The Late Middle and Upper Pleistocene Loess/Palaeosol deposits of section Tönchesberg/Neuwied Basin—Loess in the Middle and Upper Rhine area *in* Weidenfeller, M., and Zöller, L. (eds.), Loess in the Middle and Upper Rhine Area, Loessfest Field Guide—Geologisches Landesamt Rheinland-Pfalz, March 25, 1999: Geologisches Landesamt Rheinland-Pfalz, 83 p.

Freudenberger, W., and Schwerd, K., 1996, Erläuterungen zur geologischen Karte von Bayern 1: 500 000 [Explanatory notes to the geological map of Bavaria 1: 500 000]: München, Germany, Bayerisches Geologisches Landesamt, 329 p.

Friedrich, M., Kromer, B., Spurk, M., Hofmann, J., and Kaiser, K.F., 1999, Paleo-environment and radiocarbon calibration as derived from Lateglacial/Early Holocene tree-ring chronologies: Quaternary International, v. 61, no. 1, p. 27–39, https://doi.org/10.1016/S1040-6182(99)00015-4.

Frisch, U., and Kockel, F., 2004, Der Bremer-Knoten im Strukturnetz Nordwest-Deutschlands—Stratigraphie, Paläogeographie, Strukturgeologie [The Bremen node in the structural network of northwest Germany—Stratigraphy, paleogeography, structural geology]: Bremen, Germany, Universität Bremen, 379 p.

Fuhrmann, U., 1983, Kalium-Argon-Untersuchungen an neogenen Vulkaniten des Rheinischen Schildes [Potassium-argon investigations on Neogene volcanics of the Rhenish Shield]: Heidelberg, Germany, Universität Heidelberg, 157 p.

Fuhrmann, U., and Lippolt, H.J., 1985, Excess argon and dating of Quaternary Eifel volcanism—1—The Schellkopf alkali phonolite/East Eifel: Neues Jahrbuch für Geologie und Paläontologie—Monatshefte, v. 8, no. 8, p. 484–497, https://doi.org/10.1127/njgpm/1985/1985/484.

Fuhrmann, U., and Lippolt, H., 1986, Excess argon and dating of Quaternary Eifel volcanism—2—Phonolitic and foiditic rocks near Rieden, East Eifel/FRG: Neues Jahrbuch für Geologie und Paläontologie—Abhandlungen, v. 172, no. 1, p. 1–19, https://doi.org/10.1127/njgpa/172/1997/1.

Fuhrmann, U., and Lippolt, H., 1987a, K-Ar-Datierungen an Maintrapp-Basalten aus Bohrungen in Frankfurt a. M. nach der 40Ar/39Ar-Stufenentgasungstechnik [K-Ar dating of Maintrapp basalts from boreholes in Frankfurt using the 40Ar/39Ar staged degassing technique]: Geologisches Jahrbuch Hessen, v. 115, p. 245–257.

Fuhrmann, U., and Lippolt, H.J., 1987b, Excess argon and dating of Quaternary Eifel volcanism—3—Alkali basaltic rocks of the Central West Eifel/FR Germany: Neues Jahrbuch für Geologie und Paläontologie—Monatshefte, v. 4, no. 4, p. 213–236, at https://doi.org/10.1127/njgpm/1987/1987/213.

Geluk, M., Duin, E.T., Dusar, M., Rijkers, R., Van den Berg, M., and Van Rooijen, P., 1994, Stratigraphy and tectonics of the Roer Valley Graben: Geologie en Mijnbouw, v. 73, p. 129–141.

GeoSphere Austria, 2022, Erdbebenarchiv [Earthquake archive]: GeoSphere Austria—Bundesanstalt für Geologie, Geophysik, Klimatologie und Meteorologie, accessed January 20, 2026, at https://www.geosphere.at/de/karten/aktuelle-erdbeben.

Helmholtz-Zentrum Potsdam, G.F.Z., 2022, Plattform zur Abfrage von gefährdungskonsistenten Antwortspektren (UHS) für beliebige Punkte in Deutschland sowie von nationalen Erdbebengefährdungskarten nach dem Berechnungsmodell von Grünthal and others (2018) [Platform for querying Uniform Hazard Spectra (UHS) for any point in Germany as well as national earthquake hazard maps based on the calculation model of Grünthal and others (2018)]: GFZ Helmholtz-Zentrum Potsdam, ed., Deutsches GeoForschungsZentrum GFZ, accessed January 1, 2022, at http://www.gfz.de.

Giggenbach, W., Sano, Y., and Schmincke, H.-U., 1991, CO2-rich gases from Lakes Nyos and Monoun, Cameroon; Laacher See, Germany; Dieng, Indonesia, and Mt. Gambier, Australia—Variations on a common theme: Journal of Volcanology and Geothermal Research, v. 45, nos. 3–4, p. 311–323, https://doi.org/10.1016/0377-0273(91)90065-8.

Gögen, K., and Wagner, G., 2000, Alpha-recoil track dating of Quaternary volcanics: Chemical Geology, v. 166, nos. 1–2, p. 127–137, https://doi.org/10.1016/S0009-2541(99)00185-0.

Grad, M., Tiira, T., and ESC Working Group, 2009, The Moho depth map of the European Plate: Geophysical Journal International, v. 176, no. 1, p. 279–292, https://doi.org/10.1111/j.1365-246X.2008.03919.x.

Griesshaber, E., O'Nions, R., and Oxburgh, E., 1992, Helium and carbon isotope systematics in crustal fluids from the Eifel, the Rhine Graben and Black Forest, FRG: Chemical Geology, v. 99, no. 4, p. 213–235, https://doi.org/10.1016/0009-2541(92)90178-8.

Grimmer, J., Ritter, J., Eisbacher, G., and Fielitz, W., 2017, The Late Variscan control on the location and asymmetry of the Upper Rhine Graben: International Journal of Earth Sciences, v. 106, no. 3, p. 827–853, https://doi.org/10.1007/s00531-016-1336-x.

Grünthal, G., Schenk, V., Zeman, A., and Schenková, Z., 1990, Seismotectonic model for the earthquake swarm of 1985–1986 in the Vogtland/West Bohemia focal area: Tectonophysics, v. 174, no. 3–4, p. 369–383, https://doi.org/10.1016/0040-1951(90)90332-3.

Grünthal, G., Stromeyer, D., Bosse, C., Cotton, F., and Bindi, D., 2018, Correction to: Bulletin of Earthquake Engineering, v. 16, no. 10, p. 4339–4395, at https://doi.org/10.1007/s10518-018-0398-5.

Hajdas, I., Ivy-Ochs, S.D., Bonani, G., Loiter, A.F., Zolitschka, B., and Schluechter, C., 1995, Radiocarbon age of the Laacher See tephra—11,230±40 BP: Radiocarbon, v. 37, no. 2, p. 149–154, https://doi.org/10.1017/S0033822200030587.

Hann, H., Chen, F., Zedler, H., Frisch, W., and Loeschke, J., 2003, The Rand Granite in the southern Schwarzwald and its geodynamic significance in the Variscan belt of SW Germany: International Journal of Earth Sciences, v. 92, no. 6, p. 821–842, https://doi.org/10.1007/s00531-003-0361-8.

Hannemann, K., Ohrnberger, M., Lerbs, N., Domigall, D., Isken, M., Voigt, R., Vollmer, D., Bauz, R., Klicpera, J., and Sonnabend, L., 2021, High frequency array observations of December 2020 swarm at surface and borehole stations at ICDP Eger Rift site Landwüst (Vogtland)—EGU General Assembly 2021, online, April 19–30, 2021, accessed December 12, 2025, at https://doi.org/10.5194/egusphere-egu21-9561.

Heinicke, J., Woith, H., Alexandrakis, C., Buske, S., and Telesca, L., 2018, Can hydroseismicity explain recurring earthquake swarms in NW-Bohemia?: Geophysical Journal International, v. 212, no. 1, p. 211–228, https://doi.org/10.1093/gji/ggx412.

Hemmann, A., 2002, Relativrelokalisierung von Schwarmbeben in der Saxothuringischen seismotektonischen Provinz [Relative relocalization of earthquake swarms in the Saxothuringian seismotectonic province]: Jena, Germany, Friedrich-Schiller-Universität Jena, Ph.D. dissertation, 236 p.

Hensch, M., Dahm, T., Ritter, J., Heimann, S., Schmidt, B., Stange, S., and Lehmann, K., 2019, Deep low-frequency earthquakes reveal ongoing magmatic recharge beneath Laacher See Volcano (Eifel, Germany): Geophysical Journal International, v. 216, no. 3, p. 2025–2036, https://doi.org/10.1093/gji/ggy532.

Hetényi, G., Molinari, I., Clinton, J., Bokelmann, G., Bondár, I., Crawford, W.C., Dessa, J.-X., Doubre, C., Friederich, W., Fuchs, F., Giardini, D., Gráczer, Z., Handy, M.R., Herak, M., Jia, Y., Kissling, E., Kopp, H., Korn, M., Margheriti, L., Meier, T., Mucciarelli, M., Paul, A., Pesaresi, D., Piromallo, C., Plenefisch, T., Plomerová, J., Ritter, J., Rümpker, G., Šipka, V., Spallarossa, D., Thomas, C., Tilmann, F., Wassermann, J., Weber, M., Wéber, Z., Wesztergom, V., and Živčić, M., 2018, The AlpArray seismic network—A large-scale European experiment to image the Alpine orogen: Surveys in Geophysics, v. 39, no. 5, p. 1009–1033, https://doi.org/10.1007/s10712-018-9472-4.

Hofbauer, G., 2007, Der Vulkan von Oberleinleiter—Spuren eines Maars in der Nördlichen Frankenalb [The Oberleinleiter Volcano—Traces of a maar in the Northern Franconian Jura]: Jahresmitteilungen, v. 2007, p. 69–87.

Homuth, B., and Rümpker, G., 2017, The 2014–2015 earthquake series in the northern Upper Rhine Graben, Central Europe: Journal of Seismology, v. 21, no. 1, p. 83–98, https://doi.org/10.1007/s10950-016-9584-6.

Homuth, B., 2020, Mikroseismizität in Hessen—Die Erdbebenserie bei Bad Schwalbach im Taunus [Microseismicity in Hesse—The earthquake series near Bad Schwalbach in the Tanus]: Wiesbaden, Germany, Hessisches Landesamt für Naturschutz, Umwelt und Geologie, p. 187–192.

Horálek, J., Hampl, F., Boušková, A., and Fischer, T., 1996, Seismic regime of the West Bohemian earthquake swarm region—Preliminary results: Studia Geophysica et Geodaetica, v. 40, no. 4, p. 398–412, https://doi.org/10.1007/BF02300767.

Horn, P., Lippolt, H.J., and Todt, W., 1972, Kalium-Argon-Altersbestimmungen an tertiären Vulkaniten des Oberrheingrabens, I—Gesteinsalter [Potassium-argon dating of Tertiary volcanic rocks of the Upper Rhine Graben, I—Rock age]: Eclogae Geologicae Helvetiae, v. 65, no. 1, p. 131–156.

Huth, T., and Zedler, H., 2019, Entlang der kontinentalen Schweißnaht im Südschwarzwald—Die Badenweiler-Lenzkirch-Zone (BLZ) [Along the continental weld in the Southern Black Forest—The Badenweiler-Lenzkirch Zone (BLZ)]: Schriftenreihe der Deutschen Gesellschaft für Geowissenschaften, v. 94, p. 166–192.

Information Centre of the City of Karlovy Vary, 2021, Kolonnaden und Quellen [Colonnades and springs]: City of Karlovy Vary, accessed January 1, 2021, at https://www.karlovyvary.cz/de/kolonnaden-und-quellen.

Kaban, M., Tesauro, M., and Cloetingh, S., 2010, An integrated gravity model for Europe's crust and upper mantle: Earth and Planetary Science Letters, v. 296, nos. 3–4, p. 195–209, https://doi.org/10.1016/j.epsl.2010.04.041.

Kaiser, G., and Pilot, J., 1986, Weitere K-Ar-Datierungen an jungen Vulkaniten [Further K-Ar dating of young volcanic rocks]: Zeitschrift für Geologische Wissenschaften, v. 14, no. 1, p. 121–124.

Kämpf, H., Geissler, W.H., and Bräuer, K., 2007, Combined gas-geochemical and receiver function studies of the Vogtland/NW Bohemia intraplate mantle degassing field, central Europe, *in* Ritter, J.R.R., and Christensen, U.R., eds., Mantle Plumes: Berlin, Heidelberg, Germany, Springer, p. 127–158, https://doi.org/10.1007/978-3-540-68046-8_4.

Kämpf, H., Bräuer, K., Schumann, J., Hahne, K., and Strauch, G., 2013, CO_2 discharge in an active, non-volcanic continental rift area (Czech Republic)—Characterisation ($\delta^{13}C$, $^{3}He/^{4}He$) and quantification of diffuse and vent CO_2 emissions: Chemical Geology, v. 339, p. 71–83, https://doi.org/10.1016/j.chemgeo.2012.08.005.

Kämpf, H., Broge, A.S., Marzban, P., Allahbakhshi, M., and Nickschick, T., 2019, Nonvolcanic carbon dioxide emission at continental rifts—The Bublak Mofette Area, Western Eger Rift, Czech Republic: Geofluids, v. 2019, p. 1–19, https://doi.org/10.1155/2019/4852706.

Keller, J., 2001, Welded carbonatite—A new type and new occurrence of extrusive carbonatite from the Kaiserstuhl area, Germany: Journal of African Earth Sciences, v. 32, no. 1, p. A22, https://doi.org/10.1016/S0899-5362(01)90045-4.

Keller, J., Kraml, M., and Henjes-Kunst, F., 2002, $^{40}Ar/^{39}Ar$ single crystal laser dating of early volcanism in the Upper Rhine Graben and tectonic implications: Schweizerische Mineralogische und Petrographische Mitteilungen, v. 82, p. 1–10.

Kley, J., Franzke, H., Jähne, F., Krawczyk, C., Lohr, T., Reicherter, K., Scheck-Wenderoth, M., Sippel, J., Tanner, D., and van Gent, H., 2008, Strain and stress, chap. 3.3 *of* Littke, R., Bayer, U., Gajweski, D., and Nelskamp, S., eds., Dynamics of complex intracontinental basins—The central European Basin system, p. 97–124.

Kockel, F., 1998, Geotektonischer Atlas von Nordwest-Deutschland—Die paläogeographische und strukturelle Entwicklung Nordwestdeutschlands, Band 1, Geschichte der Erforschung, Datengrundlage, Methodik, großregionale Stellung NW-Deutschlands, Schollengliederung des Sockels, Typisierung der Strukturen des Oberbaues, Zeitlichkeit der Bewegungen, thermische und Reifungsgeschichte, Subsidenzgeschichte [Geotectonic Atlas of Northwest Germany—The paleogeographic and structural development of Northwest Germany, Volume 1, History of research, data basis, methodology, macro-regional position of Northwest Germany, block structure of the basement, typification of the structures of the superstructure, temporality of movements, thermal and maturation history, subsidence history]: Hannover, Germany, Bundesanstalt für Geowissenschaften und Rohstoffe (BGR), scale 1:300,000, 77-p. text.

Konstantinsbad, 2021, Konstantinsbad—Quellen [Konstantinsbad—Springs], accessed January 1, 2021, at https://www.konstantinovylazne.cz/de/konstantinsbad/interaktive-karte/.

Köppen, K.-H., 1987, Geologie und Hydrogeologie der Gerolsteiner Mulde und ihrer Umgebung [Geology and hydrogeology of the Gerolsteiner Mulde and its surroundings]: Trier, Germany, Universität Trier, Ph.D dissertation, 200 p.

Korn, M., Funke, S., and Wendt, S., 2008, Seismicity and seismotectonics of West Saxony, Germany—New insights from recent seismicity observed with the Saxonian seismic network: Studia Geophysica et Geodaetica, v. 52, no. 4, p. 479–492, https://doi.org/10.1007/s11200-008-0033-z.

Kraft, T., Wassermann, J., Schmedes, E., and Igel, H., 2006, Meteorological triggering of earthquake swarms at Mt. Hochstaufen, SE-Germany: Tectonophysics, v. 424, nos. 3–4, p. 245–258, https://doi.org/10.1016/j.tecto.2006.03.044.

Kraml, M., Keller, J., and Henjes-Kunst, F., 1995, New K-Ar, ^{40}Ar-^{39}Ar step heating and ^{40}Ar-^{39}Ar laser fusion dates for the Kaiserstuhl volcanic complex: European Journal of Mineralogy, v. 7, p. 142.

Kraml, M., Keller, J., and Henjes-Kunst, F., 1999, Time constraints for the carbonatitic intrusions of the Kaiserstuhl volcanic complex—Upper Rhine Graben, Germany: Journal of Conference Abstracts, v. 4, p. 322.

Kreemer, C., Blewitt, G., and Davis, P.M., 2020, Geodetic evidence for a buoyant mantle plume beneath the Eifel volcanic area, NW Europe: Geophysical Journal International, v. 222, no. 2, p. 1316–1332, https://doi.org/10.1093/gji/ggaa227.

Kreuzer, H., 1973, K/Ar-Datierungen an jungtertiären Basalten aus dem Vogelsberg und aus dem Raum zwischen Kassel und Göttingen [K/Ar dating of Late Tertiary basalts from the Vogelsberg and the area between Kassel and Göttingen]: Fortschritte der Mineralogie, v. 50, no. 3, p. 10–11.

Kröchert, J., Schmieder, M., Theye, T., and Buchner, E., 2009, Considerations on the age of the Urach volcanic field (Southwest Germany): Zeitschrift der Deutschen Gesellschaft für Geowissenschaften, v. 160, no. 4, p. 325–331, https://doi.org/10.1127/1860-1804/2009/0160-0325.

Landeserdbebendienst Rheinland-Pfalz, 2022, Erdbebenereignisse lokal [Earthquake events local]: Landesamt für Geologie und Bergbau Rheinland-Pfalz, accessed July 2, 2022, at https://www.lgb-rlp.de/fachthemen/landeserdbebendienstrlp/erdbebenereignisselokal.html?no_cache=1

Lang, S., 2007, Die geologische Entwicklung der Hanau-Seligenstädter Senke (Hessen, Bayern) [The geological development of the Hanau-Seligenstadt Depression (Hesse, Bavaria)]: Darmstadt, Germany, Technische Universität Darmstadt, Ph.D. dissertation, 50 p.

Langguth, H., and Plum, H., 1984, Untersuchung der Mineral- und Thermalquellen der Eifel auf geothermische Indikationen [Investigation of the mineral and thermal springs of the Eifel for geothermal indications]: Eggenstein-Leopoldshafen, Germany, Fachinformationszentrum Energie, Physik, Mathematik Karlsruhe, 176 p.

Lenz, O.K., Wilde, V., Mertz, D.F., and Riegel, W., 2015, New palynology-based astronomical and revised 40Ar/39Ar ages for the Eocene maar lake of Messel (Germany): International Journal of Earth Sciences, v. 104, no. 3, p. 873–889, https://doi.org/10.1007/s00531-014-1126-2.

Leyk, H., and Lippolt, H., 1999, 40Ar/39Ar—Untersuchungen an spätquartären Vulkaniten der Eifel—Neue Arbeitsansätze zur Datierung junger Lavaströme [Investigations on Late Quaternary volcanic rocks of the Eifel—New approaches to dating young lava flows]: European Journal of Mineralogy, v. 11, no. 1, p. 145.

LfULG, 2021, Schwarmbeben im Vogtland [Swarm earthquakes in the Vogtland region]: Sächsisches Staatsministerium für Energie, Klimaschutz, Umwelt und Landwirtschaft, accessed January 1, 2021, at https://www.geologie.sachsen.de/schwarmbeben-im-vogtland-27867.html?_cp=%7B%7D.

LfULG, 2022, ARTUS 2—Kenntnisstandsanalyse zum tektonischen Bau von Sachsen [Current knowledge analysis on the tectonic structure of Saxony]: Sächsisches Staatsministerium für Energie, Klimaschutz, Umwelt und Landwirtschaft, accessed January 1, 2022, at https://www.geologie.sachsen.de/artus-2-kenntnisstandsanalyse-zum-tektonischen-bau-von-sachsen-27594.html.

Linthout, K., Paulick, H., and Wijbrans, J.R., 2009, Provenance of basalt blocks from Roman sites in Vleuten-De Meern (the Netherlands) traced to the Tertiary Siebengebirge (Germany)—A geoarchaeological quest using petrological and geochemical methods: Geologie en Mijnbouw, v. 88, no. 1, p. 55–74, https://doi.org/10.1017/S0016774600000998.

Lippolt, H.J., 1961, Altersbestimmungen nach der K-Ar-Methode bei kleinen Argon-und Kaliumkonzentrationen [Age determination using the K-Ar method at low argon and potassium concentrations]: Heidelberg, Germany, Ph.D. dissertation, 82 p.

Lippolt, H.J., 1974, Radiogenes Alter und Ries-Sprengung [Radiogenic age and Ries blasting]: Der Aufschluss, v. 25, nos. 7–8, p. 416–419.

Lippolt, H.J., 1976, Das pliozäne Alter der Bertenauer Basalte/Westerwald [The Pliocene age of the Bertenau basalts/Westerwald]: Der Aufschluss, v. 27, p. 205–208.

Lippolt, H.J., 1983, Distribution of volcanic activity in space and time, *in* Fuchs, K., von Gehlen, K., Mälzer, H., Murawski, H., and Semmel, A., eds., Plateau uplift: Berlin, Heidelberg, Springer, p. 112–120, https://doi.org/10.1007/978-3-642-69219-2_15.

Lippolt, H.J., and Fuhrmann, U., 1980, Vulkanismus der Nordeifel—Datierung von Gang- und Schlotbasalten [Volcanism of the Northern Eifel—Dating of dyke and vent basalts]: Aufschluss, v. 31, p. 540–547.

Lippolt, H.J., and Todt, W., 1978, Isotopische Altersbestimmungen an Vulkaniten des Westerwaldes [Isotopic dating of volcanic rocks from the Westerwald]: Neues Jahrbuch für Geologie und Paläontologie, v. 6, p. 332–352.

Lorenz, V., 1978, Phreatomagmatische Vulkane in der südlichen Westeifel, ihre Alter und ihre Beziehung zum Talnetz [Phreatomagmatic volcanoes in the southern West Eifel, their age, and their relationship to the valley network]: Berlin, Nachrichten der deutschen geologischen Gesellschaft, v. 19, 30 p.

Lorenz, V., and Büchel, G., 1980, Zur Vulkanologie der Maare und Schlackenkegel der Westeifel [On the volcanology of the maars and cinder cones of the West Eifel]: Mitteilungen der Pollichia, v. 68, p. 29–100.

Erdbebendienst Bayern, 2021, Akuelle Beben [Current earthquakes]: Ludwig-Maximilians Universität München, accessed January 1, 2021, at https://www.erdbeben-in-bayern.de/erdbebendienst/.

Lustrino, M., and Wilson, M., 2007, The circum-Mediterranean anorogenic Cenozoic igneous province: Earth-Science Reviews, v. 81, nos. 1–2, p. 1–65, https://doi.org/10.1016/j.earscirev.2006.09.002.

Lyngsie, S., and Thybo, H., 2007, A new tectonic model for the Laurentia-Avalonia-Baltica sutures in the North Sea—A case study along MONA LISA profile 3: Tectonophysics, v. 429, nos. 3–4, p. 201–227, https://doi.org/10.1016/j.tecto.2006.09.017.

Mariánské Lázně Tourist Portal, 2021, Quellen [Springs]: Mariánské Lázně, accessed January 1, 2021, at https://www.marianskelazne.cz/de/marienbad-entdecken/quellen/.

May, F., 2002a, Quantifizierung des CO_2-Flusses zur Abbildung magmatischer Prozesse im Untergrund der Westeifel [Quantification of CO_2 flux to map magmatic processes in the subsurface of the West Eifel]: Düren, Germany, Shaker Verlag, 170 p.

May, F., 2002b, Säuerlinge der Vulkaneifel und der Südeifel [Acidic springs of the Vulkaneifel and the Southern Eifel]: Mainzer Geowissenschaftliche Mitteilungen, v. 31, p. 7–58.

Maystrenko, Y., Bayer, U., Brink, H.-J., and Littke, R., 2008, The central European basin system—An overview, chap. 2 *of* Littke, R., Bayer, U., Gajewski, D., and Nelskamp, S., eds., Dynamics of Complex Intracontinental Basins: Berlin, Heidelberg, Springer, 458 p. https://doi.org/10.1007/978-3-540-85085-4_2

Maystrenko, Y.P., and Scheck-Wenderoth, M., 2013, 3D lithosphere-scale density model of the Central European Basin System and adjacent areas: Tectonophysics, v. 601, p. 53–77, https://doi.org/10.1016/j.tecto.2013.04.023.

Mertes, H., and Schmincke, H.-U., 1983, Age distribution of volcanoes in the West-Eifel: Neues Jahrbuch für Geologie und Paläontologie—Abhandlungen, v. 166, no. 2, p. 260–293, https://doi.org/10.1127/njgpa/166/1983/260.

Mertz, D., Swisher, C., Franzen, J., Neuffer, F., and Lutz, H., 2000, Numerical dating of the Eckfeld maar fossil site, Eifel, Germany—A calibration mark for the Eocene time scale: Die Naturwissenschaften, v. 87, no. 6, p. 270–274, https://doi.org/10.1007/s001140050719.

Mertz, D.F., Löhnertz, W., Nomade, S., Pereira, A., Prelević, D., and Renne, P.R., 2015, Temporal–spatial evolution of low-SiO_2 volcanism in the Pleistocene West Eifel volcanic field (west Germany) and relationship to upwelling asthenosphere: Journal of Geodynamics, v. 88, p. 59–79, https://doi.org/10.1016/j.jog.2015.04.002.

Mertz, D.F., and Renne, P.R., 2005, A numerical age for the Messel fossil deposit (UNESCO World Heritage Site) derived from $^{40}Ar/^{39}Ar$ dating on a basaltic rock fragment: Courier-Forschungsinstitut Senckenberg, v. 255, p. 67–75.

Meschede, M., 2015, Geologie Deutschlands—Ein prozessorientierter Ansatz [Geology of Germany—A process-oriented approach]: Berlin, Germany, Springer-Verlag, 233 p., https://doi.org/10.1007/978-3-662-45298-1.

Meyer, W., 2013, Geologie der Eifel [Geology of the Eifel]: Stuttgart, Germany, Schweizerbart Science Publishers, 704 p.

Meyer, W., and Stets, J., 2000, Geologische Übersichtskarte und Profil des Mittelrheintales [Geological overview map and profile of the Middle Rhine Valley]: Geologisches Landesamt Rheinland-Pfalz, 1 sheet, scale 1:100,000, 49-p. text.

Meyer, W.T., and Stets, J., 2002, Pleistocene to recent tectonics in the Rhenish Massif (Germany): Geologie en Mijnbouw, v. 81, no. 2, p. 217–221, https://doi.org/10.1017/S0016774600022460.

Molinari, I., and Morelli, A., 2011, EPcrust—A reference crustal model for the European Plate: Geophysical Journal International, v. 185, no. 1, p. 352–364, at https://doi.org/10.1111/j.1365-246X.2011.04940.x.

Mrlina, J., Kämpf, H., Geissler, W.H., and Van den Bogaard, P., 2007, Proposed Quaternary maar structure at the Czech/German boundary between Mytina and Neualbentreuth (western Eger Rift, central Europe)—Geophysical, petrochemical and geochronological indications: Zeitschrift für Geologische Wissenschaften, v. 35, p. 213–230.

Müller-Sohnius, D., and Huckenholz, H., 1989, Kalium-Argon-Datierungen an tertiären Vulkaniten der Hocheifel (BRD) [Potassium-argon dating of Tertiary volcanic rocks in the Hocheifel (Germany)]: Chemie der Erde, v. 49, no. 2, p. 119–136.

Müller, K., Brandes, C., and Winsemann, J., 2019, Paleoseismic investigation of northern Germany—Final Report: Hannover, Germany, Gottfried Wilhelm Leibniz Universität Hannover, 155 p.

Negendank, J.F.W., Brauer, A., and Zolitschka, B., 1990, Die Eifelmaare als erdgeschichtliche Fallen und Quellen zur Rekonstruktion des Paläoenvironments [The Eifel maars as geological traps and sources for the reconstruction of the paleoenvironment]: Mainzer Geowissenschaftliche Mitteilungen, v. 19, p. 235–262.

Nesbor, H.-D., 2018, Das Vulkangebiet Vogelsberg [The Vogelsberg volcanic region]: Geologisches Jahrbuch Hessen, v. 139, p. 5–41.

Neunhöfer, H., and Hemmann, A., 2005, Earthquake swarms in the Vogtland/Western Bohemia region—Spatial distribution and magnitude-frequency distribution as an indication of the genesis of swarms?: Journal of Geodynamics, v. 39, no. 4, p. 361–385, https://doi.org/10.1016/j.jog.2005.01.004.

O'Nions, R., Griesshaber, E., and Oxburgh, E., 1989, Rocks that are too hot to handle: Nature, v. 341, no. 6241, p. 391, https://doi.org/10.1038/341391a0.

Oncken, O., Plesch, A., Weber, J., Ricken, W., and Schrader, S., 2000, Passive margin detachment during arc-continent collision (central European Variscides): Special Publication - Geological Society of London, v. 179, no. 1, p. 199–216, https://doi.org/10.1144/GSL.SP.2000.179.01.13.

Paulick, H., Ewen, C., Blanchard, H., and Zöller, L., 2008, The Middle-Pleistocene (~300 ka) Rodderberg maar-scoria cone volcanic complex (Bonn, Germany)—Eruptive history, geochemistry, and thermoluminescence dating: International Journal of Earth Sciences, v. 98, no. 8, p. 1879–1899, https://doi.org/10.1007/s00531-008-0341-0.

Pécskay, Z., Přichystal, A., Tomek, Č., and Zapletal, J., 2009, Nová radiometrická data pro neovulkanity severní Moravy a Slezska [New radiometric data of neovolcanic rocks of northern Moravia and Silesia] [abs.], *in* Faměra, M., Dolníček, Z., and Lehotský, T., 2009, Moravskoslezské paleozoikum, Olomouc, Czech Republic, February 10, 2009: Palacký University Olomouc, Faculty of Science, p. 15–16, accessed December 17, 2025, at https://ugv.sci.muni.cz/media/2108288/msp2009.pdf.

Pfänder, J.A., Jung, S., Klügel, A., Münker, C., Romer, R.L., Sperner, B., and Rohrmüller, J., 2018, Recurrent local melting of metasomatised lithospheric mantle in response to continental rifting—Constraints from basanites and nephelinites/melilitites from SE Germany: Journal of Petrology, v. 59, no. 4, p. 667–694, https://doi.org/10.1093/petrology/egy041.

Pharaoh, T.C., 1999, Palaeozoic terranes and their lithospheric boundaries within the Trans-European Suture Zone (TESZ)—A review: Tectonophysics, v. 314, nos. 1–3, p. 17–41, https://doi.org/10.1016/S0040-1951(99)00235-8.

Preusser, F., Rufer, D., and Schreurs, G., 2011, Direct dating of Quaternary phreatic maar eruptions by luminescence methods: Geology, v. 39, no. 12, p. 1135–1138, https://doi.org/10.1130/G32345.1.

Prinz, L., and McCann, T., 2021, Sand injectites—From source to emplacement—An example from the Miocene age Frimmersdorf Seam, Garzweiler Open-cast Mine, Lower Rhine Embayment: Special Publication—Geological Society of London, v. 493, no. 1, p. 235–258, https://doi.org/10.1144/SP493-2017-289.

Przybyla, T., Pfänder, J., Münker, C., Kolb, M., Becker, M., and Hamacher, U., 2017, High-resolution $^{40}Ar/^{39}Ar$ geochronology of volcanic rocks from the Siebengebirge (central Germany)—Implications for eruption timescales and petrogenetic evolution of intraplate volcanic fields: International Journal of Earth Sciences, v. 107, no. 4, p. 1465–1484, https://doi.org/10.1007/s00531-017-1553-y.

Rajchl, M., Uličný, D., Grygar, R., and Mach, K., 2009, Evolution of basin architecture in an incipient continental rift—The Cenozoic Most Basin, Eger Graben (central Europe): Basin Research, v. 21, no. 3, p. 269–294, https://doi.org/10.1111/j.1365-2117.2008.00393.x.

Reicherter, K., Froitzheim, N., Jarosinski, M., Badura, J., Franzke, H., Hansen, M., Hübscher, C., Müller, R., Poprawa, P., and Reinecker, J., 2008, Alpine tectonics north of the Alps *in* McCann, T., ed., The Geology of Central Europe Volume 2—Mesozoic and Cenozoic: London, United Kingdom, Geological Society of London, p. 1233–1285. https://doi.org/10.1144/CEV2P.7

Reinhold, K., 2005, Tiefenlage der "Kristallin-Oberfläche" in Deutschland [Depth of the "Crystalline Surface" in Germany]: Hannover, Germany, Bundesanstalt für Geowissenschaften und Rohstoffe (BGR), final report, 91 p.

Reinig, F., Wacker, L., Jöris, O., Oppenheimer, C., Guidobaldi, G., Nievergelt, D., Adolphi, F., Cherubini, P., Engels, S., Esper, J., Land, A., Lane, C., Pfanz, H., Remmele, S., Sigl, M., Sookdeo, A., and Büntgen, U., 2021, Precise date for the Laacher See eruption synchronizes the Younger Dryas: Nature, v. 595, no. 7865, p. 66–69, at https://doi.org/10.1038/s41586-021-03608-x.

Ribbert, K.-H., 2010, Geologie im Rheinischen Schiefergebirge—Teil 1—Nordeifel [Geology in the Rhenish Massif—Part 1—North Eifel]: Krefeld, Germany, Geologischer Dienst Nordrhein-Westfalen, 184 p.

Ribbert, K.-H., 2012, Geologie im Rheinischen Schiefergebirge—Teil 2— Bergisches Land [Geology in the Rhenish Massif—Part 2— Bergisches Land]: Krefeld, Germany, Geologischer Dienst Nordrhein-Westfalen, 192 p.

Ring, U., and Bolhar, R., 2020, Tilting, uplift, volcanism and disintegration of the South German block: Tectonophysics, v. 795, no. 228611, 15 p., https://doi.org/10.1016/j.tecto.2020.228611.

Rogge, A., and Nowag, S., 2018, Hydrogeologisches Gutachten über die staatlich anerkannten Heilquellen von Bad Pyrmont [Hydrogeological report on the state-approved mineral springs of Bad Pyrmont]: Wunstorf, Germany, GeoDienste GmbH, 123 p.

Rohrmüller, J., Kämpf, H., Geiss, E., Großmann, J., Grun, I., Mingram, J., Mrlina, J., Plessen, B., Stebich, M., Veress, C., Wendt, A., and Nowaczyk, N., 2017, Reconnaissance study of an inferred Quaternary maar structure in the western part of the Bohemian Massif near Neualbenreuth, NE-Bavaria (Germany): International Journal of Earth Sciences, v. 107, no. 4, p. 1381–1405, https://doi.org/10.1007/s00531-017-1543-0.

Rummel, L., Bartels, A., and May, F., 2021a, Dokumentation und Auswertung einer zweiten Expertenbefragung zur langfristigen Vorhersage vulkanischer Aktivität in Deutschland [Documentation and evaluation of a second expert survey on the long-term forecast of volcanic activity in Germany]: Hannover, Germany, Bundesanstalt für Geowissenschaften und Rohstoffe, 73 p.

Rupf, I., and Nitsch, E., 2008, Das geologische Landesmodell von Baden-Württemberg—Datengrundlagen, technische Umsetzung und erste geologische Ergebnisse [The geological model of Baden-Württemberg—Data basis, technical implementation and first geological results]: Freiburg im Breisgau, Germany, Landesamt für Geologie, Rohstoffe und Bergbau Baden-Württemberg, 81 p.

Schaber, K., and Sirocko, F., 2005, Lithologie und Stratigraphie der spätpleistozänen Trockenmaare der Eifel [Lithology and stratigraphy of the Late Pleistocene dry maars of the Eifel]: Mainzer Geowissenschaftliche Mitteilungen, v. 33, p. 295–340.

Schäffer, R., Bär, K., Fischer, S., Fritsche, J.-G., and Sass, I., 2021, Database of Mineral, Thermal and Deep Groundwater of Hesse, Germany: Earth System Science Data, v. 13, no. 10, p. 4847–4860, https://doi.org/10.5194/essd-13-4847-2021.

Scheck, M., Bayer, U., Otto, V., Lamarche, J., Banka, D., and Pharaoh, T., 2002, The Elbe Fault System in North Central Europe—A basement controlled zone of crustal weakness: Tectonophysics, v. 360, nos. 1–4, p. 281–299, https://doi.org/10.1016/S0040-1951(02)00357-8.

Schleicher, H., 1986, Isotopengeochemie der Alkalivulkanite des Kaiserstuhls (ein Beitrag zu ihrer Genese mit Hilfe radiogener Isotope) [Isotope geochemistry of the alkali volcanics of the Kaiserstuhl (a contribution to their genesis using radiogenic isotopes)]: Freiburg im Breisgau, Germany, Albert-Ludwigs-Universität Freiburg, habilitation thesis, 220 p.

Schloz, W., and Stober, I., 2006, Mineral-, Heil- und Thermalwässer, Solen und Säuerlinge in Baden-Württemberg [Mineral, medicinal, and thermal waters, brines, and acidic springs in Baden-Württemberg]: Freiburg im Breisgau, Germany, Landesamt für Geologie, Rohstoffe und Bergbau Baden-Württemberg, 20 p.

Schmid, R., Franz, L., Rahn, M., Gautheron, C., and Capitani, C., 2014, Petrography and geochronology of phonolites of the Hegau volcanic field, SW Germany: 12th Swiss Geoscience Meeting 2014, Fribourg, Switzerland, November 21–22, 2014, Abstract v. 114-115.

Schmid, S.M., Fügenschuh, B., Kissling, E., and Schuster, R., 2004, Tectonic map and overall architecture of the Alpine orogen: Eclogae Geologicae Helvetiae, v. 97, no. 1, p. 93–117, https://doi.org/10.1007/s00015-004-1113-x.

Schmidt, C., Schaarschmidt, M., Kolb, T., Büchel, G., Richter, D., and Zöller, L., 2017, Luminescence dating of Late Pleistocene eruptions in the Eifel volcanic field, Germany: Journal of Quaternary Science, v. 32, no. 5, p. 628–638, https://doi.org/10.1002/jqs.2961.

Schmincke, H.-U., and Mertes, H., 1979, Pliocene and Quaternary volcanic phases in the Eifel volcanic fields: Die Naturwissenschaften, v. 66, no. 12, p. 614–615, https://doi.org/10.1007/BF00405123.

Schmitt, A.K., Marks, M.A., Nesbor, H.D., and Markl, G., 2007, The onset and origin of differentiated Rhine Graben volcanism based on U-Pb ages and oxygen isotopic composition of zircon: European Journal of Mineralogy, v. 19, no. 6, p. 849–857, https://doi.org/10.1127/0935-1221/2007/0019-1776.

Schneider, G., and Bankwitz, P., 2003, Neotektonische Krustenaktivität im Schwarmbebengebiet Vogtland/NW-Böhmen [Neotectonic crustal activity in the Vogtland/NW Bohemia swarm earthquake area]: Stuttgart/Potsdam, Germany, final report DFG-Projekt.

Schnepp, E., 1996, Geomagnetic paleointensities derived from volcanic rocks of the Quaternary East Eifel volcanic field, Germany: Physics of the Earth and Planetary Interiors, v. 94, no. 1–2, p. 23–41, https://doi.org/10.1016/0031-9201(95)03096-4.

Schnepp, E., and Hradetzky, H., 1994, Combined paleointensity and 40Ar/39Ar age spectrum data from volcanic rocks of the West Eifel field (Germany)—Evidence for an early Brunhes geomagnetic excursion: Journal of Geophysical Research, v. 99, no. B5, p. 9061–9076, https://doi.org/10.1029/93JB03365.

Schöttker, K., 2022, Die Quellen—Graf Metternich [The springs— Graf Metternich], accessed January 1, 2022, at https://www.graf-metternich-quellen.de/die-quellen/.

Schreiber, U., and Rotsch, S., 1998, Cenozoic block rotation according to a conjugate shear system in central Europe—Indications from palaeomagnetic measurements: Tectonophysics, v. 299, nos. 1–3, p. 111–142, https://doi.org/10.1016/S0040-1951(98)00201-7.

Schubert, S., Jung, S., Pfänder, J.A., Hauff, F., and Garbe-Schönberg, D., 2015, Petrogenesis of Tertiary continental intra-plate lavas between Siebengebirge and Westerwald, Germany—Constraints from trace element systematics and Nd, Sr and Pb isotopes: Journal of Volcanology and Geothermal Research, v. 305, p. 84–99, https://doi.org/10.1016/j.jvolgeores.2015.08.023.

Schulz, R., Suchi, E., Öhlschläger, D., Dittmann, J., Knopf, S., and Müller, C., 2013, Geothermie-Atlas zur Darstellung möglicher Nutzungskonkurrenzen zwischen CCS und Tiefer Geothermie [Geothermal Atlas showing potential conflicts of use between CCS and deep geothermal energy]: Hannover, Germany, Leibniz-Institut für Angewandte Geophysik (LIAG), Bundesanstalt für Geowissenschaften und Rohstoffe (BGR), final report, 108 p.

Schweigert, G., 1990, Eine untermiozäne Flora von Würtingen bei Bad Urach: Jahresberichte und Mitteilungen des Oberrheinischen Geologischen Vereins, v. 72, p. 277–285. [A Lower Miocene flora of Würtingen near Bad Urach], at https://doi.org/10.1127/jmogv/72/1990/277.

Schweizerischer Erdbebendienst [SED], 2022, Schweizerischer Erdbebendienst [Swiss Seismological Service]: ETH Zürich, accessed January 3, 2022, at http://www.seismo.ethz.ch/de/home/.

Shaw, J., and Johnston, S.T., 2016, Terrane wrecks (coupled oroclines) and paleomagnetic inclination anomalies: Earth-Science Reviews, v. 154, p. 191–209, https://doi.org/10.1016/j.earscirev.2016.01.003.

Sibrava, V., and Havlicek, P., 1980, Radiometric age of Plio-Pleistocene volcanic rocks of the Bohemian Massif: Vestnik Ustredniho Ustavu Geologickeho, v. 55, no. 3, p. 129–139.

Singer, B.S., Hoffman, K.A., Schnepp, E., and Guillou, H., 2008, Multiple Brunhes Chron excursions recorded in the West Eifel (Germany) volcanics—Support for long-held mantle control over the non-axial dipole field: Physics of the Earth and Planetary Interiors, v. 169, nos. 1–4, p. 28–40, https://doi.org/10.1016/j.pepi.2008.05.001.

Sintubin, M., Debacker, T.N., and Van Baelen, H., 2009, Early Palaeozoic orogenic events north of the Rheic suture (Brabant, Ardenne)—A review: Comptes Rendus—Géoscience, v. 341, nos. 2–3, p. 156–173, https://doi.org/10.1016/j.crte.2008.11.012.

Sissingh, W., 2003, Tertiary paleogeographic and tectonostratigraphic evolution of the Rhenish Triple Junction: Palaeogeography, Palaeoclimatology, Palaeoecology, v. 196, nos. 1–2, p. 229–263, https://doi.org/10.1016/S0031-0182(03)00320-1.

Sissingh, W., 2006, Syn-kinematic palaeogeographic evolution of the West European Platform—Correlation with Alpine plate collision and foreland deformation: Geologie en Mijnbouw, v. 85, no. 2, p. 131–180, https://doi.org/10.1017/S0016774600077933.

Skapski, J., 2022, Aktuelle Erdbeben in Deutschland [Current earthquakes in Germany]: Erdbebennews, accessed January 1, 2022, at https://erdbebennews.de/.

Smit, J., van Wees, J.-D., and Cloetingh, S., 2016, The Thor suture zone—From subduction to intraplate basin setting: Geology, v. 44, no. 9, p. 707–710, https://doi.org/10.1130/G37958.1.

Staatsbad, 2022, Die 5 Heilquellen im Staatsbad Bad Brückenau [The 5 healing springs in the Staatsbad Bad Brückenau], accessed January 1, 2022, at https://www.staatsbad.de/gesundheit-im-staatsbad-bad-brueckenau/heilquellen-in-bad-brueckenau/.

Stanek, K., Domínguez-Gonzalez, L., Andreani, L., and Bräutigam, B., 2016, 3D-Modellierung des Tertiärs in der Lausitz [3D modeling of the Tertiary period in Lusatia]: Dresden, Germany, Sächsisches Landesamt für Umwelt, Landwirtschaft und Geologie, 86 p.

Stanek, K.P., Renno, A.D., and Pushkarev, Y., 2003, Die tertiaren Vulkanite in der Umgebung von Baruth [The Tertiary volcanic rocks in the vicinity of Baruth]: Zeitschrift für Geologische Wissenschaften, v. 31, p. 425–440.

Tesauro, M., Kaban, M.K., and Cloetingh, S.A., 2008, EuCRUST-07—A new reference model for the European crust: Geophysical Research Letters, v. 35, no. 5, 5 p., at https://doi.org/10.1029/2007GL032244.

The PACE TMR Network Team, and Winchester, J.A., 2002, Palaeozoic amalgamation of Central Europe—New results from recent geological and geophysical investigations: Tectonophysics, v. 360, no. 1-4, p. 5–21, https://doi.org/10.1016/S0040-1951(02)00344-X.

Thews, J.-D., 1996, Erläuterungen zur geologischen Übersichtskarte von Hessen 1:300,000 (GÜK 300 Hessen) — Teil 1—Kristallin, Ordoviz, Silur, Devon, Karbon [Explanatory notes on the geological overview map of Hesse 1:300,000 (GÜK 300 Hessen) —Part 1—Crystalline, Ordovician, Silurian, Devonian, Carboniferous]. v. 96: Wiesbaden, Germany, Hessisches Landesamt für Bodenforschung, Geologische Abhandlungen Hessen, 237 p.

Todt, W., and Lippolt, H.J., 1975a, K-AR-Altersbestimmungen an Vulkaniten bekannter paläomagnetischer Feldrichtung—I—Oberpfalz und Oberfranken [K-Ar dating of volcanic rocks with known paleomagnetic field directions—I—Upper Palatinate and Upper Franconia]: Journal of Geophysics, v. 41, p. 43–61.

Todt, W., and Lippolt, H.J., 1975b, K-Ar-Altersbestimmungen an Vulkaniten bekannter paläomagnetischer Feldrichtung—II— Sachsen [K-Ar dating of volcanic rocks with known paleomagnetic field directions—II—Saxony]: Journal of Geophysics, v. 41, p. 641–650.

Todt, W., and Lippolt, H.J., 1980, K-Ar age determinations on tertiary volcanic rocks—5— Siebengebirge, Siebengebirge-Graben: Journal of Geophysics, v. 48, no. 1, p. 18–27.

Turk, P.G., Lohse, H.H., Schürmann, K., Fuhrmann, U., and Lippolt, H.J., 1984, Petrographische und Kalium-Argon-Untersuchungen an basischen tertiären Vulkaniten zwischen Westerwald und Vogelsberg: Geologische Rundschau, v. 73, no. 2, p. 599–617, https://doi.org/10.1007/BF01824974.

Ufrecht, W., 2006, Zusammensetzung und Herkunft der Gase in den Säuerlingen von Stuttgart-Bad Canstatt und -Berg [Origin and composition of the gases in the mineral water of Stuttgart-Bad Canstatt and Berg]: Schriftenreihe des Amtes für Umweltschutz, v. 3, p. 103–114.

Ulrych, J., Ackerman, L., Balogh, K., Hegner, E., Jelínek, E., Pécskay, Z., Přichystal, A., Upton, B.G., Zimák, J., and Foltýnová, R., 2013, Plio-Pleistocene basanitic and melilititic series of the Bohemian Massif—K-Ar ages, major/trace element and Sr-Nd isotopic data: Chemie der Erde, v. 73, no. 4, p. 429–450, https://doi.org/10.1016/j.chemer.2013.02.001.

Ulrych, J., Dostal, J., Hegner, E., Balogh, K., and Ackerman, L., 2008, Late Cretaceous to Paleocene melilitic rocks of the Ohře/Eger Rift in northern Bohemia, Czech Republic—Insights into the initial stages of continental rifting: Lithos, v. 101, nos. 1–2, p. 141–161, https://doi.org/10.1016/j.lithos.2007.07.012.

Ulrych, J., Novák, J.K., Lang, M., Balogh, K., Hegner, E., and Řanda, Z., 2006, Petrology and geochemistry and KAr ages for Cenozoic tinguaites from the Ohre/Eger Rift (NW Bohemia): Neues Jahrbuch für Mineralogie. Abhandlungen, v. 183, no. 1, p. 41–61, https://doi.org/10.1127/0077-7757/2006/0059.

Ulrych, J., Lloyd, F.E., and Balogh, K., 2003, Age relations and geochemical constraints of Cenozoic alkaline volcanic series in W Bohemia—A review: Geolines (Praha), v. 15, p. 168–180

Ulrych, J., Svobodová, J., and Balogh, K., 2002, The source of Cenozoic volcanism in the Ceske stredohori Mts., Bohemian Massif: Neues Jahrbuch für Mineralogie. Abhandlungen, v. 177, no. 2, p. 133–162, https://doi.org/10.1127/0077-7757/2002/0177-0133.

Viereck, L., 1983, Geologische und petrologische Entwicklung des pleistozänen Leuzitit -Leuzitphonolith-Vulkankomplexes Rieden, Ost-Eifel [Geological and petrological evolution of the Pleistocene leucitite - leucite phonolite-volcanic complex Rieden, East Eifel]: Bochum, Germany, Ruhr-Universität Bochum, Ph.D. dissertation, 337 p.

Wagner, G., 1976, Fission track dating on apatite and sphene from the subvolcanics of the Kaiserstuhl (Germany): Neues Jahrbuch für Geologie und Paläontologie, v. 9, p. 389–393.

Wagner, G., Gogen, K., Jonckheere, R., Wagner, I., and Woda, C., 2002, Dating of the Quaternary volcanoes Komorni Hurka (Kammerbuhl) and Zelezna Hurka (Eisenbuhl), Czech Republic, by TL, ESR, alpha-recoil and fission track chronometry: Zeitschrift für Geologische Wissenschaften, v. 30, no. 3, p. 191–200.

Weber, K., 2012, Erdbeben in der Eifel und dem Neuwieder Becken [Earthquakes in the Eifel and Neuwied Basin]: Einblicke—Vom Gestern zum Heute—25 Jahre DVG, p. 91–100.

Wedepohl, K.H., 1982, K-Ar-Altersbestimmungen an basaltischen Vulkaniten der nördlichen Hessischen Senke und ihr Beitrag zur Diskussion der Magmengenese [K-Ar age determinations on basaltic volcanic rocks of the northern Hessian Depression and their contribution to the discussion of magma formation]: Neues Jahrbuch für Mineralogie. Abhandlungen, v. 144, no. 2, p. 172–196, https://doi.org/10.1127/njma/144/1982/172.

Weinlich, F., 1998, Gas flux distribution in mineral springs and tectonic structure in the western Eger Rift: Journal of the Czech Geological Society, v. 43, no. 1–2, p. 91–110.

Weinlich, F., Bräuer, K., Kämpf, H., Strauch, G., Tesař, J., and Weise, S., 1999, An active subcontinental mantle volatile system in the western Eger rift, Central Europe—Gas flux, isotopic (He, C, and N) and compositional fingerprints: Geochimica et Cosmochimica Acta, v. 63, no. 21, p. 3653–3671, https://doi.org/10.1016/S0016-7037(99)00187-8.

Weinlich, F.H., Bräuer, K., Kämpf, H., Strauch, G., Tesař, J., and Weise, S.M., 2003, Gas flux and tectonic structure in the western Eger Rift, Karlovy Vary—Oberpfalz and Oberfranken, Bavaria: Geolines (Praha), v. 15, p. 181–187.

Weinlich, F.H., Faber, E., Boušková, A., Horálek, J., Teschner, M., and Poggenburg, J., 2006, Seismically induced variations in Mariánské Lázně fault gas composition in the NW Bohemian swarm quake region, Czech Republic—A continuous gas monitoring: Tectonophysics, v. 421, no. 1–2, p. 89–110, https://doi.org/10.1016/j.tecto.2006.04.012.

Weise, S.M., Bräuer, K., Kämpf, H., Strauch, G., and Koch, U., 2001, Transport of mantle volatiles through the crust traced by seismically released fluids—A natural experiment in the earthquake swarm area Vogtland/NW Bohemia, Central Europe: Tectonophysics, v. 336, no. 1–4, p. 137–150, https://doi.org/10.1016/S0040-1951(01)00098-1.

Wilson, M., Rosenbaum, J., and Ulrych, J., 1994, Cenozoic magmatism of the Ohře Rift, Czech Republic—Geochemical signatures and mantle dynamics [Abs.]: International Volcanological Congress [IAVCEI], September 12–16, 1994, Ankara, Turkey, 1 p.

Wimmenauer, W., 2003, Erläuterungen zum Blatt Kaiserstuhl [Explanations regarding the Kaiserstuhl sheet]: Freiburg im Breisgau, Germany, Landesamt für Geologie, Rohstoffe und Bergbau Baden-Württemberg, 280 p.

Wirth, W., Plenefisch, T., Klinge, K., Stammler, K., and Seidl, D., 2000, Focal mechanisms and stress field in the region Vogtland/Western Bohemia: Studia Geophysica et Geodaetica, v. 44, no. 2, p. 126–141, https://doi.org/10.1023/A:1022150523353.

Woda, C., Mangini, A., and Wagner, G.A., 2001, ESR dating of xenolithic quartz in volcanic rocks: Quaternary Science Reviews, v. 20, no. 5–9, p. 993–998, https://doi.org/10.1016/S0277-3791(00)00043-3.

Wrede, V., 2017, Regionale Baueinheiten [Regional structural units] *in* Wrede, V., ed., Geologie im Rheinischen Schiefergebirge—Teil 3—Sauer- und Siegerland [Geology in the Rhenish Massif—Part 3—Sauerland and Siegerland]: Krefeld, Germany, Geologischer Dienst Nordrhein-Westfalen, p. 33–45.

Zhu, H., Bozdağ, E., and Tromp, J., 2015, Seismic structure of the European upper mantle based on adjoint tomography: Geophysical Journal International, v. 201, no. 1, p. 18–52, https://doi.org/10.1093/gji/ggu492.

Ziegler, P., and Dèzes, P., 2006, Crustal evolution of western and central Europe: Geological Society of London, Memoirs, v. 32, no. 1, p. 43–56, at https://doi.org/10.1144/GSL.MEM.2006.032.01.03.

Zirkler, A., Glasmacher, U., Krob, F., Zeibig, S., Olbert, J., and Dunkl, I., 2021, Magmatism in the Werra-Fulda mining district—Window into the magmatic evolution of the central European volcanic province and its interaction with evaporites: European Mineralogical Conference, 3rd, Cracow, Poland, August 29–September 2, 2021, Proceedings: Mineralogical Society of Poland.

Zolitschka, B., 1998, A 14,000 year sediment yield record from western Germany based on annually laminated lake sediments: Geomorphology, v. 22, no. 1, p. 1–17, https://doi.org/10.1016/S0169-555X(97)00051-2.

Zolitschka, B., Negendank, J.F., and Lottermoser, B., 1995, Sedimentological proof and dating of the early Holocene volcanic eruption of Ulmener Maar (Vulkaneifel, Germany): Geologische Rundschau, v. 84, no. 1, p. 213–219, https://doi.org/10.1007/BF00192252.

Zöller, L., 1991, Thermoluminescence dating of upper Pleistocene volcanoes—Paleolimnology of maar lakes, *in* Zolitschka, B., and Negendank, J.F.W., eds., Abstracts & Excursion Guide, 62 p.

Zöller, L., and Blanchard, H., 2009, The partial heat–longest plateau technique—Testing TL dating of Middle and Upper Quaternary volcanic eruptions in the Eifel Area, Germany: E&G Quaternary Science Journal, v. 58, no. 1, p. 86–106, https://doi.org/10.3285/eg.58.1.05.

Moffett Field Publishing Service Center
Manuscript approved January 14, 2026
Edited by Hayden Chaisson
Illustration support and layout by Cory Hurd

ISSN 2330-7102 (online)
https://doi.org/10.3133/pp1890C